7-18-2018

Interaction of High Molecular Weight Compounds with a, β-Unsaturated Carbonyl Moiety with Mammalian and Drosophila Melanogaster Thioredoxin Reductase

Anupama Tuladhar
atula001@fiu.edu

FLORIDA INTERNATIONAL UNIVERSITY

Miami, Florida

INTERACTION OF HIGH MOLECULAR WEIGHT COMPOUNDS WITH α, β-UNSATURATED CARBONYL MOIETY WITH MAMMALIAN AND *DROSOPHILA MELANOGASTER* THIOREDOXIN REDUCTASE

A dissertation submitted in partial fulfillment of

the requirements for the degree of

DOCTOR OF PHILOSOPHY

in

CHEMISTRY

by

Anupama Tuladhar

2018

To: Dean Michael R. Heithaus
College of Arts, Sciences and Education

This dissertation, written by Anupama Tuladhar, and entitled Interaction of High Molecular Weight Compounds with α, β-unsaturated Carbonyl Moiety with Mammalian and *Drosophila melanogaster* Thioredoxin Reductase, having been approved in respect to style and intellectual content, is referred to you for judgment.

We have read this dissertation and recommend that it be approved.

Kevin O'Shea

Raphael G. Raptis

Yuan Liu

Niclas Engene

Kathleen Rein, Major Professor

Date of Defense: July 18, 2018

The dissertation of Anupama Tuladhar is approved

Dean Michael R. Heithaus
College of Arts, Sciences and Education

Andrés G. Gil
Vice President for Research and Economic Development
and Dean of the University Graduate School

Florida International University, 2018

DEDICATION

I would like to dedicate this work to my parents and dearest husband Kiran Subedi for endless love and support. This work would not have been possible without you.

ACKNOWLEDGMENT

There are many people to acknowledge for the completion of my PhD. I am grateful towards everyone who have supported and guided me to accomplish my dream.

First and foremost, I would like to thank my advisor whose guidance, patience and persistant recommendation during these 5 years had made me the person who I am today. I also want to extend my sincere gratitude to Robert Hondal from the University of Vermont for providing valuable suggestions and the precious enzymes.

My second thought of gratitude goes out to my committee members Kevin O'Shea, Yuan Liu, Niclas Engene and Raphael Raptis who has always been there to guide and suggest. Especial thanks to Yuan Liu for providing the cells.

Last but not the least, I want to thank all my labmates (Ricky, Elyssa and John) and friends who have made these 5 years at FIU memorable and fun. I also want to thank Department of Chemistry and Biochemistry for the support throughout my PhD career.

ABSTRACT OF THE DISSERTATION

INTERACTION OF HIGH MOLECULAR WEIGHT COMPOUNDS WITH α, β-UNSATURATED CARBONYL MOIETY WITH MAMMALIAN AND *DROSOPHILA MELANOGASTER* THIOREDOXIN REDUCTASE

by

Anupama Tuladhar

Florida International University, 2018

Miami, Florida

Professor Kathleen Rein, Major Professor

The thioredoxin system is the major cellular reductant system present in the cell, whose role is to maintain cellular redox homeostasis. It does this in part, by regulating the activity of many other enzymes including ribonucleotide reductase, which is essential for DNA synthesis. It also acts as an antioxidant, reducing destructive reactive oxygen species. The thioredoxin system is comprised of thioredoxin (Trx) which reduces target protein disulfide bridges by thiol-disulfide exchange and thioredoxin reductase (TrxR) which reduces Trx back to its active state. Thioredoxin reductase is a common target for many cancer drugs including cisplatin and auranofin. Recently we have shown that the Florida red tide toxin, brevetoxin-2 (PbTx-2) can inhibit mammalian TrxR1. Brevetoxin-2 has α, β-unsaturated aldehyde moiety that was proposed to inhibit the enzyme by forming a Michael adduct. Several compounds which are similar to brevetoxin in size and functionality have a similar effect on TrxR. These compounds include antitumor and antibiotics such as manumycin A, geldanamycin, rifamycin SV and thiostrepton and toxins such as brevetoxin-3, nodularin and microcystin-LR. Manumycin A behaves as a

typical TrxR1 inhibitor while other compounds screened activate the reduction of small disulfides such as DTNB (5,5'-dithiobis-(2-nitrobenzoic acid)). Mammalian thioredoxin reductase is a homodimer with two redox center viz. N-terminal dithiol buried in the enzyme and C-terminal selenosulfide located on the flexible C-terminal tail. Modification of the C-terminal tail of TrxR by these test compounds can expose N-terminal redox thiol that could reduce DTNB. The C-terminal Sec, a nucleophile can form a Michael adduct with α, β-unsaturated carbonyl moiety of test compounds. Together with point-specific mutant enzymes (C-terminal tail truncated, dead tail and Cys mutant) and enzyme assays that are specific/dependent on C-terminal Sec were used to decipher the site-specific interaction between these test compounds and TrxR. Inhibition of TrxR at the C-terminal redox center produces a pro-oxidant known as SecTRAP (Selenium Compromised Thioredoxin Reductase-derived Apoptotic Proteins), which uses NADPH to produce superoxide radical anion as observed with manumycin A. Since many cancer drugs target TrxR the present study has the potential to discover new cancer drugs.

TABLE OF CONTENTS

CHAPTER PAGE

LIST OF TABLES

TABLE PAGE

LIST OF FIGURES

FIGURE PAGE

LIST OF ABBREVIATIONS

3’-UTR	3’-untranslated regions
Adda	(all-*S*, all-*E*)-3-amino-9-methoxy-2, 6,8-trimethyl-10-phenyldeca-4, 6-dienoic acid
Ala	Alanine
ANOVA	Analysis of variance
AP-1	Activator protein 1
ASK1	Apoptosis signal-regulating kinase 1
Asn	Asparagine
BCL6	B cell lymphoma 6 protein
BSA	Bovine serum albumin
cDNA	Complementary deoxyribonucleic acid
Deoxyman-A	Deoxy-manumycin A
Dihydroman-A	Dihydro-manumycin A
DMSO	Dimethyl sulfoxide
DmTrxR	Dorsophila melanogaster thioredoxin reductase
DNA	Deoxyribonucleic acid
DNCB	1-chloro-2,4-dinitrobenzene
DTNB	5,5’-dithiobis-(2-nitrobenzoic acid)
DTT	Dithiothreitol
EC_{50}	Effective concentration
EDTA	Ethylenediaminetetraacetic acid

EF	Elongation factor
ETS	Electron transport system
FBS	Fetal bovine serum
FOXM1	Forkhead box M1
FTase	Farnesyl transferase
Ga	Geldanamycin
GDP	Guanosine diphosphate
GM02152	Human lymphoblast cell
GPxs	Glutathione peroxidase
GR	Glutathione reductase
GSH	Glutathione
GTP	Guanosine triphosphate
HAB	Harmful algal bloom
HK-60	Human myeloid cells
HSP90	Heat shock protein 90
hTrx-1	Human thioredoxin 1
IC_{50}	Inhibition concentration
JNK MAPK	c-Jun N-terminal kinase mitogen-activated protein kinase
K. brevis	*Karenia brevis*
MALDI-MS	Matrix-assisted laser desorption ionization-mass spectrometry
MALDI-TOF-MS	Matrix assisted laser desorption-Time of flight-ionization-mass spectrometry

Man-A	Manumycin A
MAPK	Mitogen-activated protein kinases
MC-LR	Microcystin LR
MDA	Malondialdehyde
M_r	Molecular weight
MeCN	Acetonitrile
mRNA	Messenger ribonucleic acid
Msr	Methionine sulfoxide reductases
mTrxR2	Mitochondrial thioredoxin reductase
MTT	3(4,5-dimethylthiazolyl-2)-25-diphenyltetrazolium bromide
NADH	Nicotinamide adenine dinucleotide
NADPH	Nicotinamide adenine dinucleotide phosphate
NF-κB	Nuclear factor κB
NSP	Neurotoxic shellfish poisoning
OATP	Organic anion transporting polypeptides
PAGE	Polyacrylamide gel electrophoresis
PbTx	Brevetoxin
Pro	Proline
Prx	Preoxiredoxin
Prx 3	Peroxiredoxin
PSTK	O-phosphoseryl-tRNA kinase

PUFA	Polyunsaturated fatty acid
RAR	Retinoic acid receptor
Red. MC-LR	Dihydro Microcystin LR
Ref-1	Redox factor 1
Rf	Rifamycin SV
ROS	Reactive oxygen species
Sec	Selenocysteine
SECIS	Sec Insertion Sequence
SecTRAP	Selenium compromised thioredoxin reductase-derived apoptotic proteins
SepSecS	Sep-tRNA:Sec-tRNA synthase
Ser	Serine
SerRS	Seryl-tRNA synthetase
SOD	Superoxide dismutase
SPE	Solid phase extraction
TBA	Thiobarbituric acid
TBARS	Thiobarbaturic acid-reactive substances
TCEP	(tris(2-carboxyethyl)phosphine)
TEP	Tetraethoxypropane
TFA	Trifluoroacetic acid
TGR	Thioredoxin glutathione reductase
Th	Thiostrepton
TNB^{2-}	2-nitro-5-thiobenzoate anion

TNF-α	Tumor necrosis factor
tRNA	Transfer ribonucleic acid
Trolox	6-hydroxy-2,5,7,8-tetramethylchroman-2-carboxylic acid
Trx	Thioredoxin
TrxR	Thioredoxin reductase
TrxR1	Cytosolic thioredoxin reductase
Txnip	Thioredoxin interacting protein
U-937	Monocyte cell line
UV-vis	ultraviolet-visible absorption spectroscopy
α	Alpha
α-CHCA	Cyanno-4-hyrocinnamic acid
B	Beta
ºC	Degree Celsius
L	Liter
µ	Micro
λ	Lambda
m	Milli
mol	Mole
%	Percentage

Chapter 1. Introduction

Cellular homeostasis in mammalian cells is maintained principally by two redox enzymes viz. glutathione reductase (GR) and thioredoxin reductase (TrxR). These two enzymes share structural, functional and mechanistic similarities. Both utilize cysteines at the active site, reducing their substrates by thiol-disulfide exchange. The principle role of GR is the reduction of the disulfide bond of oxidized glutathione while TrxR reduces thioredoxin (Trx). In turn, thioredoxin (Trx) reduces protein disulfide bridges of numerous protein targets.

The pKa of cysteine is modulated by environment such as hydrogen bonding, co-ordinating metal ion or the helix dipole[1]. Under physiological conditions the pKa of cysteine (Figure 1) can be lowered significantly, which makes cysteine an ideal electron donor to the oxidized proteins. In addition to S, another group 6 element Se, is incorporated into the 21st amino acid, as selenocysteine (Figure 1) (Sec). While selenoproteins are rare, they are present in a wide variety of organisms from mammals to protists. Selenium (Se) is a rare non-metal that was discovered by Swedish chemist Jöns Jacob Berzelius in 1817. It is believed that the presence of Se in the enzyme active site imparts increased reactivity as well as a broad substrate range. Mammalian selenoproteins include thioredoxin reductase (TrxR), glutathione peroxidase (GPxs), iodothyronine deiodinase, methionine sulfoxide reductase 1B, selenophosphate synthetase 2 and selenoprotein P. Beside proteins, mammalian and bacterial tRNA (transfer ribonucleic acid) also contain selenium.

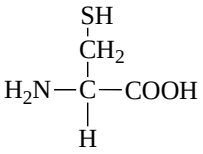

Cysteine (Cys)

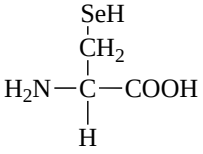

Selenocysteine (Sec)

Figure 1. Amino acids

Mammals have three different isoforms of TrxR: cytosolic represented as TrxR1, mitochondrial represented as TrxR2 and testis specific TrxR represented as thioredoxin glutathione reductase (TGR). Thioredoxin reductase regulates many cellular processes by reducing Trx and is required for the normal development of the embryo. Deletion of TrxR and the Trx gene has different impacts on developing embryos. Mitochondrial TrxR and Trx are highly expressed in metabolically active tissues such as heart, kidney and liver[2] to prevent oxidative stress and is essential for the survival of mice embryos. The deletion of the TrxR2 gene is associated with hematopoiesis, heart dysfunction and apoptosis[3], a condition similar to Keshan disease, which is related to a deficiency of Se in the diet. On the other hand, TrxR1 knockout mice embryos show retarded growth with reduced cell proliferation followed by death of the embryo without affecting the heart[4]. Thioredoxin glutathione reductase which reduces both glutathione as well as thioredoxin is specifically required during spermatogenesis. However, knockdown of the TGR gene is associated with decreased transcriptional activity of retinoic acid receptor (RAR) in mice that mediates biological processes such as cell proliferation, differentiation and development through retinoic acid[5].

1.1 The thioredoxin system

The thioredoxin system consists of TrxR, Trx, NADPH and FAD where TrxR reduces oxidized Trx in an NADPH dependent reaction, as shown in Figure 2. The reduced Trx in turn reduces targets such as insulin, ribonucleotide reductase and transcriptional factors[6]. Thioredoxin reductase belongs to the family of pyridine nucleotide disulfide oxidoreductases, which also includes other enzymes such as glutathione reductase, mercuric ion reductase and lipoamide dehydrogenase. Other roles of TrxR include antioxidant defense, cellular proliferation, DNA and protein repair, transcription of protein and its folding.

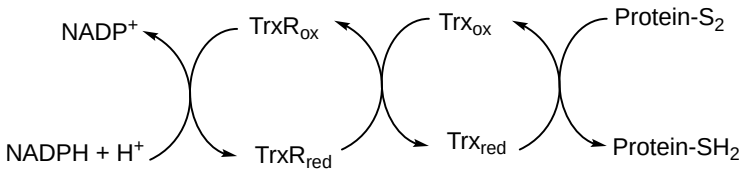

Figure 2. Electron flow of the thioredoxin system. Trx reduces many proteins and is returned to the active reduced state by TrxR in a NADPH dependent reaction

Thioredoxin reductase is present in all living organisms and has evolved significantly, with numerous homologs identified[7]. Thioredoxin reductase homologs differ in size and the number and sequence of redox centers. These variations form the basis of the classification systems. Thioredoxin reductases from lower eukaryotes and prokaryotes are low-M_r dimers of ~35 kDa subunits that utilize two redox centers: a non-covalently bound FAD and a N-terminal dithiol/disulfide (Cys-Ala-Thr-Cys). The two redox centers are juxtaposed in the oxidized form but when reduced, the N-terminal dithiol rotates to expose the dithiol towards the solvent surface facilitating reduction of Trx[8]. The oxidized disulfide then rotates to its original position to be reduced by FAD.

The high-M_r TrxR (present in numerous animals, including vertebrates, invertebrates, insects and protists) are composed of two monomers aligned antiparallel to each other. This class of TrxR has an additional C-terminal redox center, not present in the low-M_r enzymes, whose sequence varies according to the source. The C-terminal tail of higher eukaryotes is highly conserved and flexible with variable redox sites. Mammalian TrxR is composed of two high molecular weight (M_r ~55 kDa) subunits arranged such that the reducing equivalent of NADPH is transferred via the N-terminal dithiol to the C-terminal redox center of the other monomer, as shown in Figure 3.

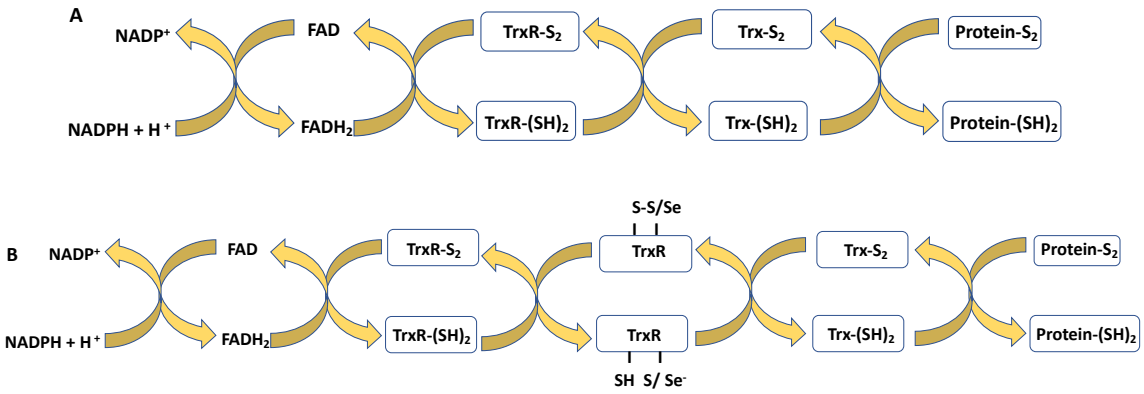

Figure 3. Electron flow from NADPH to protein disulfide bridges, via TrxR and Trx. (**A**) Prokaryotic, low-M_r TrxR. (**B**) High M_r TrxR. The C-terminal redox center in high M_r TrxR can be composed of either 2 cysteines residues or a cysteine and a selenocysteine

Thioredoxin reductase from higher organisms can be further classified into two groups on the basis of the sequence of the C-terminal redox center. *Type I* TrxR, with a vicinal selenosulfide bond (X-Cys-Sec-X) sequence is present in animals or vicinal disulfide bond (X-Cys-Cys-X) as in *Drosophilia melanogaster*. Mammals have a 16 amino acid C-terminal tail which helps to shuttle electrons received from the N-terminal dithiol to the target protein. *Type II* TrxR have redox cysteines separated as in *Plasmodium falciparum* (Cys-Gly-Gly-Gly-Lys-Cys-Gly). Detailed classification of the

C-terminal redox centers is presented in Table 1. Despite the disparity in the C-terminal redox center these TrxR share some identities and have similar mechanism of action. Table 2 displays the sequence identity of various large M_r TrxR.

Table 1. Classification of TrxR on the basis of C-terminal redox center

	Species	**C-terminal motif**
Type I	Human/Rat TrxR	-GCUG(Cytosolic/Mitochondrial)
	Caenorhabditis elegans	-GCUG (Cytosolic) -GCCG (Mitochondrial)
	Drosophila melanogaster	-SCCS (Cytosolic/Mitochondrial)
Type II	*Plasmodium falciparum*	-CGGGKCG

Table 2. Sequence identities of various large M_r TrxR. Identities were determined using Clustal Omega multiple sequence alignment software[9]

	Accession number	***Plasmodium falciparum***	***Drosophila melanogaster***	***Caenorhabditis elegans***	***Homo sapiens***
Plasmodium falciparum	CAA60574.1	100	46.25	44.98	46.41
Drosophila melanogaster	NP_524216.1	46.25	100	43.97	50.81
Caenorhabditis elegans	NP_001293761.1	44.98	43.97	100	58.38
Homo sapiens	AAB35418.1	46.41	50.81	58.38	100

1.2 Biosynthesis of selenoproteins in mammalian TrxR

In humans, three genes *TXNRD1, TXNRD2 and TXNRD3* encode for TrxR1, TrxR2 and TGR respectively. The *TXNRD1* gene is located on the chromosome 12q23.3 and the cDNA sequence has 3826 bp which encodes for 495 amino acids. The human *TXNRD1* gene is divided into 16 exons including 100 kb DNA[10]. The human mitochondrial *TXNRD2* gene is localized in chromosomal position 22q11.2 and consists of 18 exons with 67 kb DNA[11]. It has 521 amino acid residues with a molecular mass of 56.2 kDa. The *TXNRD3* gene is localized in chromosomal position 22q11.2 and has 65 kilobases in humans[12].

The C-terminal tail of mammalian TrxR is highly conserved among mammals with the sequence –Gly-Cys-Sec-Gly. The selenium of the Sec residue is derived from hydrogen selenide in a reaction catalyzed by selenophosphate synthesase2 in all eukarya/archaea and bacteria. Selenocysteine is encoded by TGA in the sequence GGC TGC TGA GGT TAA. The stop codon is normally encoded by TGA but here TAA is the true stop codon. The incorporation of Sec into selenoproteins requires recoding of the TGA which is accomplished by SECIS (Selenocysteine Insertion Sequence) element located at the 3'-untranslated region (3'-UTR) of the mRNA. The SECIS element forms a stem loop structure that guides a special tRNA to insert Sec into the growing peptide rather than to read it as termination codon.

The mechanism of Sec insertion in proteins differs between bacteria, archaea and higher eukaryotes. In eukaryotes selenoprotein synthesis requires a Sec specific tRNA ($tRNA^{sec}$) which plays the vital role in Sec incorporation into proteins. It begins with aminoacetylation of $tRNA^{sec}$ by serine, the process is catalyzed by seryl-tRNA synthetase

(SerRS). The serine hydroxyl is phosphorylated by O-phosphoseryl-tRNA kinase (PSTK) in eukarya and archaea. The enzyme Sep-tRNA:Sec-tRNA synthase (SepSecS) converts O-phosphoseryl-tRNA to selenocysteinyl-tRNA^{sec} by substitution of the phosphate group with selenophosphate[13].

Four genes are involved in incorporation of Sec in bacterial selenoproteins: *selA*, *selB*, *selC* and *selD*. The gene *selC* codes for tRNA^{sec} [14] that accepts serine at the beginning and co-translationally inserts Sec in the reaction catalyzed by Sec synthase (product of *SelA* genes)[15]. The conversion of ser-tRNA^{sec} into sec-tRNA^{sec} is catalyzed by Sec synthase where selenium is donated by selenophosphate. Selenophosphate synthetase, a product of *selD* gene catalyzes the reaction that converts the selenide to selenophosphate by the consumption of ATP[16].

The sec-tRNA^{sec} has the anticodon ACU which reads the UGA code (also a stop codon) in mRNA and co-translationally inserts Sec into the growing polypeptide chain in the presence of the SECIS element which is located after the stop codon in eukaryotes and before the stop codon in bacteria. The SECIS binding protein (SBP2) binds to the SECIS element of mRNA and along with elongation factor (EF) translates the code UGA to Sec. In bacteria, selB, a selenocysteine specific translational elongation factor and also homolgous to SBP2 in eukaryotes directly binds to SECIS and translates for Sec. The mechanism of Sec insertion is shown in Figure 4.

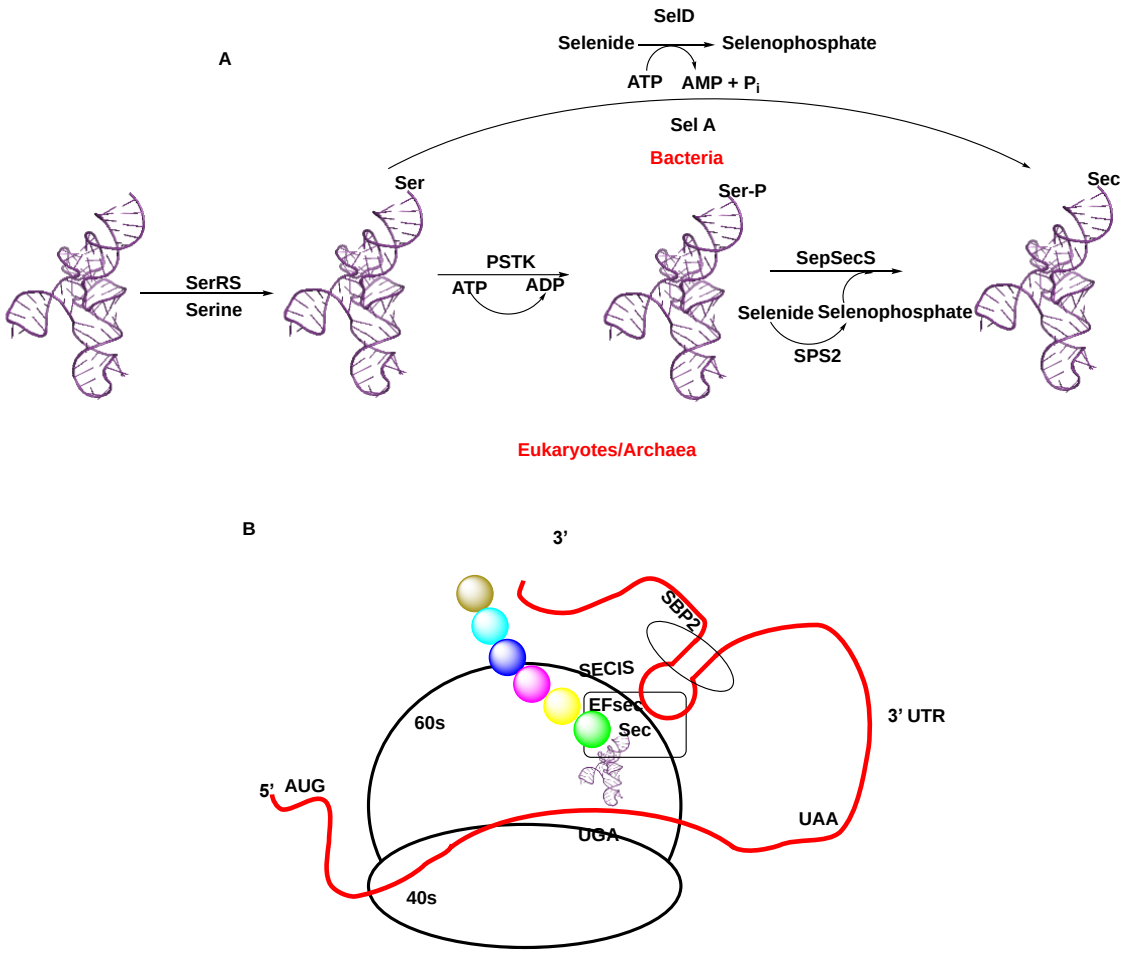

Figure 4. Insertion of Sec in eukaryotes and bacterial protein. **(A)** Incorporation of Sec in tRNA in eukaryotes and bacteria begins with attachment of L-serine to tRNA. The seryl group is phosphorylated by kinase phosphoseryl-tRNA kinase (PSTK) to O-phosphoseryl-tRNA. Selenophosphate synthase (SPS2) and SepSecS incorporates Sec in tRNA, sec-tRNAsec. In bacteria, *selA* and s*elD* catalyzes the conversion of Ser-tRNAsec to Sec-tRNAsec **(B)** Translation of mRNA to protein in eukaryotes. The sec-tRNAsec is transported to ribosome by an elongation factor at the codon UGA and SECIS binding protein (SBP2) specifically binds to SECIS element which recognizes UGA as a code for Sec and incorporates in a growing polypeptide. In bacteria, direct binding of *SelB* to SECIS codes for Sec. Adapted from reference 16

1.3 Catalytic properties of mammalian TrxR

Thioredoxin reductase is a homodimer flavoenzyme whose monomers are aligned in an antiparallel arrangement. The FAD is located in close proximity to the N-terminal redox center, which is comprised of Cys^{59} and Cys^{64} in human's TrxR1. In addition to the

N-terminal redox center the human TrxR has a C-terminal redox center which is comprised of Cys^{497} and Sec^{498}. The catalytic cycle of mammalian TrxR begins by transfer of two electrons to FAD by oxidation of one equivalent of NADPH. The reduced FAD ($FADH_2$) forms a charge transfer complex with Cys^{64}. As shown in Figure 5, the base His^{472} abstracts the proton from Cys^{59}. This reaction is thermodynamically favoured by -2.2 kcal/mol due to the presence of proton acceptor Glu^{477} which stabilizes the imidazole ring[17]. The importance of catalytic triad (His^{472}, Glu^{477} and Cys^{59}) is also supported experimentally where mutation of Glu^{477} to Lys, Ala or Gln decreases the enzymatic activity significantly (nearly 6-15 folds)[18]. The reduced Cys^{59} reduces the selenosulfide (Cys^{497}- Sec^{498}) redox site located at C-terminal tail. The new selenosulfide bond between (Cys^{59}- Sec^{498}) is then reduced by Cys^{64}. Once reduced the C-terminal redox center swings out of the pocket to reduce substrate[19].The oxidized C-terminal tail then enters a tetra peptide (Gly-Cys-Sec-Gly) pocket, a narrow groove and is reduced by the N-terminal redox center. The mammalian TrxR utilizes Sec as the formation of selenoate in comparison to thiolate is thermodynamically favoured by additional -2.3 kcal/mol due to second catalytic triad (His^{472}, Glu^{477} and Sec^{498})[17].

As compared to mammalian TrxR, DmTrxR is a homodimeric with the C-terminal redox center (-Ser-Cys-Cys-Ser). The mechanism of reduction is similar to mammalian TrxR, as shown in Figure 5. However, DmTrxR does not have Sec at C-terminal but rather uses cysteine to reduce the substrates. The reduction cycle starts by reduction of the N-terminal disulfide by the reducing equivalent obtained from the oxidation of NADPH[20]. This catalytic process of mammalian TrxR is known as a ping pong mechanism, as illustrated in Figure 5.

The mammalian TrxRs have wide substrate tolerance which is attributed to the presence of Sec. It is known to reduce Trx of other species such as *E. coli* as well as other substrates such as the diselenide selenocystine, DTNB, lipoic acid and juglone. Although the functional C-terminal tail is required for the reduction of most of the substrates, some small molecules such as DTNB and selenite have been reported to be reduced by the N-terminal redox center as well.

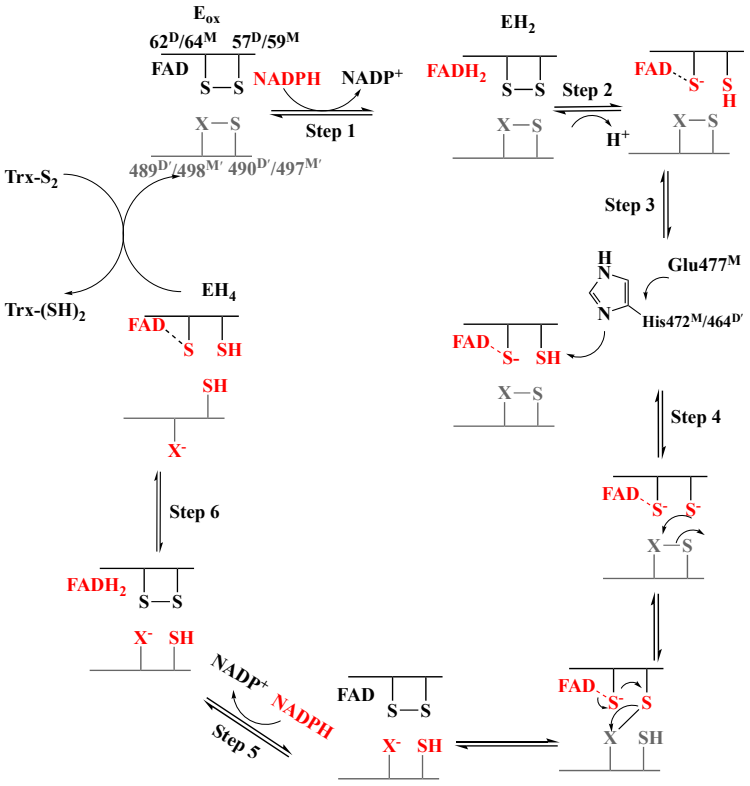

Figure 5. Catalytic cycle of mammalian (M) and *Drosophila melanogaster* (D) TrxR. DmTrxR X= Cys, mammalian TrxR X= Sec. All the reduced moieties are shown in red. **Step 1:** FAD is reduced by NADPH forming EH_2. **Step 2:** ($FADH_2$) forms a charge transfer complex with C^{64M}/C^{62D} and transfers two electrons to C^{59M}/C^{57D}, reducing the disulfide bond. **Step 3:** The histidine from catalytic triad abstract the hydrogen from C^{59M}/C^{57D}. **Step 4:** A pair of electrons moves to X from C^{59M}/C^{57D}, reducing the selenosulfide bond. **Step 5:** Second equivalent of NADPH reduces FAD. **Step 6:** C-terminal selenocysteine is oriented towards solvent surface to reduce substrates and cycle returns to **Step 1**. Adapted from reference 19

1.4 Importance of Sec in mammalian TrxR

Selenium (Se) is an essential micronutrient, but an excess dose can cause selenium poisoning with symptoms including diarrhea, hair loss, nail discoloration and brittleness, nausea, muscle pain and cramps. The recommended daily intake for Se is 55 μg/day for adults[21]. On the other hand, selenium deficiency is associated with Keshan disease characterized by myocardial necrosis and Kashin-Beck disease characterized by necrosis of cartilage tissue[22] and hypothyroidism. The selenium containing enzyme iodothyronine deiodinase has an important role in conversion of thyroxine (T4) to triiodothyronine. About 25 human enzymes have Sec as an active electron donor which includes glutathione peroxidase, deiodinases, thioredoxin reductase, selenoprotein W, selenoprotein P, selenophophate synthatase and others[23]. It is intriguing why some enzymes use Sec while the other enzyme is less dependent on the use of Sec. One reason for an enzyme to replace sulfur with selenium is to achieve high efficiency in oxidizing conditions as the oxidation of selenium is reversible under physiological conditions, as shown in Figure 6 [24].

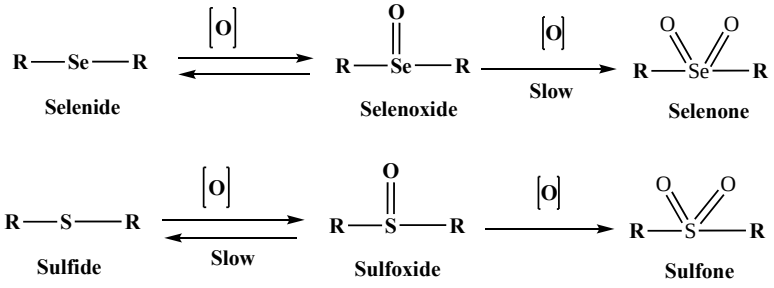

Figure 6. Comparison of reversible oxidation of selenide and sulfide

All the three mammalian TrxR isoenzymes viz. TrxR1, TrxR2 and TGR (thioredoxin/glutathione reductase) are homologous. Figure 7 shows the comparison of

different domains of mammalian TrxR isoforms. The sequence identity among different mammalian TrxR isoforms are shown in Table 3 where mTrxR2, hTGR and mTrxR1 represents mouse mitochondrial TrxR, human TGR and mouse cytoplasmic TrxR respectively.

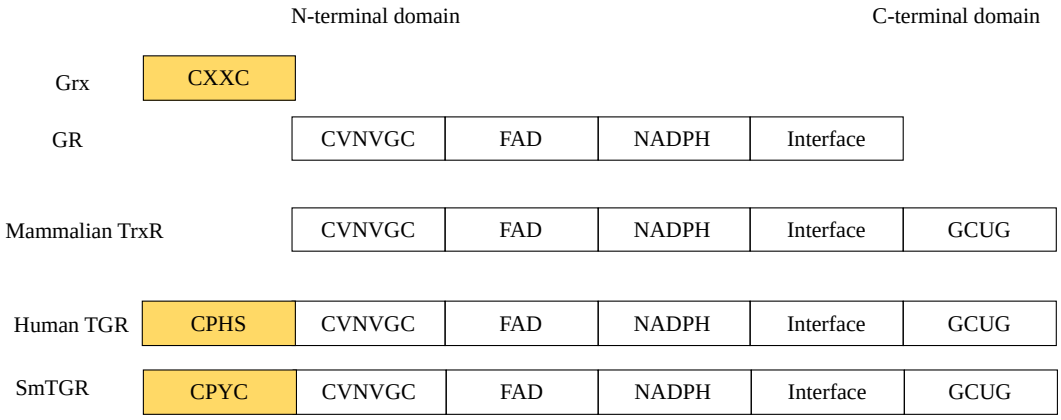

Figure 7. Comparison of different domains in glutaredoxin (Grx), glutathione reductase (GR), thioredoxin reductase (TrxR) and thioredoxin glutathione reductase (TGR). Thioredoxin reductase and TGR have N-terminal domain (CVNVGC) and C-terminal domain (GCUG) with a highly conserved redox site. These two domains are separated by the interface where two monomers interact. TGR has an extended portion with a sequence similar to Grx. Humans have single cysteine in Grx (Cys-Pro-His-Ser) while *Schistosoma mansoni* have a pair of cysteine (Cys-Pro-Tyr-Cys). Glutathione reductase on the other hand has only a single, N-terminal redox domain

Table 3. Sequence identities of different mammalian TrxR isoforms

	mTrxR2	**hTGR**	**mTrxR1**
mTrxR2	100	52	55.85
hTGR	52	100	72.14
mTrxR1	55.85	72.14	100

Among these three types of mammalian TrxR, cytosolic TrxR1 is the most extensively studied and is known to have broad substrate acceptance and can reduce bacterial as well as human Trx. The cytosolic TrxR1 is highly dependent on C-terminal

Sec to reduce Trx. Mutation of the Sec to Cys decreases the enzyme activity by ~90 fold when human Trx is used as substrate[25]. On the other hand, mutation of Sec to Cys in TrxR2 shows no such profound decrease in activity when *E. coli* Trx is used as substrate. Such vast disparity between the two isoenzymes has been attributed to the guiding bar. The guiding bar is comprised of amino acids $Trp^{407'}$, $Asn^{418'}$ and $Asn^{419'}$ and forms the hydrogen bond to $Gln^{494'-496'}$ in hTrxR [26] which is present in the same monomer. The guiding bar restricts the random motion of the C-terminal arm in TrxR1 through hydrogen bonding which renders the TrxR1 to be dependent on the nucleophilicity of Sec to reduce substrates. Mutation of Sec to Cys which is less nucleophilic greatly compromises the enzyme activity. On the other hand, the absence of guiding bar in TrxR2 allows the substrates to be reduced by both C-terminal as well as N-terminal redox center as the C-terminal tail is flexible.

Thioredoxin glutathione reductase is 65 kDa subunit primarily expressed in male germ cells and catalyzes the disulfide bond formation during protein folding[27]. Beside spermatogenesis, TGR functions as a sole disulfide enzyme required for cell growth and immune response in the phylum Platyhelminthes where other isoforms of TrxR and GR are absent[28]. Structurally, TGR includes a glutaredoxin domain (Cys-X-X-Cys) at the N-terminus. The catalytic mechanism of TGR is similar to other isoforms. However, because of the presence of the glutaredoxin domain; it can reduce both thioredoxin as well as glutathione as the name (TGR) suggests. The reduction of glutathione is carried out by the glutaredoxin domain which in turn is reduced by C-terminal selenothiol.

The broad substrate range of mammalian TrxR has been attributed to the presence of the nucleophilic Sec. Also, the low pKa ~5.6 of Sec ensures that the Sec is

deprotonated under normal physiological conditions imparting activity when compared to the Cys counterpart. However, as a result of the nucleophilic character of the Sec, mammalian TrxR is susceptible to inactivation by irreversible alkylation with numerous electrophiles.

1.5 Role of TrxR in oxidative stress

Reactive oxygen species (ROS) such as peroxide, are produced by cells in response to external (phagocytes) as well as internal (NADPH oxidase) stimuli. Cells produce ROS which act to regulate signal transduction under normal conditions. However, excess production of ROS leaves the cells under oxidative stress and is potentially a threat to cell survival. Hence, ROS are tightly regulated by antioxidants/ROS scavengers including the Trx and glutathione (GSH) systems. Thioredoxin in particular provides reducing equivalents to peroxiredoxin (Prx) that transfers the electrons to reduce H_2O_2 and ROOH to H_2O/ROH[29]. Oxidation of methionine to methionine sulfoxide results in incorrect folding of protein such as E200K prion protein[30] associated with Creutzfeldt-Jakob disease, a neurodegenerative disease. Similarly, other diseases related to misfolded proteins include Alzheimer's, Huntington's and Parkinson's. The enzyme methionine sulfoxide reductase (Msr) corrects the misfolded protein through reduction of methionine sulfoxide in a stereospecific manner by receiving the reducing equivalent of electrons from Trx. The antioxidant property of the Trx system is shown in Figure 8.

Human primary cancerous cells, such as acute lymphoblastic leukemia[31], lung[32], cervix[33] and liver[34] are known to overexpress thioredoxin which helps these cells combat

ROS. The Trx system also regulates biological functions such as modulation of transcription factors, stimulation of cell growth and inhibition of apoptosis. Apoptosis signal-regulating kinase-1 (ASK-1) is arrested in its inactive form by reduced Trx by interacting with the N-terminal coiled domain of ASK-1[35-36]. Under oxidative stress induced by ROS and tumor necrosis factor (TNF-α), oxidation of Trx stimulates ASK-1 to signal apoptosis by activating the p53 and JNK MAPK pathway[37]. On the other hand, oxidative stress downregulates the expression of thioredoxin interacting protein (Txnip), which otherwise inhibits the activity of Trx and promotes cell growth and this promotes apoptosis in vascular endothelial cells[38] and cardiomyocytes[39]. Several studies have shown that Trx is translocated into the nucleus under oxidative conditions. The nuclear Trx activates nuclear factor κB (NF-κB) transcriptional activities that controls gene expression. In the cytoplasm, NF-κB exists as heterotrimeric complex with inhibitor I-κB. When I-κB dissociates under the influence of stimuli, the NF-κB migrates to the nucleus and promotes cancer growth[40]. Another transcription factor AP-1 (Activator protein 1), which regulates expression of genes involved in cell growth, is also indirectly activated by nuclear Trx via interaction with Ref-1[41] (redox factor 1), as shown in Figure 9.

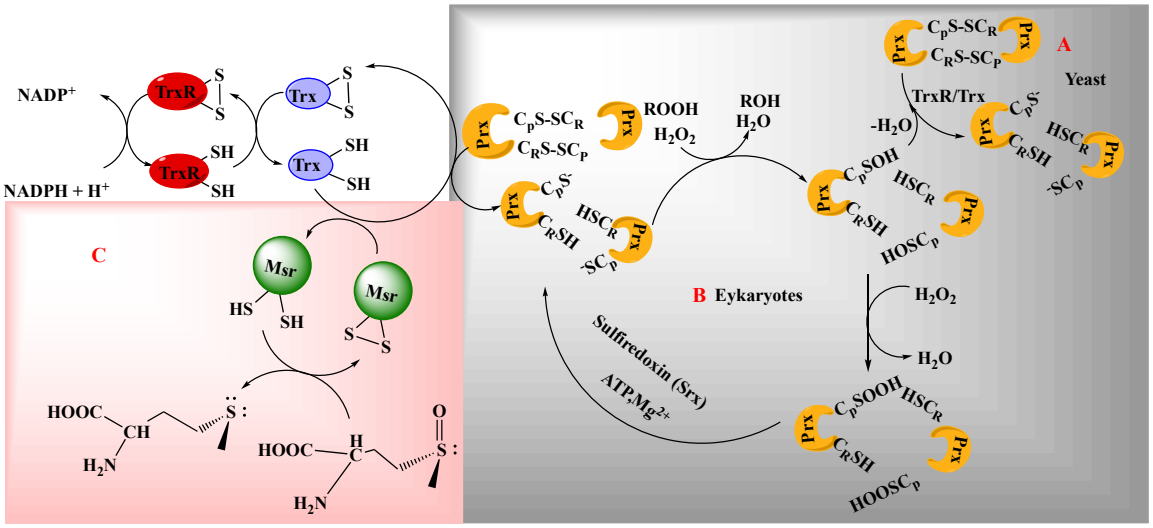

Figure 8. Antioxidant properties of thioredoxin reductase. (**A**) Peroxidredoxin (Prx) scavenges peroxides such as H_2O_2, lipid peroxides (ROOH) and preoxynitrite ($ONOO^-$). The C^{47} and C^{170} are highly conserved in Prx family and is the part of active catalysis. C^{47}-SH is prone to oxidation by peroxides to C^{47}-SOH so called peroxidatic C(C_p). The resolving C^{170} (C_R) forms disulfide linkage with C^{47}-S-S-C^{170} in yeast after oxidation. This disulfide bond is reduced by Trx which is reduced by TrxR in NADPH dependent reaction. (**B**) However, in eukaryotic Prx, cysteine sulfenic acid (C-SOH) is further oxidized into cysteine sulfinic acid (Cp-SOOH) which is then reduced by sulfiredoxin. (**C**) Catalytic mechanism of methionine sulfoxide reductases. The nucleophilic cysteine of Msr attacks the methionine sulfoxide to convert it to active methionine. The oxidized Msr reductase is then reduced by Trx system. Adapted from reference 29,30

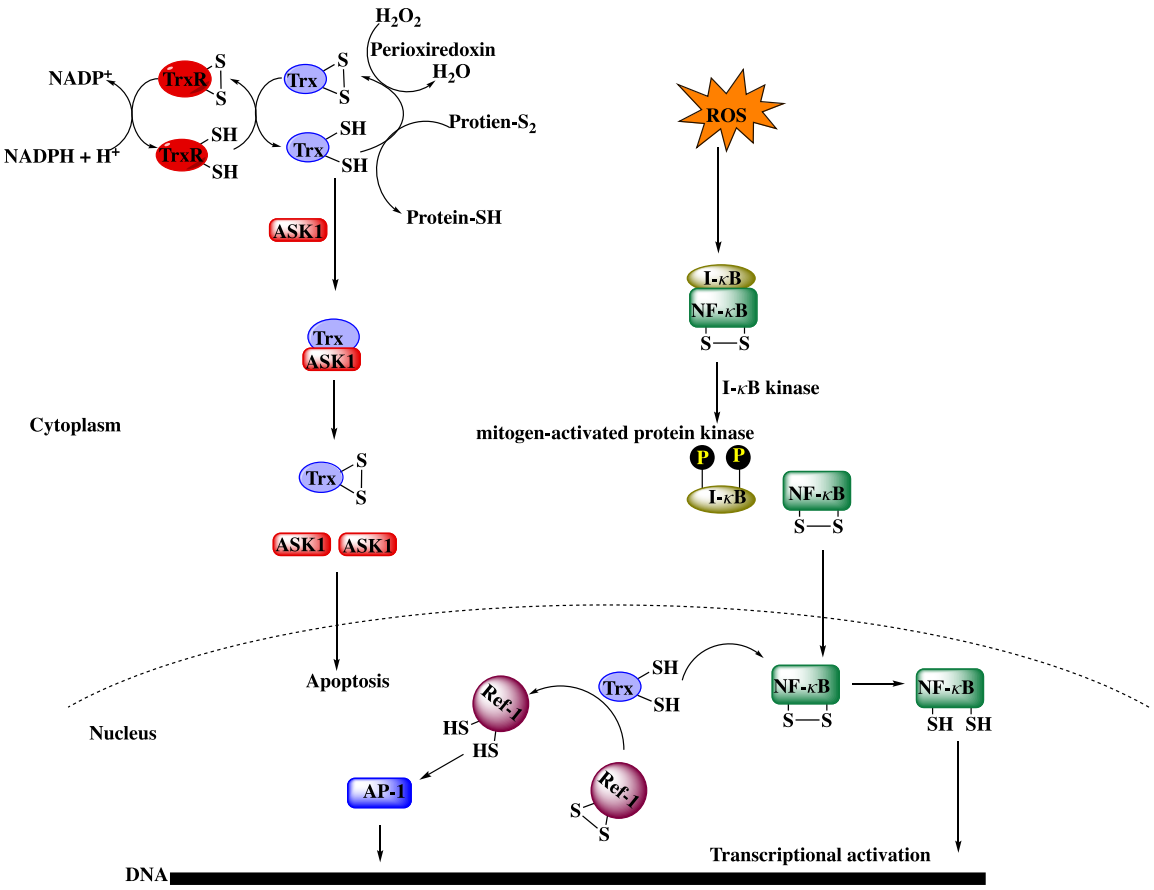

Figure 9. Redox signaling of transcription factor by thioredoxin system in cells. Trx negatively regulates apoptosis by arresting ASK-1 in an inactive form. The oxidation of Trx releases ASK-1 which induces apoptosis by activating p32 MAP kinase pathway. Under an oxidative stress Trx is translocated into nucleus where it reduces NF-κB and increases its DNA binding activity. Adapted from references 36,40

1.6 Thioredoxin system in reference to cancer

All aerobic organisms produce ROS, a necessary evil which exists in internal balance with antioxidants. External and internal stimuli, shown in Figure 10, perturb the internal balance and promote ROS generation. These ROS include hydroxyl anion (OH^-), superoxide anion ($O_2^{-\cdot}$), hydrogen peroxide (H_2O_2) and nitric oxide (NO), primarily produced by inhibition of TrxR, NADPH oxidase in mitochondria as the result of cellular respiration. Superoxide and H_2O_2 function as the mediators of nuclear transcription

factors such as NF-κB and activator protein-1. Hydrogen peroxide activates redox sensitive kinases such as protein kinase B, protein kinase C, mitogen activated protein kinase and is also required for insulin and growth factor-induced tyrosine kinase signaling. To maintain the cellular homeostasis, an organism develops internal defense systems of antioxidants which fight off excess ROS. Reactive oxygen species in general are produced by normal cells, for transduction of signal, to regulate transcriptional factor and to fight phagocytic invasion. However, production of excess ROS becomes harmful to cells and can lead to oxidative stress, ultimately leading to mutagenesis and apoptosis. Study of different cancer cells, viz. cervical[33], lung[42], hepatoma[43], squamous carcinoma cell[44], pancreatic cancer cells[45], all show elevated Trx-1. It is believed that the increased Trx activity helps cancer cells fight against ROS and decreases apoptosis. In order to fight cancer, the cellular defense mechanism continuously produces more antioxidants. The imbalance in ROS and antioxidants is the driving force for cancerous cells to thrive. The cells have two types of antioxidants: enzymes that the cells produce naturally and lower molecular weight antioxidants that can be externally supplemented. Both kinds of antioxidants act in a similar manner by scavenging ROS. The enzymes can continuously renew their redox property while lower molecular weight antioxidants need to be regulated via enzyme activity through redox reactions once the antioxidant is oxidized. Low molecular weight antioxidants such as vitamin C in human myeloid cells (HK-60)[46], tocopherol in brine shrimp[47,38], and the use of Trolox (6-hydroxy-2,5,7,8-tetramethylchroman-2-carboxylic acid) a water-soluble vitamin E analog in mouse thymocytes[48], have been reported to prevent oxidative stress induced apoptosis.

Inhibition of the thioredoxin system has proven to be a successful approach to control cancerous cell growth. Several thioredoxin system inhibiting drugs, such as cisplatin, auranofin and others, have been approved by the FDA for cancer treatment and more drugs are continuously discovered. Most of these cancer drugs affect the C-terminal moiety of thioredoxin reductase inhibiting the enzymatic property and producing the oxidative milieu in cancerous cells. The inhibition of C-terminal moiety increases the ROS in many cellular processes described above, ultimately leading to apoptosis of cancerous cells.

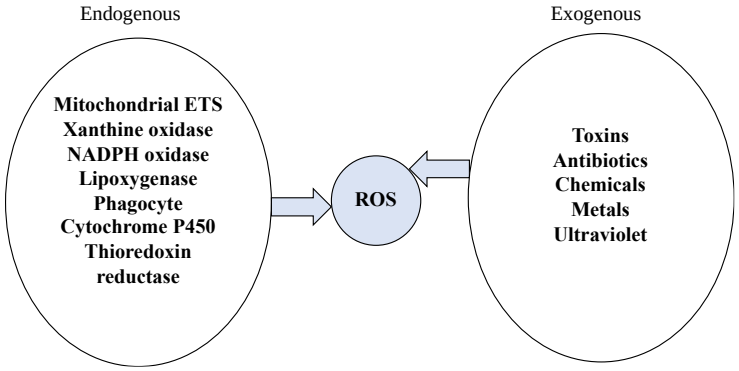

Figure 10. Sources of ROS

1.7 Mammalian thioredoxin reductase and inhibitors

The broad substrate tolerance of mammalian TrxR is believed to be due to the increased enzyme activity attributed to the presence of Sec. The reduced TrxR shuttles electrons through Trx to other substrates (Figure 11A). But mammalian TrxR alone can also reduce other substrates, as shown in Figure 11B. The activity of TrxR is inhibited by naturally occurring compounds curcumin (an important key constituent of turmeric and known to have antioxidant and anti-inflammatory property). In addition to organic inhibitors, some organometallic compounds also inhibit thioredoxin reductase. Known

TrxR inhibitors are listed in Table 4. Most of the known inhibitors interact with the C-terminal Sec, covalently modifying the enzyme. However, some of the metal-based compounds may interact with TrxR in different way. The crystal structure of TGR and auranofin reveals the gold atom coordinated between N-terminal Cys^{154} and Cys^{159}, Cys^{520} and Cys^{574} and NADPH binding pocket of *Schistosoma mansoni* TGR[49]. Cisplatin, a platinum compound, also interacts at the C-terminal Sec. At the same time, it is a DNA alkylator which interacts with nitrogen (N-7) of guanine base, unwinding the DNA helix through intra-strand crosslink[50], leading ultimately to apoptosis as a result of DNA damage. Another derivative of cisplatin, 5-Nitro-2-furancarbohydrazide derivatives interact with Sec through cisplatin and N-terminal Cys through the nitrofuran moiety[51].

The organic inhibitors on the other hand, activate the NADPH oxidase activity of TrxR by inhibiting the C-terminal redox center. In the absence of functional or intact C-terminal redox center, TrxR is converted to a pro-oxidant which causes the N-terminal redox center to oxidize NADPH to $NADP^+$ and produce superoxide anion, as shown in equation below.

$$NADPH + 2O_2 \xrightarrow{TrxR} H^+ + 2O_2^{\cdot -} + NADP^+$$

Such a pro-oxidant enzyme is also called SecTRAP (selenium compromised thioredoxin reductase-derived apoptotic protein)[52]. The ROS produced as a result inactivates redox regulating enzymes. Thus, the oxidized environment inside the cell becomes lethal. Because of their TrxR inhibiting properties some compounds such as cisplatin are approved for the treatment of testicular and ovarian cancers[53]. Many of these inhibitors are electrophiles and have α, β-unsaturated aldehyde or carbonyl group.

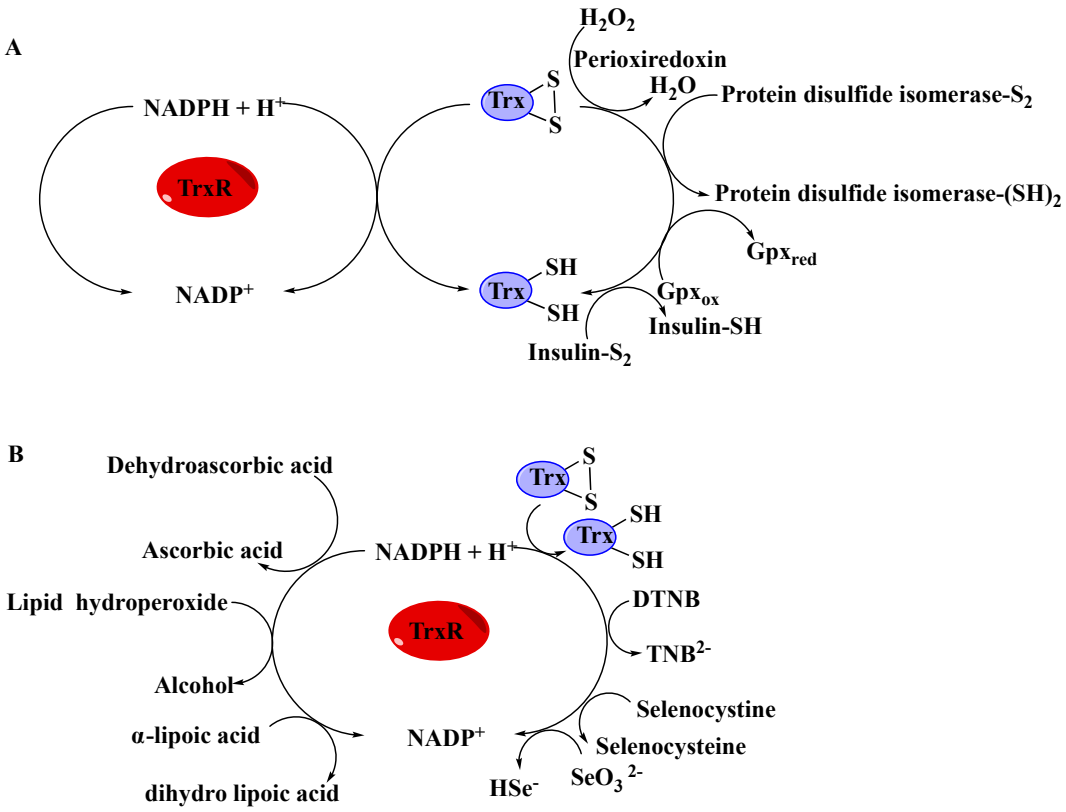

Figure 11. Substrates for mammalian TrxR. **(A)** Substrates reduced indirectly via Trx **(B)** Substrates reduced directly by TrxR.

Table 4. Table of TrxR inhibitors

Inhibitor type	Enzymes	IC_{50}	Site of reaction
Cisplatin Cisplatin derivative 5-Nitro-2-furancarbohydrazides	Human placental TrxR, induce NADPH oxidase, crosslink DNA, apoptosis	~25 μM[54] 16 μM[42]	C^{497} and U^{498} N-terminal C
Auranofin	*Schistosoma mansoni* TGR[49]		Between C^{154} and C^{159} Between C^{520} and C^{574} NADPH binding pocket
Arsenic trioxide[55]	Human TrxR1	0.25 μM	C^{497} and U^{498} possibly N-terminal
DNCB	Human TrxR1, induce NADPH oxidase		C^{497} and U^{498}
Juglone (5-Hydroxy-1,4-napthoquinone)	Inhibits TrxR, induce NADPH oxidase		
Curcumin[56]	Rat TrxR1, NADPH oxidase activity, generates superoxide anion	3.6 μM	C^{497} and U^{498}
Mansonone F	NADPH oxidase activity, generates superoxide anion	5.2 ± 0.6 [57]	
Mercuric chloride [58]	Inhibits TrxR	7.2 nM	

Chapter 2. Objectives and Rationale

2.1 Preliminary studies

Karenia brevis, a dinoflagellate responsible for Florida red tide occurs ubiquitously in the Gulf of Mexico. It is well known for the production of neurotoxins known as brevetoxins (PbTx). Brevetoxins (PbTxs) are polycyclic polyether ladders with 11 fused rings and have a molecular weight around 900 Da. Brevetoxin-3 and PbTx-2 are the most abundant of the brevetoxins with allylic alcohol and α, β- unsaturated aldehyde at K-ring side chains, respectively as shown in Figure 12.

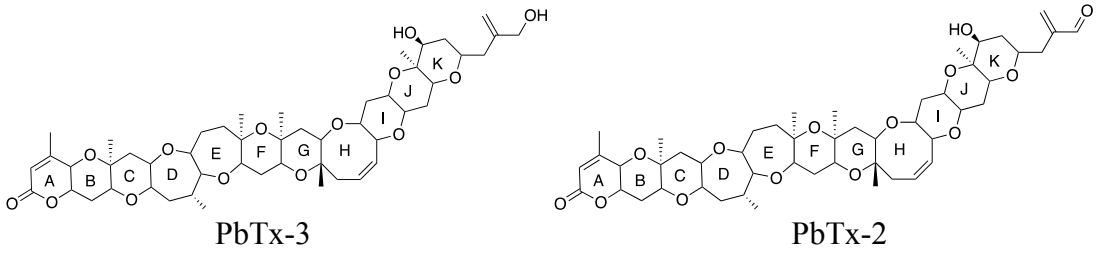

Figure 12. Structure of PbTx-3 and PbTx-2

PbTxs are neurotoxins that bind to site 5 of the voltage-gated sodium channel of excitable membranes resulting in sodium influx into the cell and membrane depolarization, thus affecting the central nervous system as well as skeletal muscle[59]. The influx of sodium is believed to be the mechanism of the neurotoxic effects. However, several studies have reported increases in indicators of oxidative stress in manatee[60] and loggerhead turtles[61] that have been exposed to brevetoxins. The increase in oxidative stress is the indicative of an alternate mechanism of toxicity, which may broaden the range of effects of PbTx. In *K. brevis* cells, PbTx is localized in the chloroplast and is associated with a protein, thioredoxin[62]. Studies with mammalian thioredoxin reductase

(TrxR1) show that PbTx-2 inhibits the reduction of Trx with an IC_{50} of 25 μM[63], as shown in Figure 13A. However, it activates the DTNB reduction (Figure 13B) in an unprecedented way.

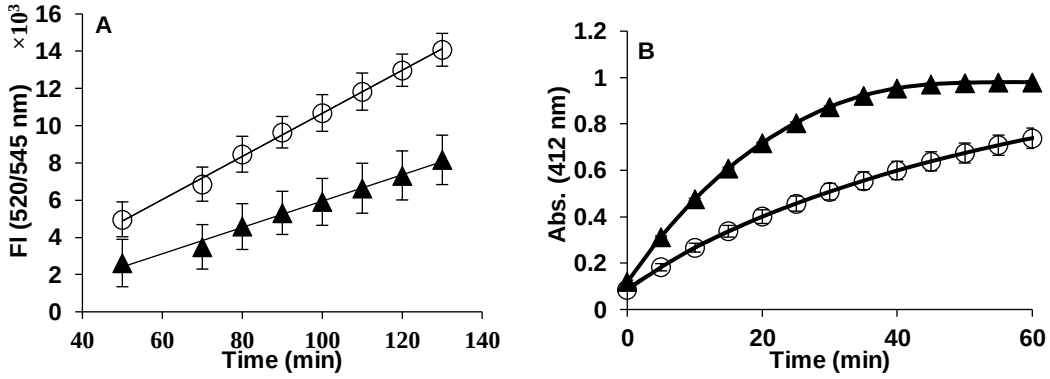

Figure 13. (**A**) TrxR1/Trx inhibition by PbTx-2 (20 μM, ▲); control (only DMSO, ○). (**B**) DTNB reduction by rat recombinant TrxR1(0.56 μM) in the presence of PbTx-2 (18 μM, ▲); control (only DMSO, ○). Adapted from reference 63

2.2 Rationale

The structure of many known inhibitors of TrxR have an α, β- unsaturated ketone/aldehyde functional group such as curcumin[56], juglone, PbTx-2[63], mitomycin C[64] and many more. In many cases, the inhibitors, such as curcumin and possibly PbTx-2, acts as a Michael acceptor to the selenol of Sec. However, PbTx-2 activates reduction of DTNB by TrxR1 and inhibit insulin reduction, which has not been previously observed. The dual effect was attributed to the combination of the α, β- unsaturated aldehyde functional group and the large size of the brevetoxin molecule which might act as a wedge preventing the modified C-terminal tail from entering the tetrapeptide pocket and preventing reduction of the C-terminal redox center while at the same time, exposing the N-terminal redox center. We reasoned that other molecules with similar properties might

behave in the same fashion. Several compounds were identified that fit the desired criteria: an α, β- unsaturated carbonyl functional group and Mr over 500 amu. These compounds belong to broad categories that include toxins such as brevetoxin-3 (PbTx-3), microcystin LR (MC-LR) and nodularin (Figure 14) as well as antibiotics such as geldanamycin (Ga), rifamycin SV (Rf) and thiostrepton (Th), as shown in Figure 15. These compounds have alternative targets in vivo; however, TrxR may also be a common target for all these test compounds.

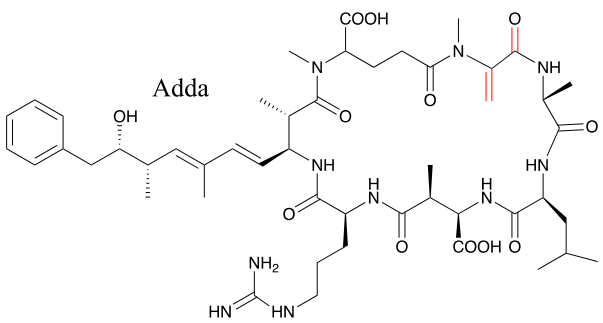

Microcystin-LR (MC-LR)

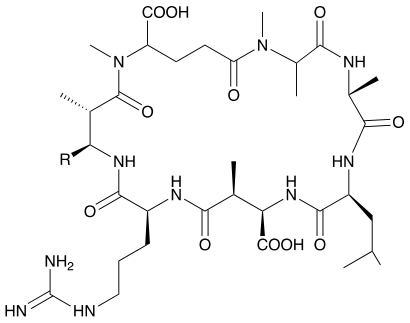

Reduced Microcystin-LR

(R = Adda group same as MC-LR)

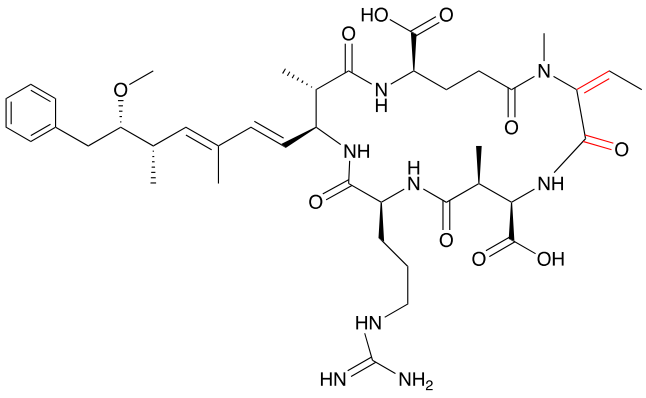

Nodularin

Figure 14. Test compounds (toxins) to be screened with TrxR. The bonds in red are α, β-unsaturated carbonyl moiety and shows the possible site of forming Michael adduct with Sec of TrxR

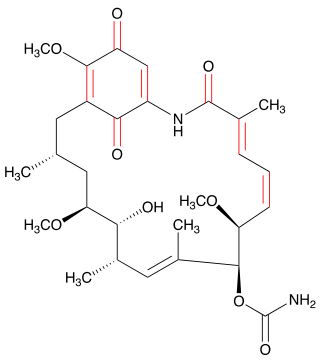

Geldanamycin

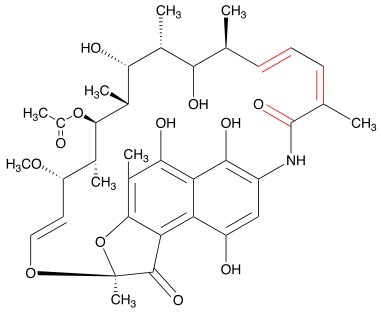

Rifamycin SV

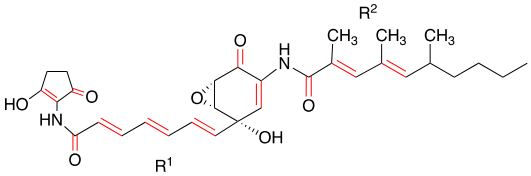

Manumycin A

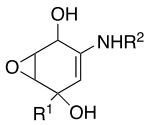

Dihydro-manumycin A

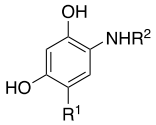

Deoxy-manumycin A

R^1 and R^2 are same as manumycin A

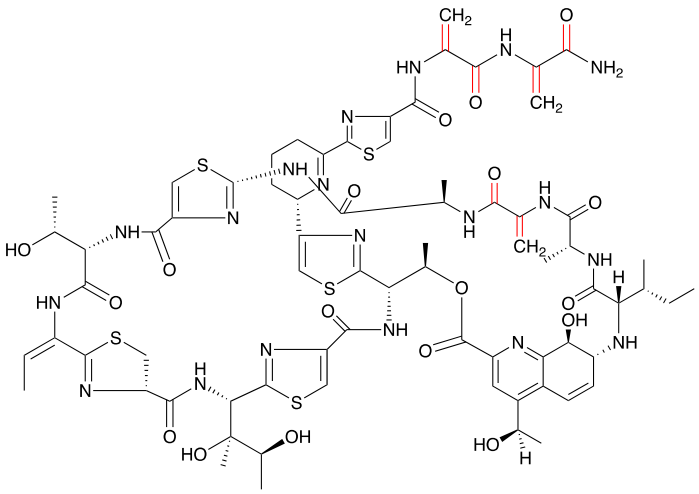

Thiostrepton

Figure 15. Test compounds (antibiotics) to be screened with TrxR. The bonds in red are α,β-unsaturated carbonyl moiety and shows the possible site of forming Michael adduct with Sec of TrxR

2.3 Research objectives

1. The first objective of this research is to determine if molecules which are similar in size and functionality to PbTx-2 will have the same dual effect on TrxR as does PbTx-2. These compounds will be screened for the effect on DTNB, insulin and selenocystine reduction by cytosolic TrxR1, mitochondrial (mTrxR2) and (*Drosophila melanogaster*) DmTrxR. All three enzymes have similar mechanism of action to reduce their substrates but varies in homology.
2. The second objective of this work shall focus on understanding the mechanism of inhibition/activation induced by these test compounds by employing site specific mutants of mTrxR2 and DmTrxR.
3. The third objective is to evaluate the necessity of the functional group α, β-unsaturated carbonyl for inhibition of TrxR by considering specifically the above mentioned test compounds that have this functional group.
4. Inhibition of TrxR is known to produce NADPH oxidase activity and increase the ROS. The current research will also study if TrxR inhibition by these test compounds is the source of ROS in vitro as well as in vivo using cellular model such as human lymphoblast cell particularly with PbTx-2.

2.4 DTNB reduction by TrxR1 in the presence of α, β-unsaturated carbonyl compounds

Ellman's reagent (5,5'-dithiobis-(2-nitrobenzoic acid)) or DTNB, contains a disulfide bond that is susceptible to attack by a nucleophile such as thiol or selenol with the release of yellow colored 2-nitro-5-thiobenzoate (TNB^{2-})[65]. The reaction occurs in a stoichiometric ratio, as shown in Figure 16.

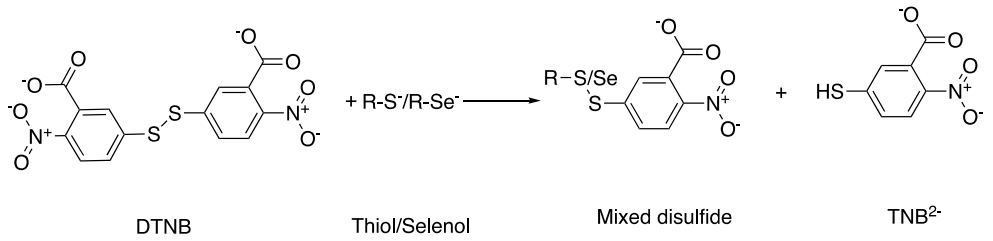

Figure 16. Stoichiometric reaction of DTNB and nucleophile

Small molecule substrates, such as DTNB[66] and juglone[67], are known to be reduced by both N-as well as C-terminal redox active site. The reduction of DTNB by TrxR1 in the presence of the above mentioned test compounds resulted in activation at various degree except for Man-A, as shown in Figure 17. Such activation might be the result of a conformational change that results from the interaction with the C-terminal Sec by an electrophile[25]. Table 5 represents the relative rate of activation experienced by individual test compounds as compared to the control. The enzyme activity of the control is 634 ± 47.2 NADPH mol/min-mol enzyme.

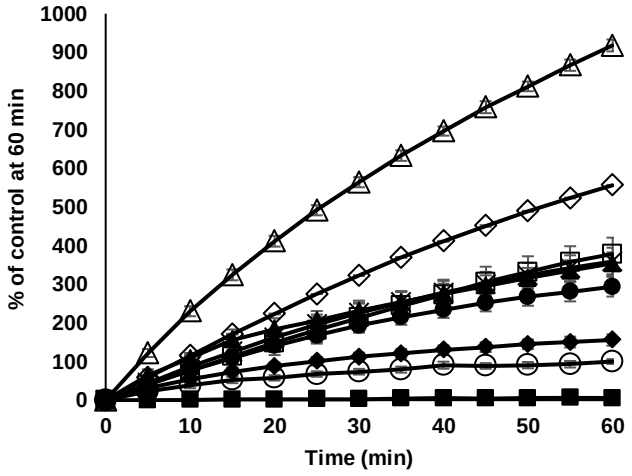

Figure 17. Reduction of DTNB (2 mM) by TrxR1 (5.12 nM) in the presence of test compounds (20 µM). PbTx-3 (△); MC-LR (◇); Th (□); Ga (×); PbTx-2(▲); Rf (●); Nodularin (◆); Man-A (■) and Control (○)

Table 5. Relative rate of test compounds (20 μM) as compared to wild type TrxR1(5.12 nM) in DTNB reduction (2 mM)

Compounds	Relative rate
PbTx-3	6.04**
PbTx-2	2.60**
MC-LR	3.32**
Dihydro MC-LR	3.55**
Nodularin	1.47**
Ga	2.67**
Rf	2.33**
Th	2.35**
Man-A	0.05**
Dihydroman-A	0.91
Deoxyman-A	0.10**

2.5 Enzymes to be used in this study

The enzymes used in this research are listed in Table 6. Two isoforms of human TrxR: cytoplasmic and mitochondrial, and a TrxR that belong to a different class, insecta (DmTrxR) were used. Although they are all homodimers with similar mechanism of action, each enzyme has different roles and different substrate specificity. All of these enzymes utilize a C-terminal Sec for reducing substrates. The C-terminal Sec site is also susceptible to inhibition by many electrophiles. Substitution of the C-terminal Sec by less nucleophilic Cys or rendering the C-terminal unfunctional can reveal the in-depth mechanism of interaction of the test compounds with TrxR. The dead tail mutant of mTrxR and DmTrxR rely solely on their N-terminal redox centers to reduce their substrates and could reveal valuable information of where the test compounds are

interacting. In addition to the truncated version, the dead tail mutant does not have the active C-terminal redox center. In the absence of the C-terminal tail, the test compounds could react with exposed N-terminal thiol and shut down the truncated enzyme completely. On the other hand, the dead tail enzyme which has a non-functional tail may prevent the test compound from interacting with the N-terminal redox center. By the use of different class and mutants the complete picture of mechanism of action between test compounds and TrxR could be elucidated. Furthermore, these enzymes will illustrate the role and necessity of C-terminal Sec in TrxR and α, β-unsaturated functional moiety in test compounds for the activation that is observed in DTNB reduction.

Table 6. List of enzymes screened for DTNB reduction with α, β-unsaturated carbonyl compounds

Enzymes	**C-terminal redox center**
TrxR1 (GCUG)	GCUG
mTrxR2 (GCUG)	GCUG
mTrxR2 (GCCG)	GCCG
mTrxR2 (GSSG)	Dead tail mutant (GSSG)
mTrxR2 (Δ8)	8 amino acid truncated enzyme at C-terminal
DmTrxR (SCCS)	SCCS
DmTrxR (SCUG)	SCUG
DmTrxR (Δ8)	8 amino acid truncated enzyme at C-terminal

2.6 Conclusion

All of the test compounds activate the DTNB reduction of TrxR1, except for Man-A. Man-A shows a characteristic behavior of typical inhibitor by preventing reduction of DTNB, which suggest a possible reaction at C-terminal redox center. As the redox center is modulated by the test compounds that activate DTNB reduction, it could be concluded that these test compounds interact with the C-terminal tail in some novel manner not observed until now. This will be the subject of studies reported herein.

Chapter 3. Manumycin-A, a potent inhibitor of mammalian thioredoxin reductase-1 and activator of thioredoxin reductase-2

3.1 Objective

A literature search of compounds which are similar in size and functionality to brevetoxin, included the farnesyl transferase inhibitor manumycin-A (Man-A). Man-A has numerous electrophilic sites that might contribute to the formation of a Michael adduct with the Sec residue of TrxR or alkylation via the epoxide. Initial screening in a DTNB reduction assay indicated that Man-A is indeed a TrxR inhibitor. The objective of the work presented in this chapter is to understand the mechanism of inhibition of TrxR1 by Man-A. This shall be accomplished by using enzyme assays that are dependent upon TrxR and Trx and a selenol specific probe. Both cytosolic TrxR1 and mitochondrial TrxR2 (mTrxR) as well as TrxR2 mutants that have point mutations in the C-terminal redox center shall be evaluated. The reactive site at Man-A will also be determined using derivatives of Man-A, dihdyro-manumycin A and deoxy-manumycin A.

3.2. Introduction

Man-A (Figure 18) is a bacterial secondary metabolite that was first isolated from *Streptomyces parvulus* as a result of a random screening program for farnesyl transferase (FTase) inhibitors[68]. FTase catalyzes the post-translational farnesylation of proteins including the Ras family of proteins. FTase links the farnesyl isoprenyl moiety to the carboxy terminal of Ras. The farnesylation of Ras allows its mobilization to lipid rich cell membrane by increasing the hydrophobicity. Ras is a guanosine nucleotide binding protein. When localized to the cell membrane, the Ras bound GDP (Guanosine

diphosphate) is phosphorylated to GTP (Guanosine triphosphate), activating Ras and initiating the cascade of phosphorylation that triggers Ras-MAPK (mitogen-activated protein kinases) signaling. Ras proteins regulate numerous functions, which are related to cell growth, proliferation and cell signaling. They function by binding to and activating several effector proteins which regulate critical cellular processes including transcription, translation, cell-cycle progression and calcium signaling[69]. FTase inhibitors block farnesylation such that Ras remains in the cytosol and does not stimulate its downstream targets. Ras is the most frequently mutated oncogene in human cancers with as many as 25% of known human tumors having mutated Ras[70]. FTase inhibitors have been discovered and developed for the treatment of cancers[71-72] as well as progeria[73] and parasitic infections[74-77]. Man-A inhibits rat brain FTase with a K_i of 1.2 μM[68] and has shown antitumor activity in a variety of cancer cell types[78-79] and tumor models[80-81].

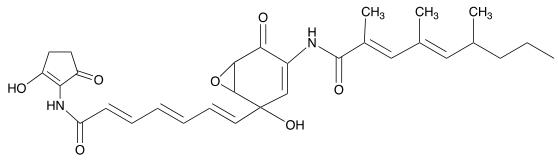

Figure 18. Manumycin A

The tumoricidal activity of manumycin was initially attributed to the inhibition of FTase preventing activation of Ras. However, it soon became apparent that the cytotoxicity of Man-A included pathways which were independent of Ras. Numerous studies report the induction of reactive oxygen species (ROS) or more specifically, superoxide radical anion ($O_2^{-\cdot}$) in Man-A treated cells and tumors[82-91].

The thioredoxin system is a major regulatory system for the maintenance of redox homeostasis of the cell. The reduced TrxR reduces Trx which then reduces other proteins. But the reduced TrxR is susceptible to attack by electrophiles. The electrophilic sites of Man-A, as shown in Figure 19, include the central epoxide and the cyclohexeneone, the cyclopenteneone and the two polyunsaturated carbonyls of the side chains. These functional groups could react with the nucleophilic Sec of TrxR.

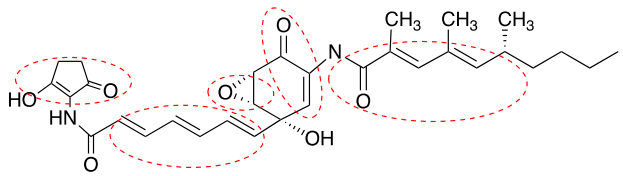

Figure 19. Electrophilic sites present in Man-A

3.3. Results and Discussion

3.3.1 DTNB as a substrate for TrxR1 and mTrxR WT and mutants

The cytosolic TrxR1 and mitochondrial TrxR2 enzymes studied in this chapter are presented in Table 7.

Table 7. Enzymes used in screening Man-A

Enzymes (C-terminal sequence)	Type
TrxR1 (GCUG)	Cytosolic recombinant rat wild type
mTrxR2 (GCUG)	Wild type (WT)
mTrxR2 (GCCG)	Cysteine mutant
mTrxR2 (GSSG)	Serine mutant “dead tail”
mTrxR2 (Δ8)	Truncated mutant

The DTNB reduction by TrxR1 after incubation with 5 μM Man-A for 60 min showed complete inhibition (Figure 20A) as a typical inhibitor such as auranofin or curcumin but unlike PbTx-2. The inhibition of TrxR1 by Man-A appeared to be time dependent. When reduced TrxR1 was pre-incubated with Man-A the initial rate (V_0) of DTNB reduction was reduced to 25.4% of the control. On the other hand, when Man-A was not pre-incubated with TrxR1, V_0 was 49.1% of the control (Figure 20B). The initial rates are calculated based on the polynomial regression of the trend line.

Dose response curves for the inhibition of DTNB reduction by Man-A confirmed that TrxR1 inhibition by Man-A is indeed time dependent. When pre-incubated for 60 minutes the IC_{50} was 272 (±29) nM whereas the IC_{50} increased to 1586 (±128) nM without pre-incubation. At higher concentration (5 μM), both the pre-incubated and not pre-incubated samples have the same inhibition (Figure 21A). These data indicate that the inhibition of Man-A by TrxR1 is time dependent at lower concentrations. For the concentration of 1 μM, the reaction was completed within 10 minutes. (Figure 21B).

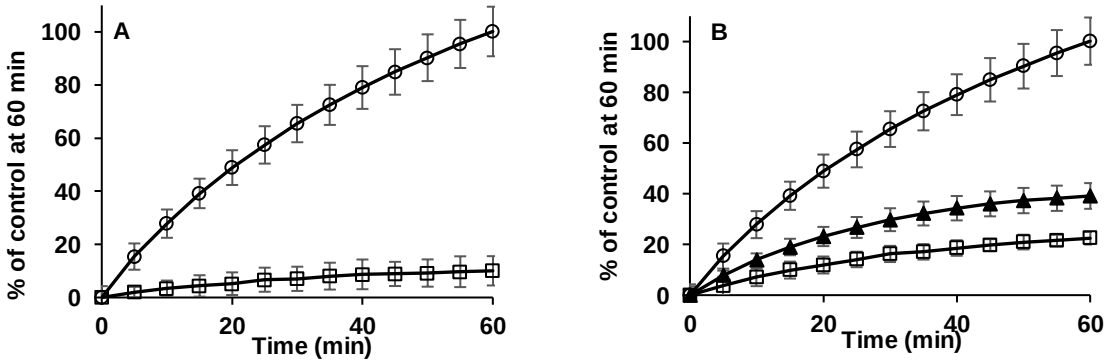

Figure 20. Reduction of DTNB by TrxR1 in the presence of Man-A (**A**) Inhibition of DTNB (2 mM) reduction by TrxR1 (5.6 nM) after sixty minutes incubation with Man-A (5 μM, □); Control (DMSO only, ○). (**B**) Effect of pre-incubation of Man-A with reduced TrxR1 (5.6 nM) on DTNB reduction. Reduced TrxR1 pre-incubated (□) and not pre-incubated (▲) with Man-A (1800 nM)

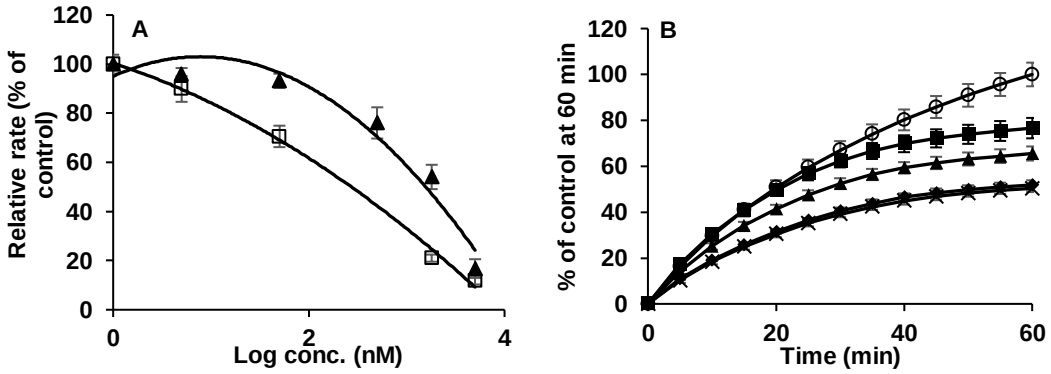

Figure 21. (**A**) Inhibition of DTNB (2 mM) reduction by TrxR1 (5.6 nM) in the presence of Man-A (0-5000 nM). Sixty minutes pre-incubation with Man-A (□). No pre-incubation (▲). Results are expressed as initial rates relative to control (no Man-A). (**B**) Time course of inhibition of DTNB reduction by TrxR1 (5.6 nM) in the presence of Man-A (1μM). Control (DMSO only, ○) Incubation times 15 min (×); 10 min (◆); 5 min (▲); 2 min (■) after Man-A addition

Man-A appears to be a typical inhibitor of TrxR1, inhibiting DTNB reduction. On the other hand, the effect of Man-A on mTrxR2 was quite different. Man-A activates the DTNB reduction by mTrxR2 enzymes (Figure 22) to different degrees. In this way, Man-A behaves towards mTrxR2 in the same way that PbTx-2 behaves towards TrxR1. The mTrxR2 (GCCG) mutant is capable of using the C-terminal redox center to reduce its substrates. Indeed, numerous isoforms of TrxR function effectively with a C-terminal GCCG. However, both the mTrxR2 (GSSG) and the mTrxR2 (Δ8) depend solely on the N-terminal redox center for DTNB reduction. It is noteworthy that the highest level of activation, 4.9-fold when compared to the mTrxR2 (GSSG) control, is observed in the dead tail mutant with. The truncated mutant in which the N-terminal redox center is already exposed showed the smaller activation of 2.5-fold compared to control. These data, taken together suggest that Man-A binds to mTrxR2 at or near the C-terminal tail, preventing the tail from tucking into the tetrapeptide pocket and exposing the N-terminal redox center. The truncated mutant already has the N-terminal redox center exposed and

therefore experiences the smallest activation among the mTrxR2 mutants. The WT and cysteine mutant of mTrxR experienced 1.5 and 4.5-fold activation respectively when compared to their controls, as shown in Table 8.

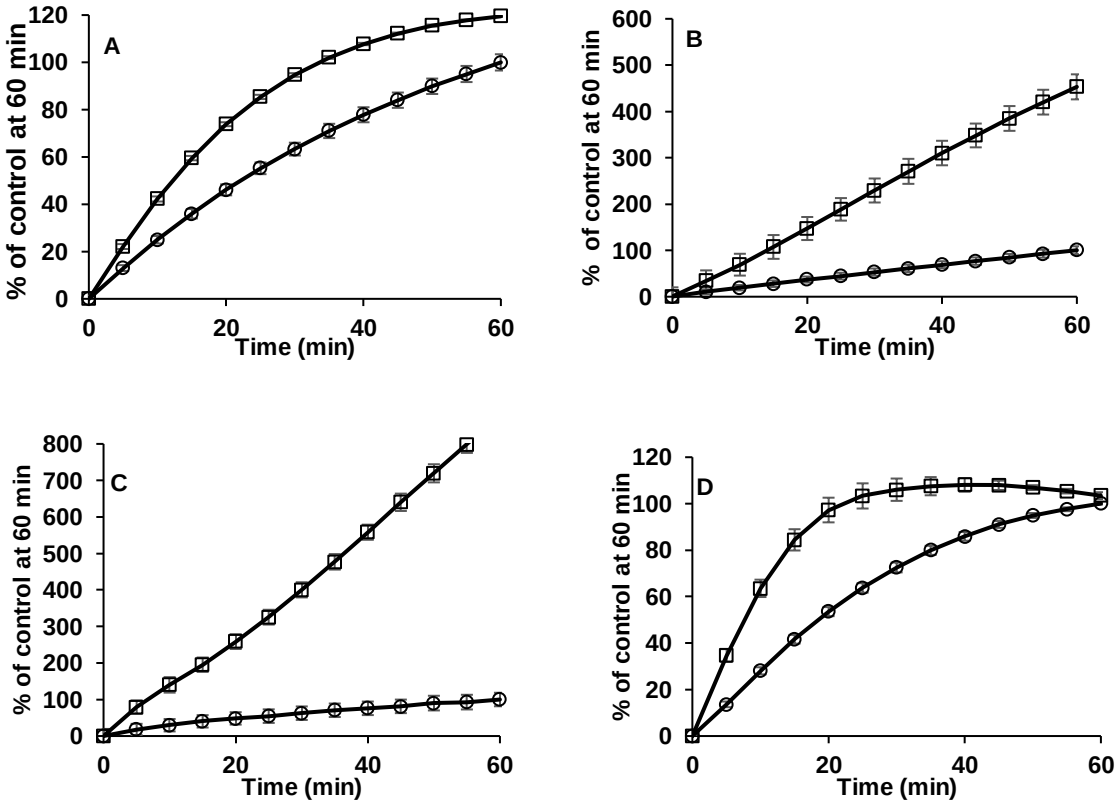

Figure 22. Reduction of DTNB (2 mM) by mTrxR (5.12 nM) in the presence of Man-A. (**A**) mTrxR2 (GCUG) (WT) (**B**) mTrxR2 (GCCG); C. mTrxR2 (GSSG) and D. mTrxR2 (Δ8). Control (DMSO only, ○); Man-A (6 μM, □)

Table 8. Relative rate of DTNB reduction by mTrxR2 in the presence of Man-A (6 μM) as compared to their respective control. The consumption of DTNB was calculated from standard curve of TNB^{2-}

mTrxR2 enzyme	Relative rate
mTrxR2 (CGUG)	1.56**
mTrxR2 (GCCG)	4.54**
mTrxR2 (GSSG)	4.85**
mTrxR2 (Δ8)	2.45**

The number of asterisks indicate significant differences compared with control (** p <0.01)

3.3.2 Irreversible inhibition of TrxR1 by Man-A

In an effort to determine if the inhibition of TrxR1 by Man-A is reversible, the DTNB reduction assay was performed as before however, after 1 hour incubation of pre-reduced TrxR1 with 2.45 μM Man-A, the mixture was passed through a gel filtration column (MW cutoff of 6000 amu) followed by a 30 min incubation with additional NADPH. Gel filtration should remove all unbound Man-A from the solution and the subsequent 30 min incubation should allow for reestablishing equilibrium. As shown in Figure 23, this treatment still resulted in complete inhibition of TrxR1 demonstrating that the inhibition of TrxR1 by Man-A is irreversible. It is particularly important to note that Man-A has no effect on the rate of DTNB reduction when incubated with TrxR1 which has not been reduced with NADPH. When oxidized TrxR1 is incubated with Man-A for 30 min, followed by gel filtration to remove Man-A, TrxR1 activity is restored completely upon reduction with NADPH. This observation demonstrates that either the N-terminal or C-terminal redox centers, or both must be reduced for Man-A to have an effect on TrxR1. Furthermore, it suggests that one or both are sites of reactivity with Man-A.

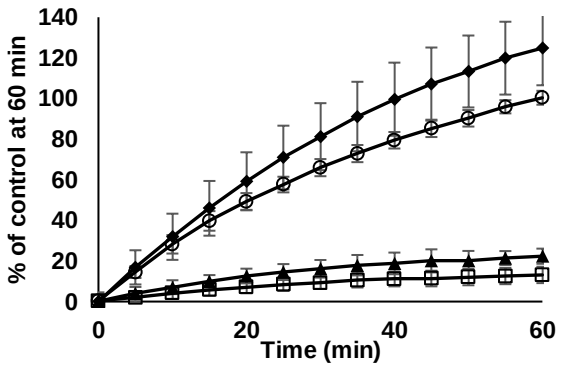

Figure 23. Test of irreversibility of inhibition of DTNB reduction by TrxR1 (5.2 nM) in the presence of Man-A (2 μM). TrxR1 reduced only after removal of Man-A by gel filtration (◆); Control (no Man-A, ○); Man-A not subjected to gel filtration (▲); Man-A removed by gel filtration after incubation with reduced TrxR1 (□)

On the other hand, when the mTrxR enzymes were treated with Man-A in an identical manner, the enzymes were no longer activated after passing through a size exclusion gel. This suggests that the Man-A can be removed and that the interaction between Man-A and the mTrxR enzymes is non-covalent or is at least reversible as shown in Figure 24.

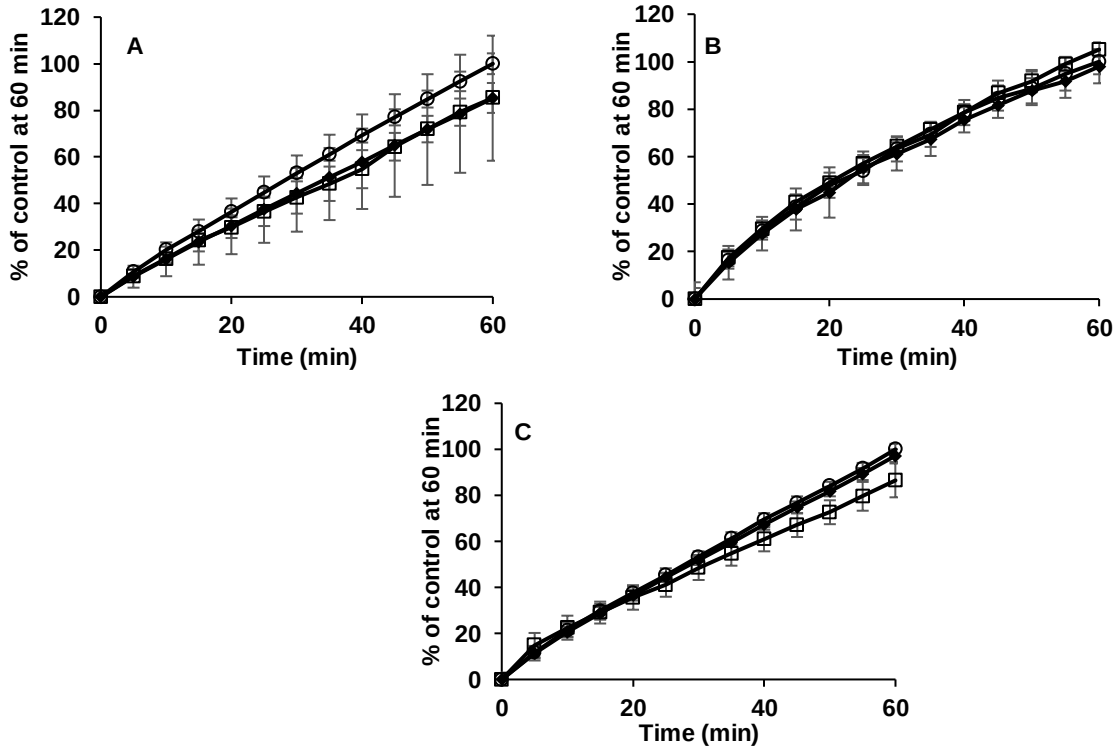

Figure 24. Test of irreversibility of inhibition of DTNB (2 mM) reduction by (**A**) mTrxR2 (CGUG) (**B**) mTrxR2 (GCCG) (**C**) mTrxR2 (GSSG) (5.2 nM) in the presence of Man-A (4.2 µM). mTrxR reduced only after removal of Man-A by gel filtration (◆); Control (no Man-A, ○); Man-A removed by gel filtration after incubation with reduced TrxR1 (□)

3.3.3 TrxR/Trx insulin reduction in the presence of Man-A

The effect of Man-A on the thioredoxin system was examined using an assay which is based on the reduction of eosin modified insulin by Trx[92]. In this two-enzyme assay, oxidized Trx is continuously reduced by TrxR1 with reducing equivalents ultimately provided by NADPH. The fluorescent signal is only possible when insulin is reduced by Trx. This means the electron flow should follow the sequence a shown in Figure 25. When the electron flow is disrupted by inhibition of TrxR1, the insulin reduction is prevented and as a result no fluorescence is observed. The dose response curve for Man-A and TrxR1 shown in Figure 26 indicates that Man-A inhibits insulin reduction by TrxR1 with an IC_{50} of 572 (± 88) nM.

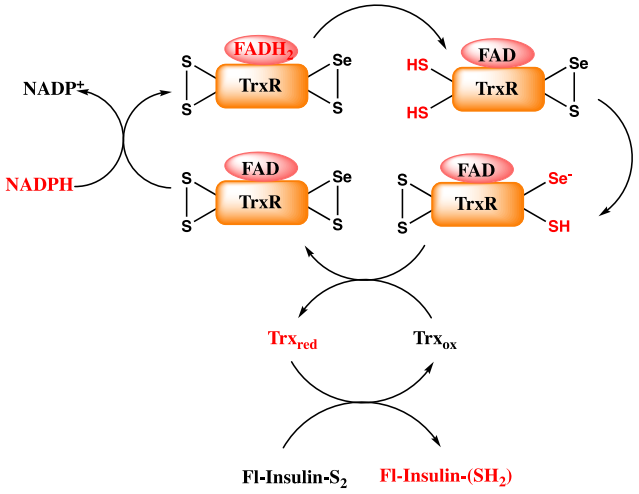

Figure 25. TrxR/Trx insulin reduction

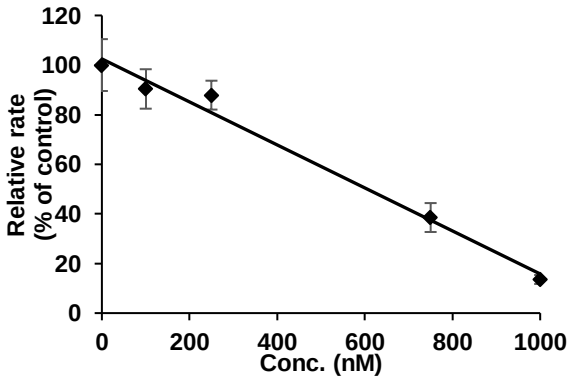

Figure 26. Dose-response curve with increasing concentration of Man-A (0-1000 nM) TrxR1/Trx insulin reduction assay. Results expressed as percent inhibition by Man-A vs. concentration

Man-A inhibits both insulin reduction and DTNB reduction by TrxR1 but activates DTNB reduction and inhibits insulin reduction by mTrxR2 enzymes in a similar manner to PbTx-2 with TrxR1[63] (Figure 27). This inhibition observed in insulin reduction suggests Man-A interferes at the C-terminal tail so as to prevent the electron flow towards thioredoxin. Both insulin reduction and gel filtration experiment suggest that Man-A forms a covalent adduct with TrxR1 and either a reversible covalent or a non-covalent adduct with mTrxR2 (GCUG).

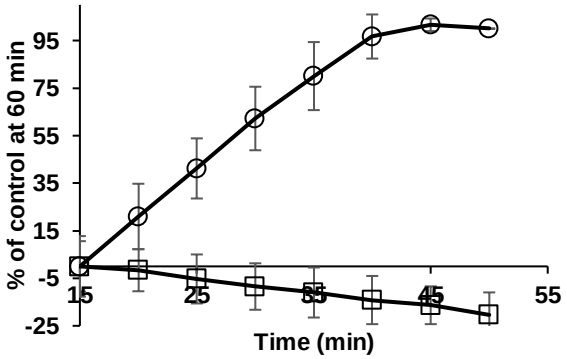

Figure 27. Inhibition of insulin reduction by mTrxR2 (CGUG) (200 nM) in the presence of Man-A (10 μM, □); Control (no Man-A, ○)

3.3.4. Reactivity of Man-A with seleno-*L*-cysteine and reduced TrxR1

Numerous electrophiles inhibit mammalian TrxR by alkylating the C-terminal Sec. These electrophiles are mainly α, β-unsaturated carbonyl compounds that irreversibly react with TrxR. Inspection of the Man-A structure reveals numerous potential sites of reactivity. In addition to the epoxide, any of the four mono- or poly unsaturated carbonyl groups of Man-A may alkylate the Sec of TrxR. The selenol selective probe Sel-green was used to evaluate the reactivity of Man-A with Sec. The strongly nucleophilic, reduced selenol undergoes nucleophilic aromatic substitution with the probe, which then releases the fluorophore as shown in Figure 28. When Sec is alkylated it will not react with the probe and fluorescence will be suppressed. Figure 29A demonstrates that the release of fluorescent reporter by Sec is inhibited in the presence of Man-A indicating that Man-A reacts with Sec. A similar experiment with TrxR1 was performed to evaluate the reactivity of Man-A as presented in the Figure 29B. Man-A treated TrxR1 resulted in 15 % inhibition.

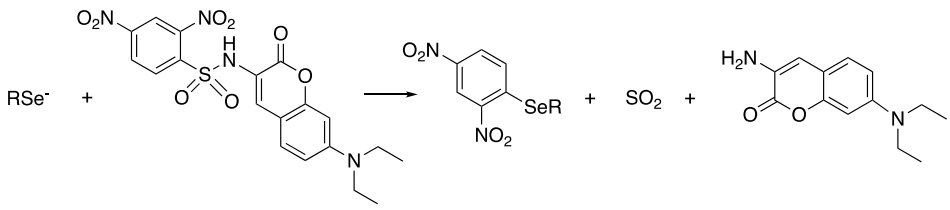

Figure 28. Reaction of Sel-green probe. Adapted from reference 93

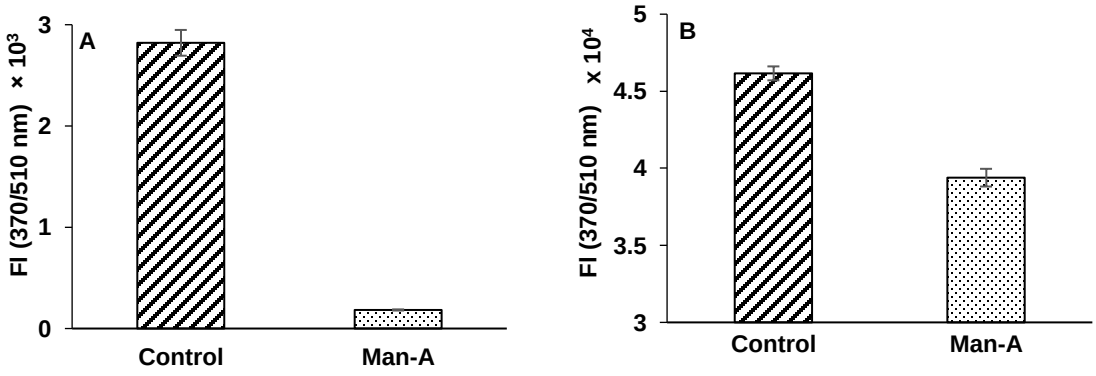

Figure 29. (**A**) Reaction of reduced selno-*L*-cysteine (20 μM) with Sel-green probe (20 μM) in the presence of Man-A (20 μM). (**B**) Reaction of TrxR1 (4.2 μM) with Sel-green probe (48 μM) in the presence of Man-A (20 μM). Data represented at 60 min

3.3.5. Determining the reactive site of Man-A

Many electrophilic sites in Man-A are susceptible to nucleophilic attack by Sec. Identification of electrophilic site responsible for TrxR1 inhibition was evaluated with two derivatives of Man-A; deoxy-manumycin A, which lacks both the epoxide and the cyclohexenone and dihydro-manumycin A which lacks the cyclohexenone (Figure 30). The selenol selective probe Sel-green[93] was used to evaluate the reactivity of Man-A derivatives with Sec. Under the same conditions used for Man-A, deoxy-Man A reduced the fluorescence by 24.6% compared to control and dihydro-Man A showed no reduction of fluorescence, indicating that Man-A reacts readily with Sec while its derivatives do not

as shown in Figure 31. This suggests the possible reactive site at Man-A is the cyclohexanone moiety.

Figure 30. Structure of Man-A derivatives. (**A**) Deoxy-manumycin-A. (**B**) Dihydro-manumycin-A. R1 and R2 are identical to Man-A

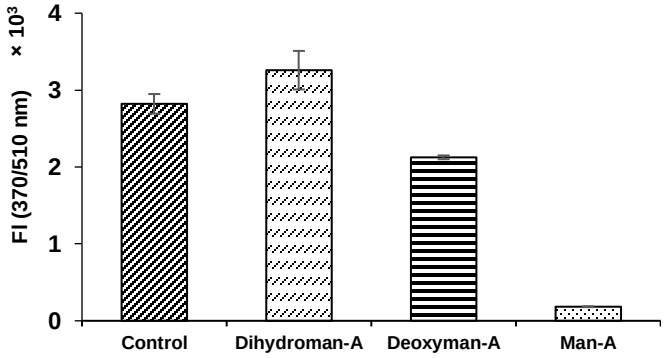

Figure 31. Reaction of reduced seleno-*L*-cysteine (20 μM) with Sel-green probe (20 μM) in the presence of Man-A and derivatives (20 μM). Data represented at 60 min

3.3.6. TrxR1/Trx insulin reduction in the presence of Man-A derivatives

Neither deoxy-Man-A nor dihydro-Man-A inhibits insulin reduction by the TrxR1/Trx system at concentrations of 20 μM as shown in Figure 32. This result is consistent with the reactivity of Man-A and its derivatives with Sec. While Man-A has several electrophilic sites, the site of reactivity with TrxR1 must be the α, β-unsaturated ketone. Even though deoxy-manumycin A showed some reactivity with Sec, it did not inhibit insulin reduction. This could possibly be due to steric hindrance due to large size of TrxR1 as compared to Sec.

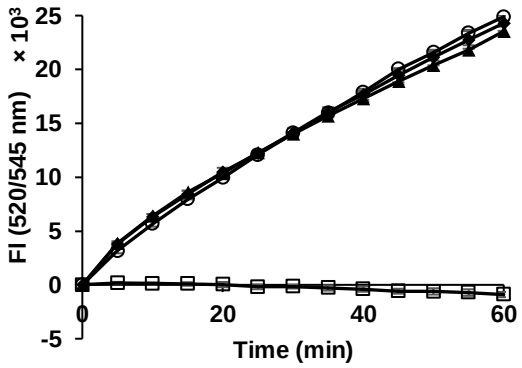

Figure 32. Insulin reduction by TrxR1/Trx in the presence of 20 μM each of deoxy-man-A (▲); dihydro-man-A (◆); Man-A (□); Control (DMSO only, ○)

3.3.7. NADPH oxidase activity of TrxR in the presence of Man-A

The chemical modification of the C-terminal Sec of TrxR1 yields a SecTRAP (selenium compromised thioredoxin reductase-derived apoptotic proteins)[52], promoting both apoptosis and necrosis via oxidative stress and increased intracellular reactive oxygen species (ROS) production. Both curcumin and juglone modified TrxR1 have demonstrated strongly induced NADPH oxidase activity, producing $O_2^{-\bullet}$ in the presence of oxygen via the N-terminal (Cys^{59}/Cys^{64}) redox center[67, 94-95]. In addition to increased ROS, Man-A treated cells have shown NADPH oxidase activity[88], decreased TrxR1 activity[85] and decreased Trx expression[87]. One reason for activation of NADPH oxidase activity may be due to the alkylation of TrxR1, producing a SecTRAP. Transfection of cells with SOD and TrxR cDNA or pre-treatment with ROS scavengers has been shown to block the adverse effects of Man-A[96]. The NADPH consumption by TrxR1 in the absence of a disulfide substrate was examined (Figure 33A). When pre-incubated with 62.5 μM Man-A, the consumption of NADPH by TrxR1 is increased 5-fold relative to the control.

Superoxide can reduce cytochrome c, and in the presence of Man-A treated TrxR1, it was monitored over time with and without the addition of SOD (Figure 33B). If superoxide is produced by Man-A treated TrxR1, then the addition of SOD should inhibit cytochrome c reduction. This was indeed the case. The rate of cytochrome c reduction was decreased to control level in the presence of SOD when compared to the Man-A treated sample alone.

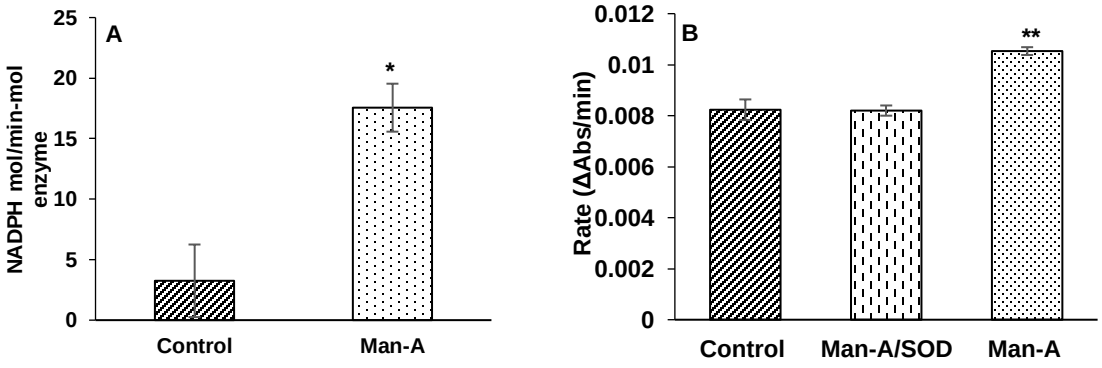

Figure 33. (**A**) NADPH consumption by TrxR1 (0.2 μM) induced by Man-A (62.5 μM). (**B)** Reduction of cytochrome c (100 μM) by $O_2^{-\bullet}$ generated by TrxR1 (100 nM) in the presence of Man-A (62.5 μM); Man-A and SOD (62.5 μM and 6 unit/well); control (DMSO only). The number of asterisks indicate significant differences compared with control (p <0.05)

As shown in Figure 34, Man-A also induces NADPH oxidation in mTrxR and mTrxR mutants to varying degrees. When compared to control, Man-A increased NADPH consumption by mTrxR2 (GCUG) by 4.4-fold, the cysteine mutant by 3.4-fold, the dead tail mutant by 14-fold and the truncated mTrxR2 by 4.4-fold (SeeTable 9).

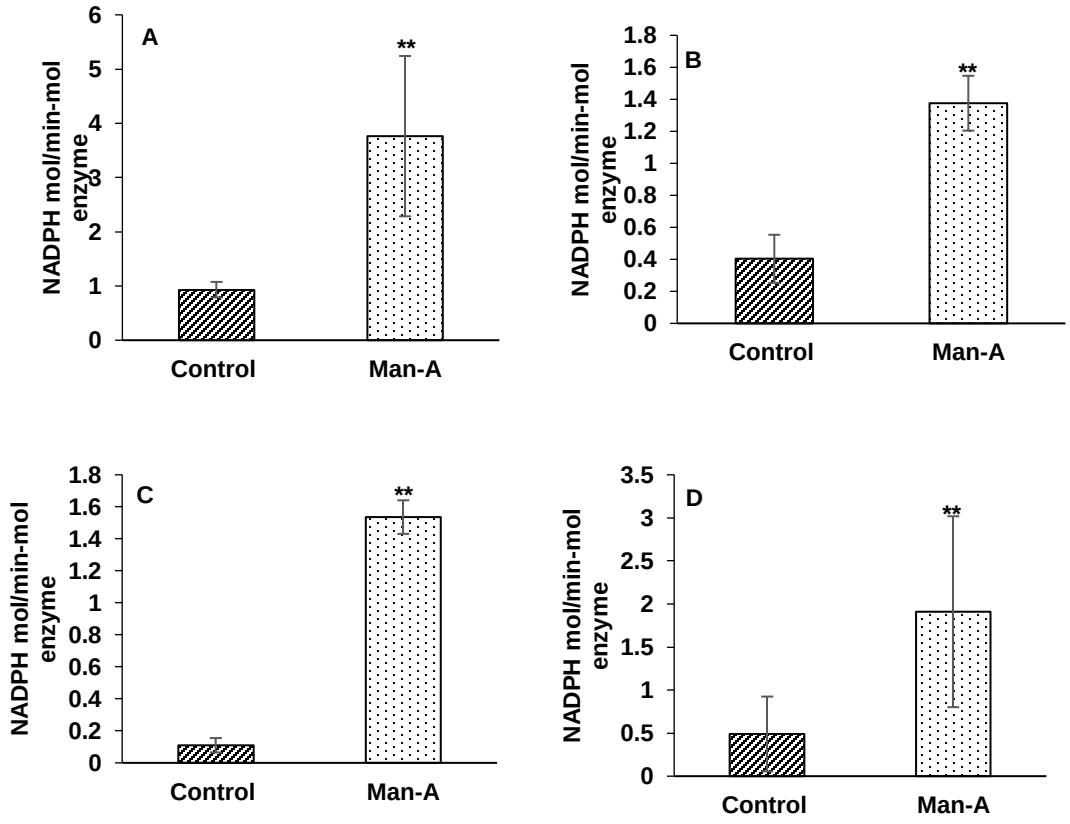

Figure 34. NADPH oxidase activity of mTrxR (0.2 μM) induced by Man-A (38.5 μM). (**A**) mTrxR2 (GCUG); (**B**) mTrxR2 (GCCG); (**C**) mTrxR2 (GSSG); (**D**) mTrxR2 (Δ8). The data is represented as NADPH consumption by mTrxR variants in the presence of Man-A. The number of asterisks indicate significant differences compared with control (* p <0.05, ** p <0.01)

Table 9. NADPH consumption by TrxR in the presence of Man-A. NADPH consumed expressed as NADPH mol/min-mol enzyme

	TrxR1	**mTrxR2 (GCUG)**	**mTrxR2 (GCCG)**	**mTrxR2 (GSSG)**	**mTrxR2 (Δ8)**
Control	3.25 ± 2.99	0.93 ± 0.14	0.40 ± 0.15	0.11 ± 0.04	0.49 ± 0.43
Man-A	17.6 ± 1.98*	3.76 ± 1.48**	1.38 ± 0.17**	1.53 ±0.10**	1.9 ± 1.10**

The number of asterisks indicate significant differences compared with control (* p <0.05, ** p <0.01)

3.3.8 Reactivity of TrxR1 and mTrxR variants with substrate selenocystine in the presence of Man-A

Reduction of selenocystine is believed to require a functional C-terminal redox center with either Cys or Sec, but both are not required. However, the rate is much faster when Sec is present[25]. The diselenide bond undergoes nucleophilic attack by the C-terminal reduced Cys/Sec forming the new diselenide or selenosulfide bond with the substrate selenocystine. This diselenide or selenosulfide bond is then reduced by an N-terminal thiol as shown in Figure 35. This mechanism further illustrates the inability of the dead tail (GSSG) and truncated (Δ8) mutants to reduce selenocystine. The rate of selenocystine reduction is measured by monitoring the consumption of NADPH. Comparison of Figure 36A and Figure 36B indicates that in the presence of Sec, NADPH consumption is significantly faster and can be attributed to the presence of selenocystine as a substrate. Given that Man-A react with TrxR1 in a time dependent manner, in the absence of pre-incubation, Man-A induced 1.3-fold enhancement with TrxR1 and 2.5-fold ehhancement as compared to mTrxR2 (CGUG) control. This also points out to the fact that initially Man-A reacts with Cys in a reversible manner and later forms a covalent adduct with Sec of TrxR1.The rate of NADPH consumption for the mTrxR2 (GCCG) mutant is very slow when compared to the mTrxR2 (CGUG) (Figure 36C and Table 10). This demonstrates the importance of Sec in selenocystine reduction. In the presence of Man-A (38.5 μM), the rate of selenocystine reduction for mTrxR2 (GCCG) is comparable to that of the control.

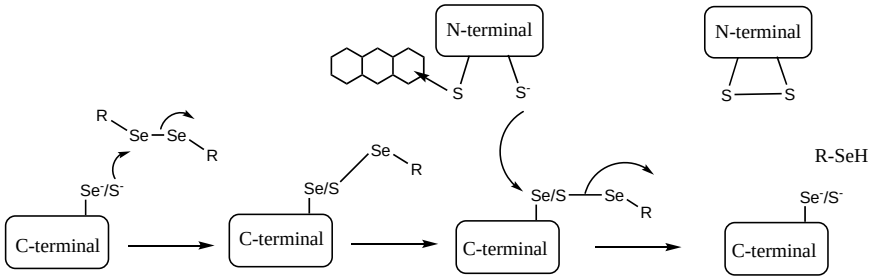

Figure 35. Mechanism of reduction of selenocystine by mammalian TrxR. Adapted from reference 25

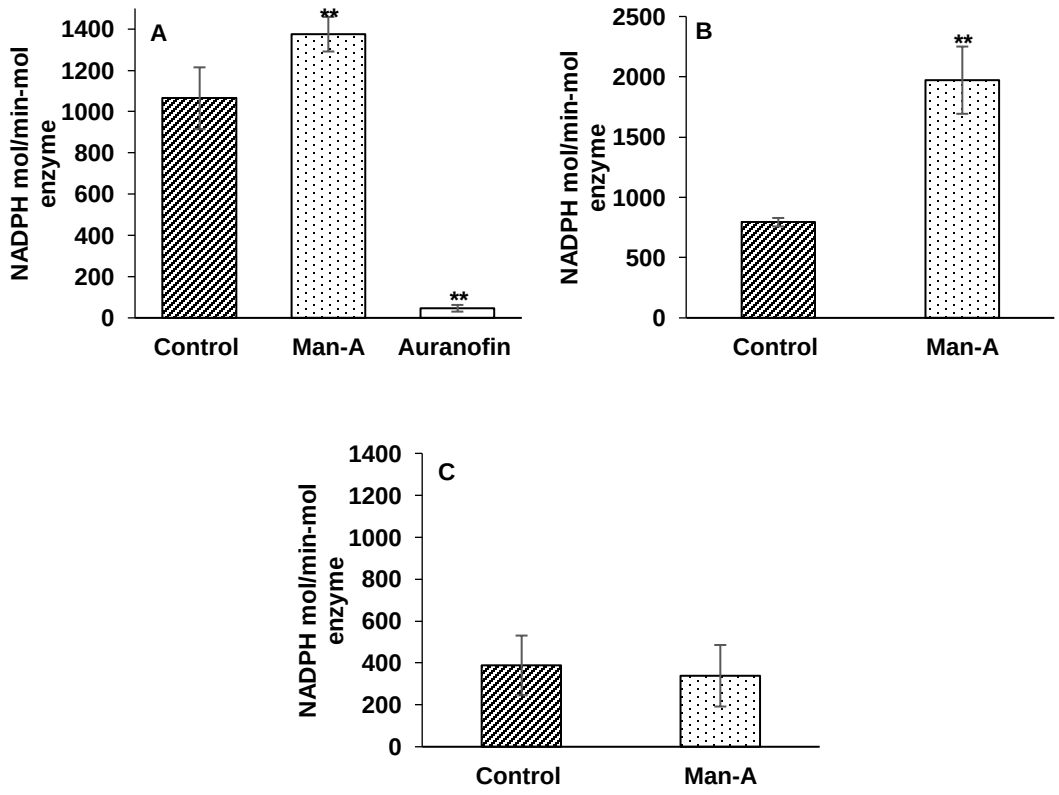

Figure 36. Selenocystine reduction by TrxR (20 nM) in the presence of Man-A (38.5 μM) without incubation. (**A**) TrxR1; (**B**) mTrxR2 (CGUG); (**C**) mTrxR2 (GCCG). The data is expressed as NADPH consumption. The number of asterisks indicate significant differences compared with control (* p <0.05, ** p <0.01)

Table 10. Rate of selenocystine reduction by TrxR in the presence of Man-A without incubation. Data expressed as NADPH mol/min-mol enzyme

	TrxR1	**mTrxR2 (GCUG)**	**mTrxR (GCCG)**
Control	1065 ± 150	794 ± 35.1	388 ± 142
Man-A	1375 ± 84.0**	1972 ± 278**	338 ± 147

The number of asterisks indicate significant differences compared with control (* p <0.05, ** p <0.01)

However, after 15 minutes incubation of Man-A with reduced TrxR prior to addition of selenocystine resulted in complete inhibition as comparable to auranofin with TrxR1. Considering the fact the reaction of Man-A with TrxR1 is time dependent (at least 10 minutes), as shown in Figure 21B, 15 minutes incubation of Man-1 with TrxR1 ensures an equilibrium time required for alkylation at Sec thus inhibiting selenocystine reduction (Figure 37A and Table 11). The cysteine mutant, mTrxR2 (GCCG) when incubated with Man-A inhibited the reduction of selenocystine reduction, as shown in Figure 37B and Table 11. However, Man-A reacts with mTrx2 (GCUG) by activating the reduction of selenocystine by 1.6-fold suggesting the C-terminal Sec is free.

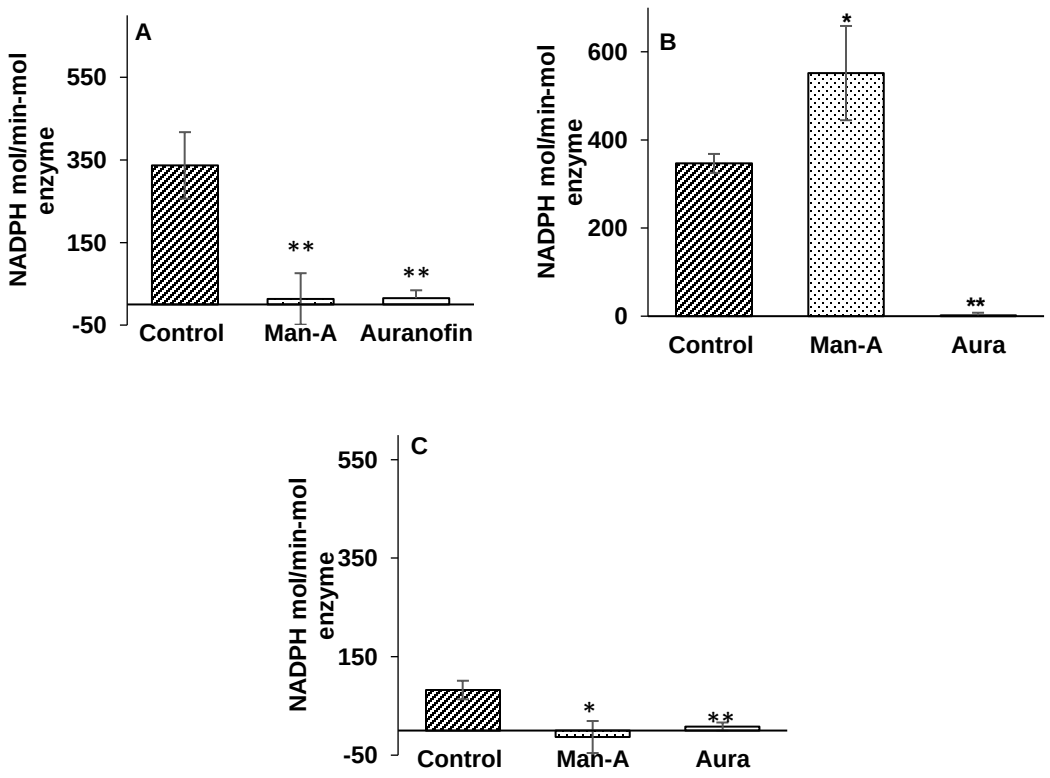

Figure 37. Selenocystine reduction by TrxR (20 nM) after 15 minutes incubation with Man-A (38.5 μM). The substrate was added after incubation of 15 minutes. (**A**) TrxR1; (**B**) mTrxR2 (CGUG); (**C**) mTrxR2 (GCCG). The data is expressed as NADPH consumption during reduction of selenocystine. The number of asterisks indicate significant differences compared with control (* p <0.05, ** p <0.01)

Table 11. Rate of selnocystine reduction by TrxR after 15 minutes ncubation with Man-A. Data expressed as NADPH mol/min-mol enzyme

	TrxR1	**mTrxR2 (GCUG)**	**mTrxR (GCCG)**
Control	337 ± 80.5	347 ± 21.5	82.2 ± 18.8
Man-A	13.3 ± 62.4**	552 ± 107*	-13.2 ± 32.5*
Auranofin	15.2 ± 19.0**	1.67 ± 6.14**	8.00 ±8.35**

The number of asterisks indicate significant differences compared with control (* p <0.05, ** p <0.01)

3.3.9 Reactivity of TrxR1 and mTrxR2 (GCUG) with substrate hydrogen peroxide in the presence of Man-A

Reduction of hydrogen peroxide requires C-terminal Sec as the Cys mutant[97-98] is unable to do so. The nucleophilic Sec is oxidized to selenic acid (-SeOH) by H_2O_2 which in turn is reduced by adjacent Cys[497]. In the presence of Man-A, as shown in Figure 38 and Table 11, the reduction of H_2O_2 is inhibited 12-fold by TrxR1 and 1.5-fold by mTrxR2 (GCUG) as compared to its respective controls. The inhibition also emphasizes the interaction of Man-A initailly with Cys[497] which would prevent reduction of oxidized Sec.

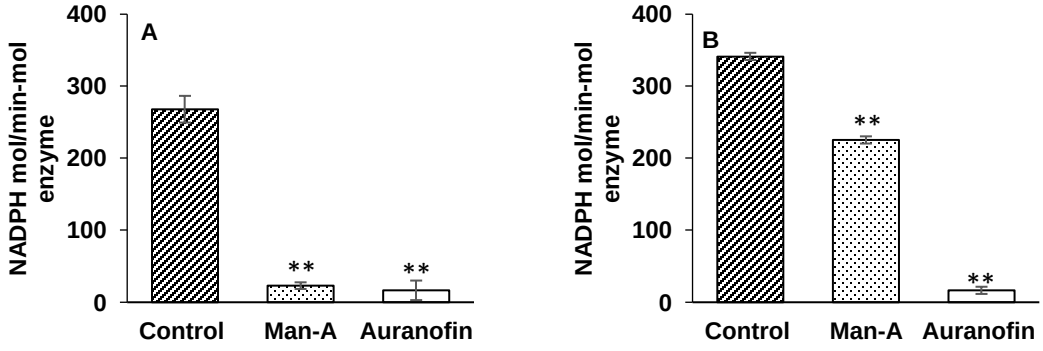

Figure 38. Hydrogen peroxide reduction by TrxR (50 nM) in the presence of Man-A (38.5 μM) and auranofin (38.5 μM). (**A**) TrxR1; (**B**) mTrxR2 (CGUG). The data is expressed as NADPH consumption during reduction of H_2O_2 (50 mM). The number of asterisks indicate significant differences compared with control (* p <0.05, ** p <0.01)

Table 12. Rate of H_2O_2 reduction by TrxR in the presence of Man-A and auranofin. Data expressed as NADPH mol/min-mol enzyme

	TrxR1	**mTrxR2 (GCUG)**
Control	268±18.5	341 ±8.20
Man-A	23.0±4.62**	225 ± 17.6**
Auranofin	16.6±13.6**	16.6 ±5.71**

The number of asterisks indicate significant differences compared with control (* p <0.05, ** p <0.01)

When incubated for 15 minutes with reduced TrxR, Man-A completely inhibited reduction of H_2O_2 (14-fold) as comparable to auranofin. While pre-incubation results in only partial inhibition (1.3-fold) with mTrxR2 (GCUG), as shown in Figure 39 and Table 13. These results also corroborate that Man-A initially interacts with Cys^{497} of TrxR1. The inhibition of H_2O_2 reduction by mTrxR2 (GCUG) in the presence of Man-A (1.3-fold) could be due to the non-covalent interaction with mTrxR2 (GCUG).

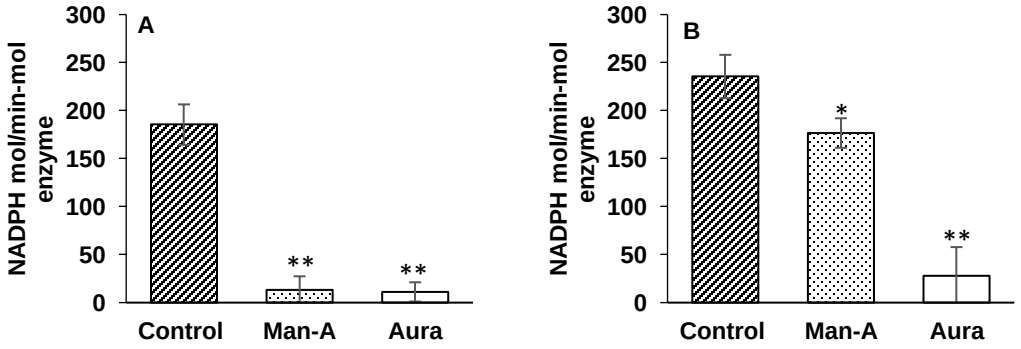

Figure 39. Hydrogen peroxide reduction by TrxR (50 nM) after 15 minutes incubation with Man-A (38.5 μM) and auranofin (38.5 μM). (**A**) TrxR1; (**B**) mTrxR2 (CGUG). The data is expressed as NADPH mol/min-mol enzyme during reduction of H_2O_2 (50 mM). The number of asterisks indicate significant differences compared with control (* p <0.05, ** p <0.01)

Table 13. Rate of H_2O_2 reduction by TrxR after 15 minutes incubation with Man-A and auranofin. Data expressed as NADPH mol/min-mol enzyme

	TrxR1	**mTrxR2 (GCUG)**
Control	185 ±21.0	235 ± 22.6
Man-A	13.3 ± 14.1**	177 ± 15.4*
Auranofin	11.1 ±10.0**	27.9 ± 29.9**

The number of asterisks indicate significant differences compared with control (* p <0.05, ** p <0.01)

3.3.10 Reactivity of Man-A in cell homogenate

Man-A has many electrophilic sites that can be the targets of numerous nucleophiles in vivo and prevent it from reacting with TrxR. In order to determine if Man-A could inhibit TrxR under physiological conditions, TrxR1 activity of human lymphoblast (GM02152) cell lysate in the presence of Man-A (1 μM) was analyzed using the insulin reduction assay. The ratio of initial rates of insulin reduction for control:Man-A treated sample is 2.3:1. There appears to be a longer induction time in the Man-A treated sample as shown in Figure 40A. However, the manufacturer of the assay kit recommends comparing rates between 15 and 45 minutes. Here the relative rates for control: Man-A treated sample is 1.2:1. This induction time may be due to the presence of numerous endogenous nucleophiles which may be susceptible to react with Man-A. Comparing the percent of TrxR1 inhibition at sixty minutes, the Man-A treated cell homogenate show only 26 % inhibition as compared to control (DMSO) treated cells as shown in Figure 40B.

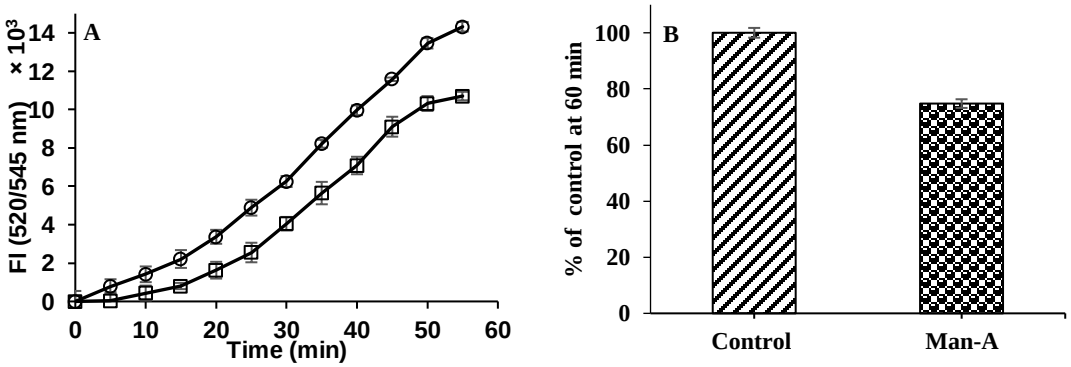

Figure 40. (**A**)TrxR1/Trx insulin reduction assay with cell homogenate (GM02152, 15.6 μg of protein) in the presence of Man-A (1 μM). (**B**) Data in A represented as bar graph. Man-A (□); Control (DMSO only, ○)

3.4 Conclusion

The summary of all the enzymatic assays in the presence of Man-A are given in Table 14. Man-A acts as a typical irreversible inhibitor of human TrxR1, inhibiting both DTNB and Trx reduction. The low IC_{50} of 272 nM for DTNB reduction in the presence of Man-A suggest that it is a potent inhibitor of TrxR1.

Table 14. Summary of TrxR activity in the presence of Man-A

Enzymes	**TrxR1**	**mTrxR2 (GCUG)**	**mTrxR2 (GCCG)**	**mTrxR2 (GSSG)**	**mTrxR2 (Δ8)**
DTNB reduction	Inhibit	Activate	Activate	Activate	Activate
Insulin reduction	Inhibit	Inhibit	-	-	-
DTNB reduction after size exclusion	Inhibit	No activation	No activation	No activation	-
NADPH oxidase	Activate	Activate	Activate	Activate	Activate
Selenocystine reduction	Activate	Activate	Activate	-	-
Selenocystine reduction (15 minutes incubation)	Inhibit	Activate	Inhibit	-	-
H_2O_2 reduction	Inhibit	Inhibit	-	-	-
H_2O_2 reduction (15 minutes incubation)	Inhibit	Inhibit	-	-	-

On the other hand, Man-A behaves in an unprecedented way, similar to PbTx-2 with WT and mutants of mTrxR2 by activating DTNB and inhibiting insulin reduction. Insulin reduction requires a functional C-terminal tail and the substitution of C-terminal

redox center Cys/Sec with Ser, truncation or alkylation should result in inhibition in insulin reduction as shown in Figure 41.

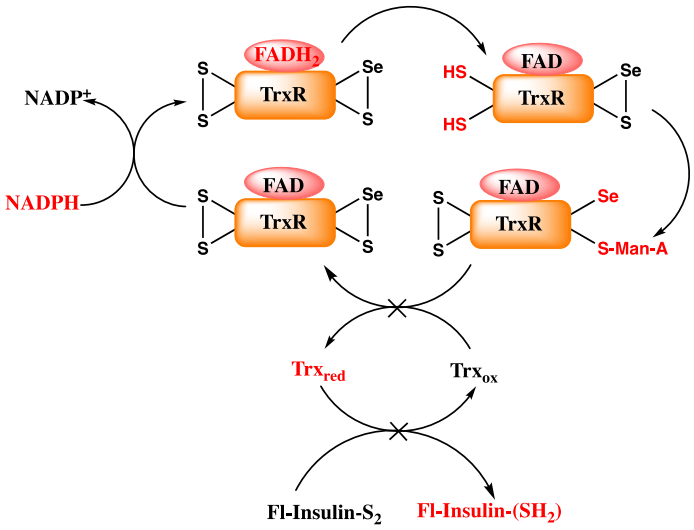

Figure 41. TrxR/Trx inhibition mechanism and in the presence of Man-A

Man-A forms an irreversible adduct with TrxR1 as Man-A incubated TrxR1 completely inhibited DTNB reduction even after passage through a size exclusion gel. In contrast to TrxR1, Man-A failed to activate DTNB reduction after passage through a size exclusion gel filter with mTrxR mutants. One possible explanation for this result would be that Man-A forms a reversible adduct with mTrxR or non-covalently interacts with the C-terminal tail of mTrxR.

Surprisingly, the reduction of selenocystine by TrxR1 was not inhibited by Man-A rather enhanced in absence of pre-incubation. This observation suggests that in the presence of Man-A, TrxR1 retains an unmodified Sec residue. This is contradictory to the earlier conclusion that Man-A reacts with Sec of TrxR1. It is generally believed that efficient selenocystine reduction requires a Sec residue in the C-terminal redox center, as the rate of selenocystine reduction by the mTrxR2 (GCCG) mutant is only about 1/3 that

or the WT enzyme[25]. However, the proposed mechanism of selenocystine reduction does not involve the C-terminal Cys residue. This raises the possibility that it is the Cys residue to be modified in TrxR1 under the given condition. Given the relative nucleophilicities of thiols vs selenols, this conclusion seems counterintuitive. The crystal structure of human TrxR1 (GCCG) revealed three possible conformations. In solution the more favorable conformation of reduced TrxR1 has the Cys^{497} more accessible than the Sec^{498} residue[26]. Reaction of Man-A with Cys^{497} could leave the Sec^{498} residue free to reduce selenocystine, as shown in Figure 42.However, when pre-incuabated with reduced TrxR, Man-A induced inhibition of both selnocystine and H_2O_2 reduction by TrxR1 revealing the reaction of Sec is not instant and is time dependent, as shown in Figure 42.

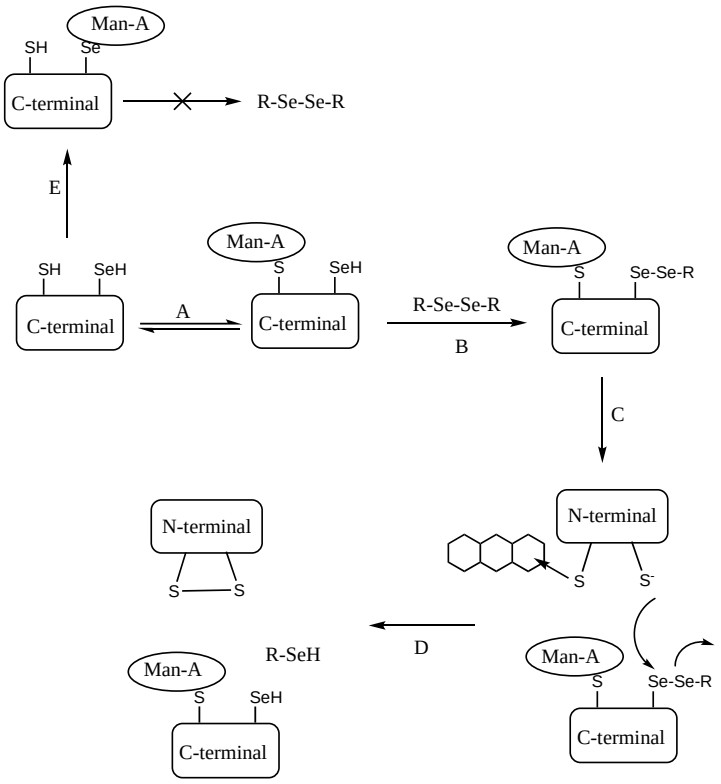

Figure 42 . The hypothesized mechanism of reduction of selenocystine in the presence of Man-A (**A)** non-covalent interaction between Man-A and Cys^{497} of TrxR (**B**) Nucleophilic attack of Sec^{498} on diselenide bond of selenocystine (R-Se-Se-R) (**C**) The new diselenide bond formed between Sec^{498} and Sec of selenocystine resolved by N-terminal redox center **(D)** Covalent interaction between Man-A and Sec^{498} of TrxR

The DTNB reduction by TrxR1 in the presence of Man-A derivatives, suggests the central cyclohexenone is the reactive site in man-A. This functional group is absent in deoxy-man-A and dihydro-man-A. This conclusion is supported by the failure of these derivatives to inhibit insulin reduction by TrxR1 and decreased reactivity with seleno-*L*-cysteine by deoxy-man-A and no reactivity with dihydro-man-A. If Man-A reacted at the C-terminal Sec, it could form Michael adduct as shown in Figure 43.

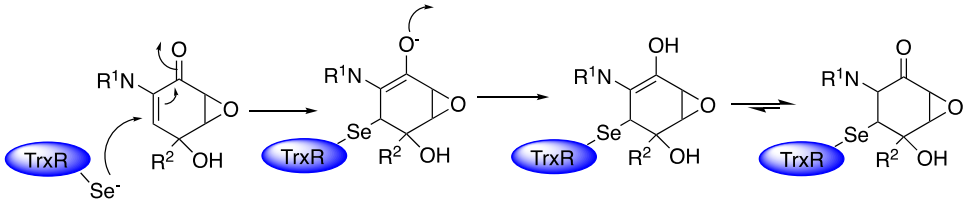

Figure 43. Proposed mechanism of reactivity of Man-A with TrxR1 after pre-incubation

Inhibition of TrxR at the C-terminal tail produces a SecTRAP and activates NADPH oxidase in cells. Reaction of Man-A with Cys^{497} may prevent the C-terminal tail to efficiently swing back into tetrapeptide binding pocket and hence interrupts the electron flow. In the presence of Man-A, NADPH oxidase activity was increased in both TrxR1 and mTrxR enzymes with a maximum of 14-fold in the dead tail mutant. These results could explain apoptosis induced by the production of $O_2^{-\cdot}$ anion that was previously unknown.

The Man-A treated cell homogenate showed a longer induction time as compared to control in the insulin reduction assay. The presence of numerous nucleophiles which could be possible targets of Man-A in addition to TrxR in living cell. This research reveals the TrxR system is a cellular target of Man-A. Not only does Man-A inhibit Ras and downstream processes, it also interferes with redox homeostasis and stimulates ROS production as shown in Figure 44.

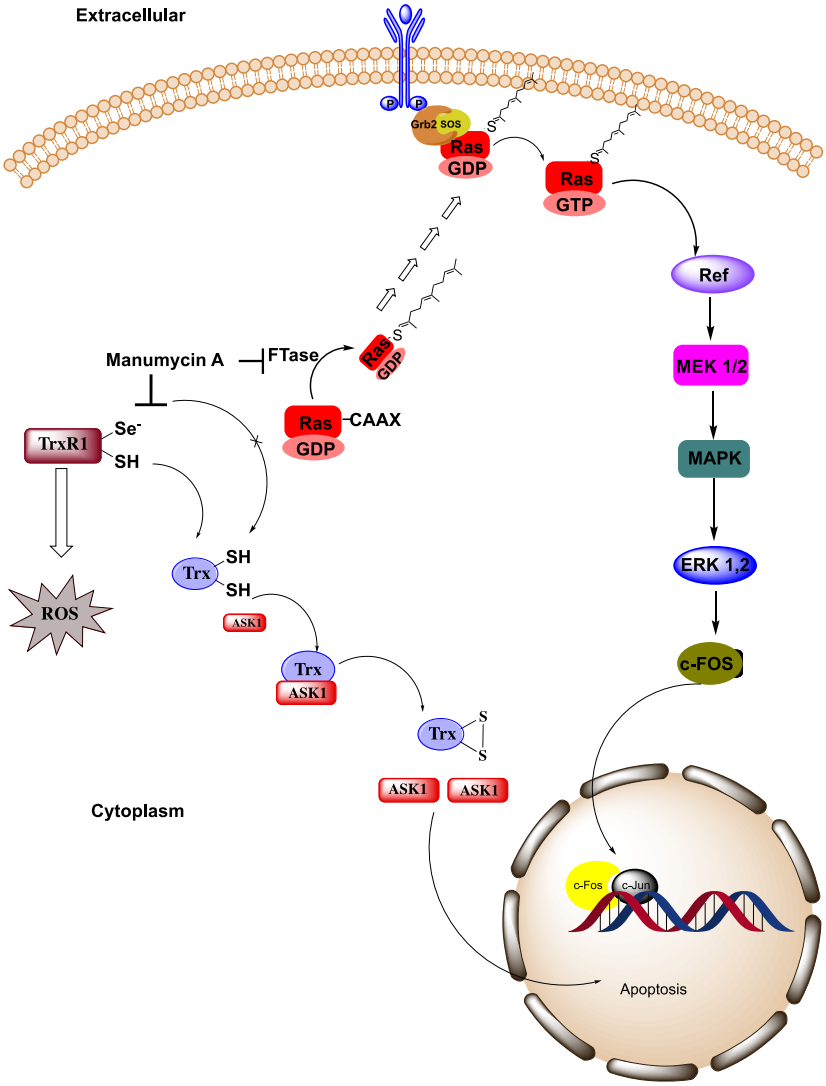

Figure 44. The cellular effects of Man-A as an inhibitor of FTase and TrxR1. FTase causes posttranslational modification of Ras which initiates a cascade of phosphorylation that triggers Ras-MAPK (mitogen-activated protein kinases) signaling. Inhibition of TrxR1 by Man-A activates NADPH oxidase, increasing the production of ROS. Inhibition of TrxR also prevents the reduction of Trx. Reduced Trx binds the ASK1 protein which is released when Trx is oxidized. Release of ASK1 activates many proteins such as AP-1 which are related to apoptosis. Posttranslation modification of Ras adapted from 99

3.5 General materials and methods

Manumycin A, deoxymanumycin A and dihydromanumycin A were purchased from Adipogen Life Sciences and used without further purification. Man-A and its derivatives were reported by the manufacturer to be >95% pure by HPLC and 1H NMR.

Man-A and its derivatives were analyzed by HESI MS (Bruker Evo-Q Elite Triple-Quadrupole) operating in positive ion mode and the anticipated *m/z* for M+1 was observed in all cases. Cytochrome c was purchased from Lee biochemical and superoxide dismutase was purchased from MP Biomedicals. Enzyme assay kit (fluorescent TrxR/Trx) and rat recombinant TrxR1 were purchased from Cayman Chemical. Mitochondrial TrxR and mutants, *Drosophila melanogaster* TrxR and mutants were gift from Dr. Robert Hondal from University of Vermnont. All other reagents were purchased from Sigma-Aldrich or Fisher Scientific and used without further purification. The TrxR/Trx assay was performed according to the kit manufacturer's instructions with noted exceptions below. UV-vis and fluorescence measurements were performed in 384 well microplates using a Synergy® 2 (BioTek Instrument, Inc.) or an Infinite® M1000 PRO (Tecan Group Ltd.) microplate reader. All assays were performed in triplicate. All assays were performed in triplicate. Results are presented as an average of three trials ±standard deviation. Error limits on graphs represent the standard deviation of three trials.

3.5.1 DTNB reduction assay

(General DTNB reduction) The assay was performed in 384 well black flat bottom plates in a final volume of 100 μL. TrxR enzymes (6.4 nM or 7.04 nM) were reduced with NADPH (102 μM or 117 μM) in assay buffer (50 mM Tris-HCl, 1 mM EDTA pH 7.5) for 30 minutes at room temperature. Test compounds (0.625 mM in 25 % DMSO or MeOH) was added for a concentration of 25 μM. The mixture was incubated for an additional thirty minutes at room temperature. DTNB (20 μL, 10 mM in 0.1 M sodium phosphate and 1 mM EDTA, pH 8.0) was added to the TrxR/test compound mixture (80 μL) to initiate the reaction. Final concentrations: 5.12 nM or 5.6 nM TrxR;

20 μM test compound; 2 mM DTNB. The reduction of DTNB was monitored by measuring absorbance at 412 nm every 5 minutes for 1 hour. **(Method A** Pre-incubation with Man-A/test compounds. Rat recombinant TrxR1 (6.4 nM) was reduced with NADPH (102 μM) in assay buffer (50 mM Tris-HCl, 1 mM EDTA pH 7.5) for 30 minutes at room temperature. The mixture was incubated for an additional thirty minutes with final Man-A concentration of 0, 5, 50, 500, 1800, 5000 nM. DTNB (20 μL, 10 mM) in 0.1 M sodium phosphate and 1 mM EDTA, pH 8.0 was added to 80 μL of reduced TrxR mixture and reduction of DTNB was monitored by measuring absorbance at 412 nm every 5 minutes for 1 hour. **(Method B)** Without pre-incubation with Man-A. The assay was performed as described above except that Man-A and DTNB were added simultaneously after NADPH reduction of TrxR. All results are expressed as percent of control at termination (60 minutes).

3.5.2 Standard curve for TNB^{2-}

Standard curve for TNB^{2-} was obtained by reducing DTNB with DTT (1,4-dithiothreitol). Various concentration of DTT (0, 0.05 mM, 0.1 mM, 0.2 mM and 0.4 mM) was prepared in 50 mM Tris-Cl, 1 mM EDTA pH 7.5. DTNB was prepared in 0.1 M sodium phosphate and 1 mM EDTA, pH 8.0. The production of TNB^{2-} was measured at 412 nm.

3.5.3 Time course inhibition of DTNB reduction by TrxR

The assay was performed in 384 well black flat bottom plate in a final volume of 100 μL. Rat recombinant TrxR1 (6.4 nM) was reduced with NADPH (102 μM) in assay buffer (50 mM Tris-HCl, 1 mM EDTA pH 7.5) for 30 minutes at room temperature. Man-A (10 μL in 25% DMSO) was added for final concentrations of 1 μM and incubated for

15, 10, 5 and 2 min. DTNB (20 µL, 10 mM in 0.1 M sodium phosphate and 1 mM EDTA, pH 8.0) was added to the TrxR/Man-A (80 µL) to initiate the reaction. The reduction of DTNB was monitored by measuring absorbance at 412 nm every 5 minutes for 1 hour.

3.5.4 Irreversible inhibition of TrxR

TrxR enzymes (80 nM) were reduced with NADPH (1.34 mM) in assay buffer (50 mM Tris-HCl, 1 mM EDTA pH 7.5) for 30 minutes at room temperature. The reduced TrxR was divided into three aliquots viz. control (TrxR/no test compound), TrxR/ test compound and TrxR/test compound not subjected to gel filtration. A fourth of TrxR/ test compound solution was not reduced with NADPH. A solution of test compound (11 µL in 25% DMSO) was added to the TrxR samples (280 µL) for concentrations of Man-A (2.6 µM for TrxR1) and the other test compound (5.5 µM). The control sample was substituted with an equal volume of 25% DMSO instead of test compound solution. Samples were incubated for 1 hour at ambient temperature, after which they were passed through a Micro Bio-spin P-6 gel column of MW limit of 6000 (Bio-rad). One sample containing test compound was not passed through the gel filtration column. All samples (280 µL) were re-reduced with (20 µL, 1.34 mM) NADPH for 30 minutes. Finally, the DTNB assay was performed as described above by adding 20 µL of 10 mM DTNB to 80 µL of enzyme/ test compound mixture and the absorbance was monitored at 412 nm every 5 minutes for 1 hour. Final concentrations: 5.2 nM TrxR, 2 µM Man-A for TrxR1, 4.2 µM for other test compounds.

3.5.5 TrxR/Trx insulin reduction

The assay was performed in 384 well black flat bottom plate in a final volume of 100 µL. Rat TrxR-1 (125 nM) was pre-reduced for 30 min with NADPH (335 µM) in the presence of test compounds (25 µM) in assay buffer (0.2 mg/mL BSA, 50 mM Tris-Cl, 1 mM EDTA pH 7.5). Human Trx (1 µM) was added for a Trx concentration of 125 nM. This solution was incubated for an additional 30 minutes. Fluorescent substrate (20 µL, 0.4 mg/mL, eosin labeled bovine insulin) was added to the enzyme/ test compound solution (80 µL) to initiate the reaction. Final concentrations: 100 nM TrxR; 20 µM test compounds; 100 nM hTrx-1. The fluorescence was monitored at λex/λem= 520nm/545 nm every 5 minutes for 1 hour. Insulin reduction with mTrxR2 (CGUG) except the mTrxR2 (CGUG) and hTrx-1 concentrations were doubled.

3.5.6 Reaction of Sel-green probe with seleno-*L*-cysteine

A stock solution of seleno-L-cystine (500 µL, 156 µM) was reduced with 1.5 equivalent of immobilized TCEP (>8 µmol/mL) for 1 hour. After reduction, the immobilized TCEP was removed by centrifugation at 14,000 X g, for 10 minutes. The reduced *L*-selenocystiene (20 µL, 312 µM) was incubated with test compounds (10 µL, 625 µM) for 1 hour. Sel-green (20 µL, 100 µM) was added to *L*-selenocysteine test compound mixture (80 µL) and fluorescence monitored at λex/λem= 370 nm/510 nm every 5 minutes for 1 hour.

3.5.7 NADPH consumption by TrxR

The assay was performed in 384 well black flat bottom plates in a final volume of 100 µL. NADPH (7.5 µL, 2.68 mM) in assay buffer (50 mM Tris-HCl, 1 mM EDTA pH 7.5) was added to a solution (92.5 µL) of rat recombinant TrxR-1 or mTrxR2 or mutants

(0.21 µM) and Man-A (68 µM/42 µM) or test compounds (42 µM) in assay buffer and the absorbance was monitored at 340 nm for 30 minutes. Final concentrations: TrxR (0.2 µM), Man-A (62.5 µM/38.5 µM), test compounds (38.5 µM), NADPH (200 µM). NADPH mol min/mol-enzyme was calculated from the standard curve of NADPH.

3.5.8 Standard curve for NADPH

Standard curve for NADPH was obtained from calibration of NADPH of various concentrations (0, 50 µM, 100 µM, 250 µM and 500 µM) NADPH in 50 mM Tris-HCl, 1 mM EDTA pH 7.5. The absorbance of NADPH was monitored at 340 nm.

3.5.9 Superoxide radical anion production by TrxR in the presence of Man A

The NADPH oxidase activity induced by Man-A was determined by monitoring the reduction of cytochrome c by $O_2^{\cdot-}$ and measuring the absorbance of reduced cytochrome C at 550 nm. The assay was performed in 384 well black flat bottom plate in a final volume of 100 µL. Cytochrome c (10 µL, 1 µM), NADPH (7.5 µL, 2.68 mM), Man-A (2.5 µL, 2.5 mM/DMSO) or 2.5 µL DMSO were combined. The reaction was initiated by addition of rat TrxR1 (10 µL, 1 µM). The production of superoxide was confirmed by addition of 6 units SOD/well in parallel samples. SOD is used to quench superoxide generated by TrxR.

3.5.10 Selenocystine reduction by TrxR1 and mTrxR variants

The assay was performed in a 384 well black flat bottom plates in a final volume of 100 µL. TrxR enzymes (25 nM) were reduced with NADPH (251 µM) in the presence of test compounds (48 µM) in assay buffer (in 50 mM Tris-HCl, 1 mM EDTA pH 7.5). The reaction was initiated by the addition of *L*-selenocystine (20 µL, 599 µM in assay buffer) to the enzyme test compound mixture (80 µL) either immediately or after

incubation for 15 minutes. Final concentrations: 20 nM TrxR; 38.5 μM test compound; 120 μM selenocystine. The consumption of NADPH was monitored by measuring absorbance at 340 nm for 10 minutes.

3.5.11 Reduction of hydrogen peroxide by TrxR1 and mTrxR2 (GCUG)

The assay was performed in a 384 well black flat bottom plate in a final volume of 100 μL. Hydrogen peroxide (20 μL, 250 mM) in assay buffer (50 mM Tris-HCl, 1 mM EDTA pH 7.5) was added to a solution (80 μL) of TrxR enzyme (62.5 nM), NADPH (200 μM) and test compounds (48 μM) in assay buffer, either immediately or after incubation for 15 minutes. Final concentrations: 50 nM TrxR; 38.5 μM test compound; 50 mM H_2O_2. The consumption of NADPH was monitored by measuring absorbance at 340 nm for 10 minutes. The potent TrxR inhibitor auranofin (38.5 μM) was used as a control.

3.5.12 Preparation of cell lysate for biochemical assays

The human lymphoblast cell line (GM02152) was purchased from Coriell institute. Cells were cultured in Roswell Park Memorial Institute (RPMI) 1640 medium supplemented with 15 % fetal bovine serum (FBS) and 2 μM sodium selenite and were maintained in a humidified incubator at 37°C and 5% CO_2 until they reach log phase.

For TrxR/Trx assay GM02152 cells were seeded in 75 cm2 flasks containing growth medium. The cells were harvested by centrifugation (720 X g, 4 minutes) when log phase was reached. The cells were lysed by addition of 100 μL lysis buffer (10 mM Tris-HCl, 200 mM KCl, 2 mM EDTA, 40% glycerol, 0.2% TritonX-100, pH 7.5) followed by rotation at 4°C for 2 hours. Cellular debris was removed by centrifugation at 17000 X g at 4°C for 30 minutes. Protein concentration of the lysate was determined by the Bradford

method using Coomassie protein assay reagent in triplicate. Typical concentration of the lysate ranged from 10-15 mg/ml.

3.5.13 TrxR/Trx inhibition assay with cell lysate

The assay was performed in 384 well black flat bottom plate in a final volume of 100 μL. Cell lysate (15.6 μg protein in lysis buffer) was reduced with NADPH (5 μL, 4 mg/ml). Man-A (in 25% DMSO) was added for a final concentration of 1 μM. After 30 minutes, human Trx (10 μL, 1 μM) was added and incubated for an additional 30 minutes. Fluorescent substrate (20 μL, 0.4 mg/ml, eosin labeled bovine insulin) was added to the enzyme/Man-A solution (80 μL) to initiate the reaction. The fluorescence was monitored at λex/λem= 520nm/545 nm every 5 minutes for 1 hour.

Chapter 4. Effect of brevetoxin-2 and brevetoxin-3 on TrxR1, mTrxR and DmTrxR

4.1 Objective

The activity of brevetoxin (PbTx) towards TrxR1 is unique in comparison to other known TrxR1 inhibitors. Both PbTx-2 and PbTx-3 activate reduction of DTNB by TrxR1. The insulin reduction assay reveals that PbTx-2 inhibits the reduction of Trx by TrxR1 in a dose-dependent manner but PbTx-3 has no effect. Because PbTx-2 has an α, β-unsaturated side chain and PbTx-3 does not, the mechanism of inhibition was assumed to be the formation of a Michael adduct with the C-terminal redox site (Sec). However, the adduct of PbTx-2 and TrxR1 was not observed by mass spectroscopy. Hence the main objective of Chapter 4 is to understand the interaction between brevetoxins and TrxR in the activation of DTNB reduction and inhibition of Trx reduction. To accomplish this goal the site-specific mutant enzymes of mTrxR and DmTrxR will be used. The marine life exposed to red tide exhibit increased indicators of oxidative stress. The second objective of this chapter is to characterize indicatiors of oxidative stress in brevetoxin treated human lymphoblast cells and to determine if antioxidant treatments can mitigate the effect, whcih will be achieved by using a cellular model (human lymphoblast cells) and antioxidants, Trolox (6-hydroxy-2,5,7,8-tetramethylchroman-2-carboxylic acid) and Vitamin C.

4.2 Introduction

Blooms of the famous Florida red tide, caused by the dinoflagellate *K. brevis,* are characterized by an obnoxious odor and dense red or brown patches near the water surface. This dinoflagellate exists naturally along the Gulf of Mexico and west coast of

Florida, blooming annually between late summer and fall. However, the bloom exacerbates as a result of some natural phenomenon such as increased water temperature, hurricane, floods etc. Another possible bloom promoter is eutrophication related to an increase in nutrients such as phosphorus and nitrogen. *Karenia brevis* is well known for the production of neurotoxins known as the brevetoxins (PbTx) which may concentrate in shellfish and fishes that feed on these dinoflagellates. The harmful algal bloom (HAB) is accompanied by mortalities of marine mammals such as manatees and costal species of fish and birds[100] as a result of PbTx exposure. It also has detrimental impacts on human health and economies resulting from beach and shellfish bed closures.

Brevetoxins (PbTxs) are polycyclic polyether ladders. They can be differentiated into two distinct backbones type A and type B as shown in Figure 45[101]. The molecules have 10-11 fused rings and have a molecular weight around 900 Da. At least 12 different structures have been identified having different combinations of backbone and side chains and are designated from PbTx-1, 2, 3….[102] as shown in Table 15. PbTx-2 with the B-type backbone is the most abundant while PbTx-1 with the A-type backbone is most potent[103].

Brevetoxins are neurotoxins that can poison humans through ingestion of contaminated shellfish, inhalation of aerosolized toxin or through dermal exposure during swimming. A particular type of poisoning called Neurotoxic Shellfish Poisoning (NSP) is the result of consumption of shellfish contaminated with PbTxs. This poisoning is characterized by gastrointestinal and neurological symptoms such as nausea, vomiting, arrhythmias, ataxia, slurred speech and dizziness. Neurological symptom includes partial paralysis and respiratory distress [104].

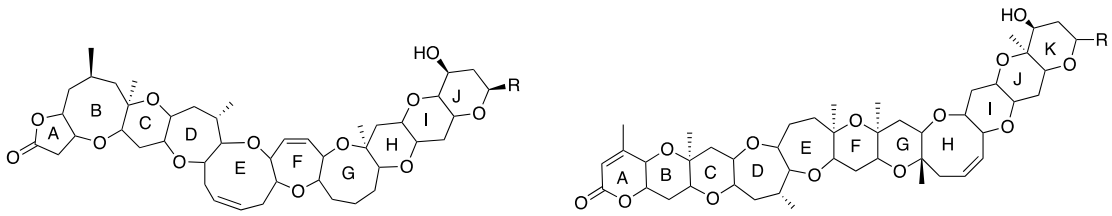

Brevetoxin A backbone Brevetoxin B backbone

Figure 45. PbTx structure

Table 15. Side chain at K-ring of brevetoxin A and brevetoxin B

Brevetoxin A	**Side chain at K-ring (R)**	**Brevetoxin B**	**Side chain at K-ring (R)**
PbTx-1	$CH_2C(=CH_2)CHO$	PbTx-2	$CH_2C(=CH_2)CHO$
PbTx-7	$CH_2C(=CH_2)CH_2OH$	PbTx-3	$CH_2C(=CH_2)CHOH$
PbTx-10	$CH_2CH(CH_3)CH_2OH$	PbTx-5	[PbTx-2],C-38 OAc
		PbTx-6	[PbTx-2]27,28 ring epoxide
		PbTx-8	CH_2COCH_2Cl
		PbTx-9	$CH_2CH(CH_3)CH_2OH$

The biotransformation of PbTx in rat hepatocytes[105], *Porites astreoides*[106] and a monocyte cell line (U-937) has been a well-studied topic. Brevetoxin-1 and 2 form conjugates as Michael adducts, with glutathione and cysteine at the α, β-unsaturated aldehyde[60]. It is also oxidized by cytochrome P450[107]. A few studies have shown that PbTx induces oxidative stress in animals and cells. The indicators of oxidative stress include a decrease in intracellular glutathione[108] in a monocyte cell line (U-937), reduced lymphocyte proliferation and decreased level of SOD (superoxide dismutase) in manatees[60], DNA damage of human lymphocyte[109] and Jurkat E6-1 cell line[110].

4.3 Results and Discussion

4.3.1 DTNB as a substrate for TrxR1

The DTNB reduction of TrxR1 is activated by 2.6-fold and 6-fold in presence of PbTx-2 and PbTx-3 respectively (Figure 46). In the case of PbTx-2, this activation of DTNB was attributed to modification of C-terminal tail of TrxR1 which allows DTNB to be reduced by the N-terminal redox center [63].

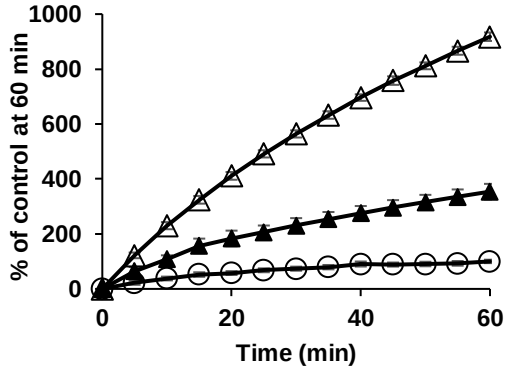

Figure 46. DTNB reduction of TrxR1 in the presence of PbTx-2 (20 μM, ▲) and PbTx-3 (20 μM, △); Control (○). Adapted from reference [63]

4.3.2 TrxR/Trx insulin reduction in the presence of PbTx-2 and PbTx-3

Brevetoxin-2 inhibits Trx reduction by TrxR1 and hence affects the reduction of insulin, while PbTx-3 has no effect (Figure 47). The inhibition of insulin reduction by TrxR1 in the presence of PbTx-2 was attributed to the covalent adduct formed by α, β-unsaturated aldehyde group of PbTx-2 with Sec of TrxR1, which was further supported by the lack of inhibition by the allylic alcohol in PbTx-3.

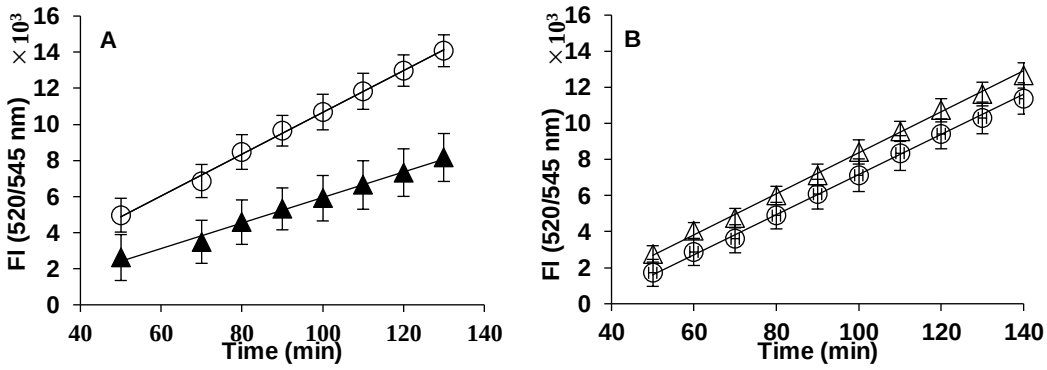

Figure 47. Insulin reduction by TrxR/Trx system. (**A)** PbTx-2 (20 μM, ▲); (**B)** PbTx-3 (20 μM, △). Adapted from [63]

4.3.3 Reactivity of PbTx-3 with seleno-*L*-cysteine

Although PbTx-3 does not inhibit Trx reduction by TrxR1, it does react with selenocysteine (Figure 48) in a reaction monitored by release of fluorophore from Sel-green probe[93] In comparison to Sec of TrxR1, selenocysteine is a small molecule and could easily react with α, β-unsaturated lactone at A-ring of PbTx-3. Despite Sec in TrxR1 being a nucleophile, it is less available due to the large and complex nature of the enzyme causing steric hindrance.

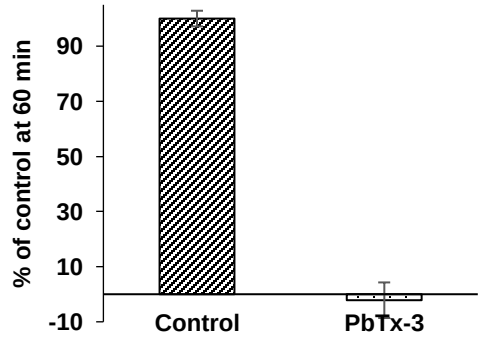

Figure 48. Reaction of reduced seleno-*L*-cysteine (20 μM) with Sel-green probe (20 μM) after incubation with the PbTx-3 (20 μM for 60 min)

4.3.4 DTNB as a substrate for mTrxR2 variants

Both PbTx-2 and PbTx-3 induce activation of DTNB reduction by all mTrxR enzymes (Figure 49). As reported in Table 16, the highest degree of activation is observed with the dead tail mutant, mTrxR2 (GSSG) by 10-fold, which has a nonfunctional C-terminal tail and reduction is only possible via the N-terminal redox center. The activation observed with the dead tail and truncated mutant also emphasize that these compounds does not necessarily have to interact with Sec for activation of DTNB reduction. Furthermore, the maximum activation of the dead tail mutant demonstrates that the brevetoxins act by exposing the N-terminal redox center.

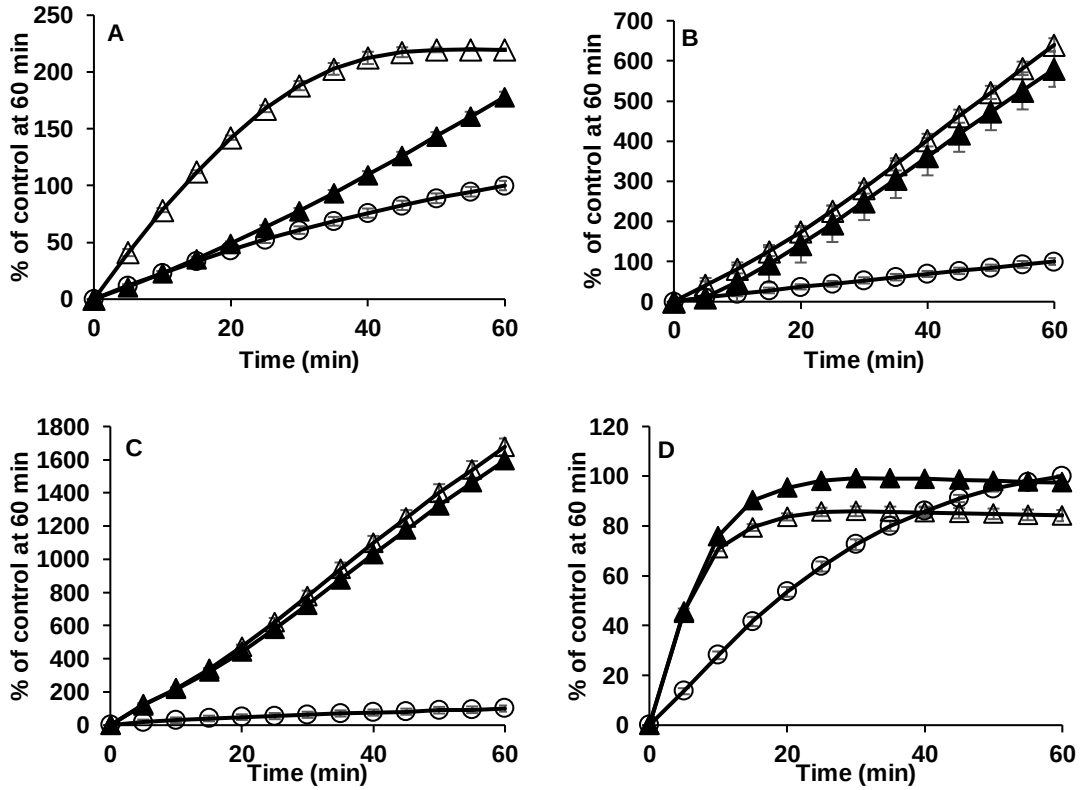

Figure 49. Reduction of DTNB (2 mM) by mTrxR in the presence of PbTx-2 and PbTx-3 (20 μM). (**A**) mTrxR2 (GCUG) (5.12 nM); (**B**) mTrxR2 (GCCG) (5.12 nM); (**C**) mTrxR2 (GSSG) (5.12 nM); (**D**) mTrxRΔ8 (10 nM). The control sample was prepared by adding an equal volume of DMSO. PbTx-3 (△); PbTx-2(▲) and Control (○)

Table 16. Enzyme activity expressed as TNB^{2-} mol/min-mol enzyme for mTrxR control and activation of DTNB reduction reported as relative rate for PbTx-2 and PbTx-3 with respect to control. The consumption of DTNB was calculated from standard curve of TNB^{2-}

	mTrxR2 (GCUG)	**mTrxR2 (GCCG)**	**mTrxR2 (GSSG)**	**mTrxR2 (Δ8)**
Control	785 ± 11.0	249 ± 23.2	226 ± 17.0	995 ± 65.5
PbTx-3	3.25**	3.99**	10.07**	2.29**
PbTx-2	1.37**	4.39**	9.06**	2.60**

The number of asterisks indicate significant differences compared with control (** p <0.01)

4.3.5 DTNB as a substrate for DmTrxR variants

The activation observed in DmTrxR (Δ8) enzymes also accentuate that the C-terminal Sec is not required for activation observed in DTNB reduction as shown in Figure 50. The enzyme activity increased in the presence of PbTx-2 and PbTx-3 as shown in Table 17.

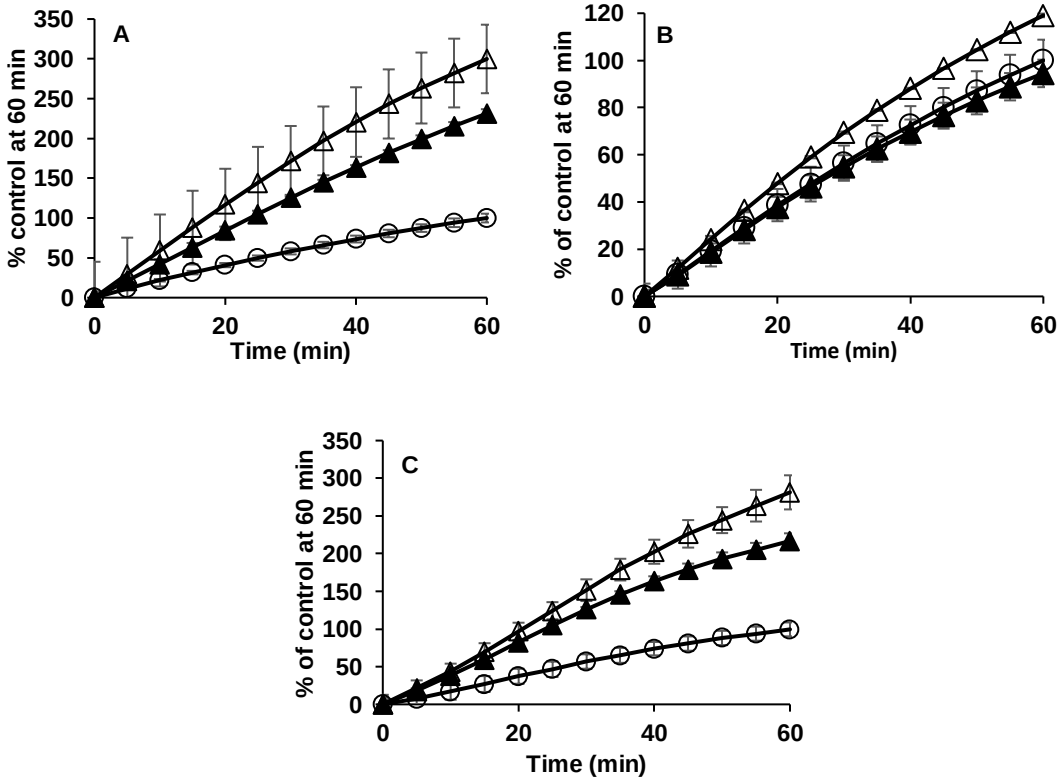

Figure 50. Reduction of DTNB (2 mM) by DmTrxR in the presence of PbTx-2 and PbTx-3 (20 µM). (**A**) DmTrxRSCUG (10 nM); (**B**) DmTrxRSCCS (50 nM); (**C**) DmTrxRΔ8 (10 nM). The control sample was prepared by adding an equal volume of DMSO. PbTx-3 (△); PbTx-2(▲) and Control (○)

Table 17. Enzyme activity expressed as TNB^{2-} produced mol/min-mol enzyme for DmTrxR control and activation of DTNB reduction reported as relative rate for PbTx-2 and PbTx-3 with respect to control. The consumption of DTNB was calculated from standard curve of TNB^{2-}

	DmTrxR (SCUG)	**DmTrxR (SCCS)**	**DmTrxR (Δ8)**
Control	70.4 ± 2.25	34.5 ± 10.3	24.6 ± 5.03
PbTx-3	2.97**	1.59*	2.12**
PbTx-2	2.08**	1.26	2.69**

The number of asterisks indicate significant differences compared with control (* p <0.05, ** p <0.01)

4.3.6 Irreversible inhibition TrxR by PbTx-2

The C-terminal Cys and Sec of TrxR are both nucleophiles and can readily react with electrophilic α, β-unsaturated carbonyl of PbTx-2. In order to determine if the PbTx-2 covalently formed an adduct with C-terminal redox center of TrxR, DTNB reduction was performed as usual with TrxR1, mTrxR2 (GCUG) and mTrxR2 (GCCG). However, after 1-hour incubation of pre-reduced TrxR1 with 4.2 μM PbTx-2, the mixture was passed through a gel filtration column (MW cutoff of 6000 amu) followed by a 30 minutes incubation with additional NADPH (Figure 51). The gel filtration should remove unbound PbTx-2 and the additional 30 minutes incubation should reestablish equilibrium. It is important to note that unlike Man-A, PbTx-2 at 4.2 μM when passed through the gel filtration column did not activate DTNB reduction by any of the enzymes meaning that the interaction between the enzymes (TrxR1, mTrxR2 (GCUG) and mTrxR2 (GCCG)) and PbTx-2 is either non-covalent or reversible.

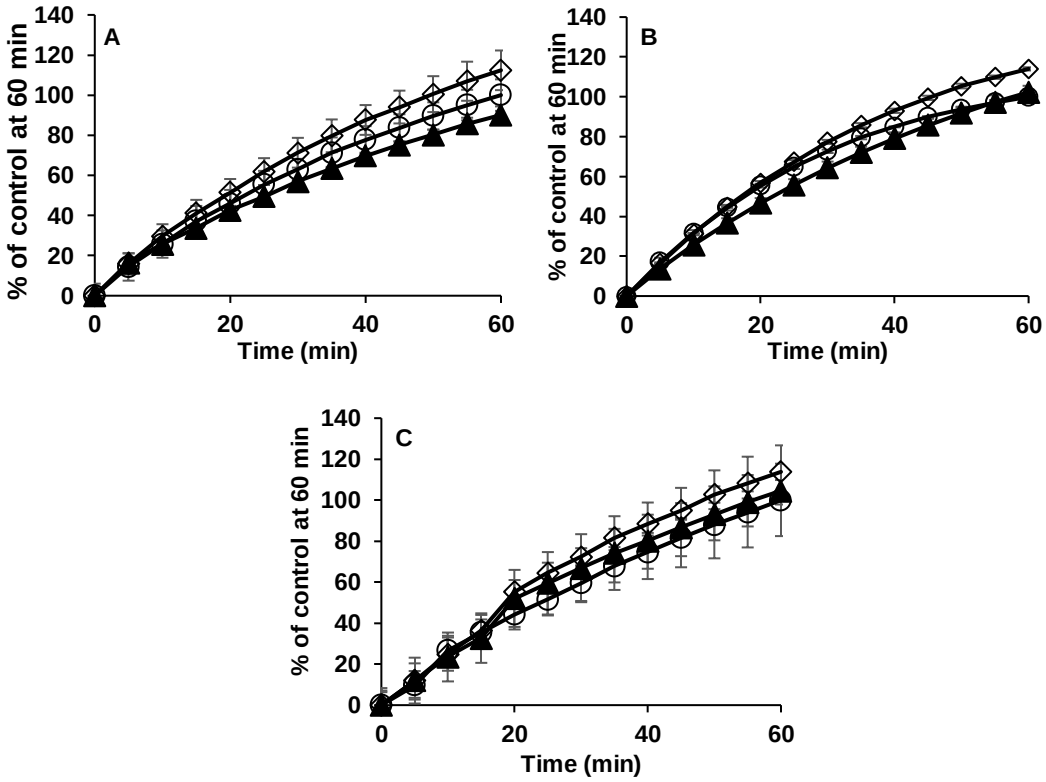

Figure 51. Test of irreversibility of inhibition of DTNB reduction by TrxR (5.2 nM) in the presence of PbTx-2 (4.2 μM). (**A**) TrxR1; (**B**) mTrxR2 (GCUG); (**C**) mTrxR2 (GCCG). TrxR reduced only after removal of test compounds by gel filtration (◆); Control (no test compound, ○); Test compound removed by gel filtration after incubation with reduced TrxR1(▲)

4.3.7 Reactivity of TrxR1 and mTrxR variants with substrate selenocystine in the presence of PbTx-2 and PbTx-3

Reduction of selenocystine requires the C-terminal redox center with either Sec/Cys[25] although the rate is much faster when Sec is present and uncompromised. The consumption of NADPH in the presence of selenocystine, is monitored as a proxy for selenocystine reduction. Comparison of the controls for Figure 52B, Figure 52C and Table 18 demonstrates that the mTrxR2 (GCCG) reduces selenocystine at a much slower rate than the wild type enzyme (Figure 52C) [mTrxR2 (GSSG) does not reduce selenocystine and was not included in this experiment]. Auranofin completely inhibited reduction of selenocystine which suggest it interacts at C-terminal redox site, possibly

Sec (Figure 52A). In the absence of pre-incubation, the reduction of selenocystine by TrxR is not compromised by both PbTx-2 and PbTx-3, as shown in Figure 52A, indicating the Sec residue of TrxR is available to reduce selenocystine.

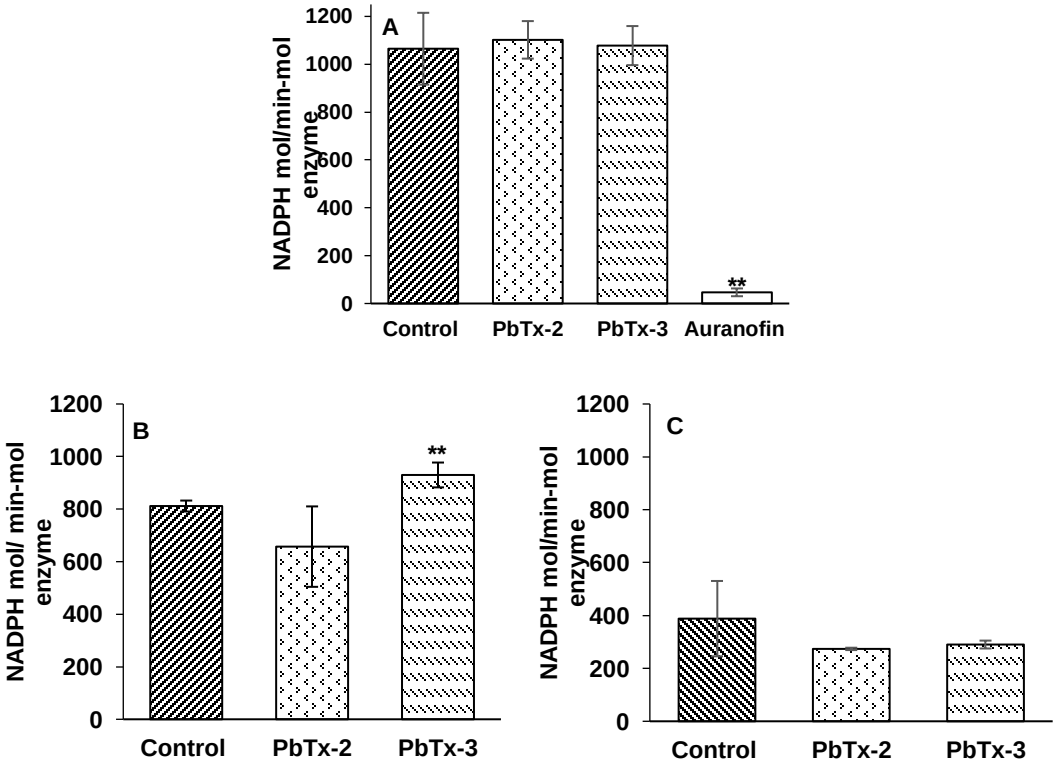

Figure 52. Reduction of selenocystine by TrxR (20 nM) in the presence of PbTx-2 and PbTx-3 (38.5 μM) and auranofin (62.5 μM). (**A**) TrxR1; (**B**) mTrxR2 (GCUG); (**C**) mTrxR2 (GCCG). The number of asterisks indicate significant differences compared with control (* p <0.05, ** p <0.01)

Table 18. Rates of of selenocystine reduction by TrxR enzymes in the presence of PbTx-2 and PbTx-3. NADPH consumption expressed as NADPH mol/min-mol enzyme

	TrxR1	**mTrxR2 (GCUG)**	**mTrxR2 (GCCG)**
Control	1065 ± 150	794 ± 35.1	388 ± 142
PbTx-2	1102 ± 78.4	657 ± 153	274 ± 4.43
PbTx-3	1078 ± 81.6	929 ± 47.2**	290 ± 14.9

The number of asterisks indicate significant differences compared with control (** p <0.01)

On the other hand, the selenocystine reduction was enhanced by 1.2-fold by mTrxR2 (GCUG) and 1.6-fold by mTrxR2 (GCCG) in the presence of PbTx-2 after incubation for 15 minutes, as shown in Figure 53 and Table 19. The enhancement of selenocystine reduction also supports that Sec remains free while PbTx-2 might interact with Cys in a reversible manner.

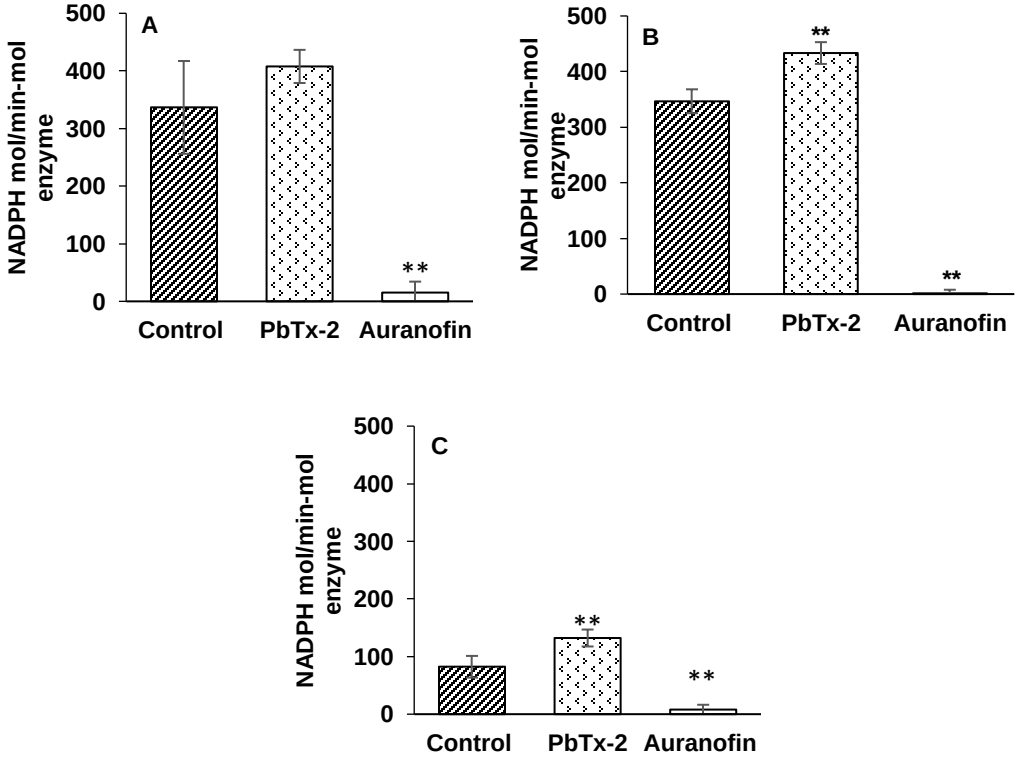

Figure 53. Reduction of selenocystine by TrxR (20 nM) after 15 minutes incubation with PbTx-2 and auranofin (38.5 μM). (**A**) TrxR1; (**B**) mTrxR2 (GCUG); (**C**) mTrxR2 (GCCG). The number of asterisks indicate significant differences compared with control (* p <0.05, ** p <0.01)

Table 19. Rates of of selenocystine reduction by TrxR enzymes after 15 minutes incubation with PbTx-2 and auranofin. NADPH consumption expressed as NADPH mol/min-mol enzyme

	TrxR1	mTrxR2 (GCUG)	mTrxR2 (GCCG)
Control	337 ± 80.5	347 ± 21.5	82.3 ± 18.8
PbTx-2	408 ± 28.7	433 ± 19.6**	132 ± 14.7**
Auranofin	15.2 ± 19.0**	1.67 ± 6.14**	8.00 ±8.35**

The number of asterisks indicate significant differences compared with control (* p <0.05, ** p <0.01)

4.3.8 Reactivity of TrxR1 and mTrxR2 (GCUG) with substrate hydrogen peroxide in the presence of PbTx-2

Brevetoxin-2 decreased the H_2O_2 reduction to 1.4-fold of that of mTrxR2 (GCUG) control in absence of pre-incubation. The reduction of H_2O_2 requires the Sec residue to be free[97-98] and the decrease with mTrxR2 (GCUG) signifies a non-covalent or reversible interaction of PbTx-2 withthe Sec residue. On the other hand, TrxR1 has no effect with as shown in Figure 54 and Table 20.

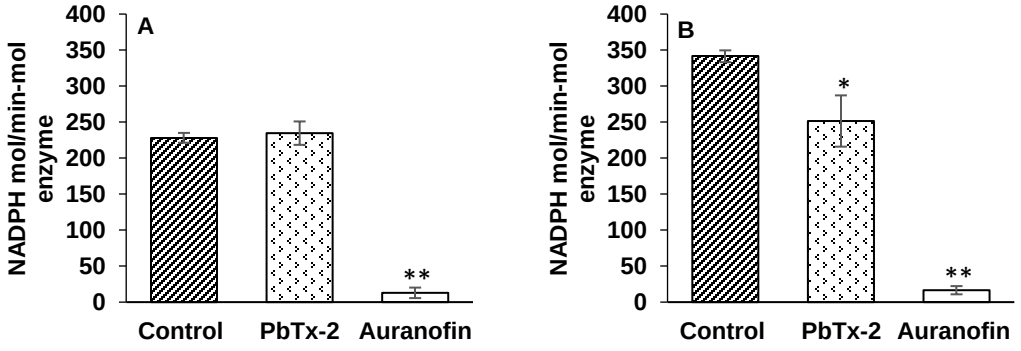

Figure 54. Hydrogen peroxide reduction by TrxR (50 nM) in the presence of PbTx-2 and auranofin (38.5 μM). **(A)** TrxR1; **(B)** mTrxR2 (CGUG). The data is expressed as NADPH consumption during reduction of H_2O_2. The number of asterisks indicate significant differences compared with control (* p <0.05, ** p <0.01)

Table 20. Rate of H_2O_2 reduction by TrxR in the presence of PbTx-2. NADPH consumption expressed as NADPH mol/min-mol enzyme

	TrxR1	**mTrxR2 (GCUG)**
Control	228 ± 6.84	341±8.20
PbTx-2	235 ± 16.2	251± 35.6*
Auranofin	12.89 ±7.29**	16.6 ±5.71**

The number of asterisks indicate significant differences compared with control (* p <0.05, ** p <0.01)

The hydrogen peroxide reduction was inhibited by 1.4-fold by TrxR1 and activated by 1.4-fold by mTrxR2 (GCUG) in the presence of PbTx-2 after incubation for 15 minutes, as shown in Figure 55 and Table 21, corroborating the the non-covlent or reversible interaction of PbTx-2 with Cys.

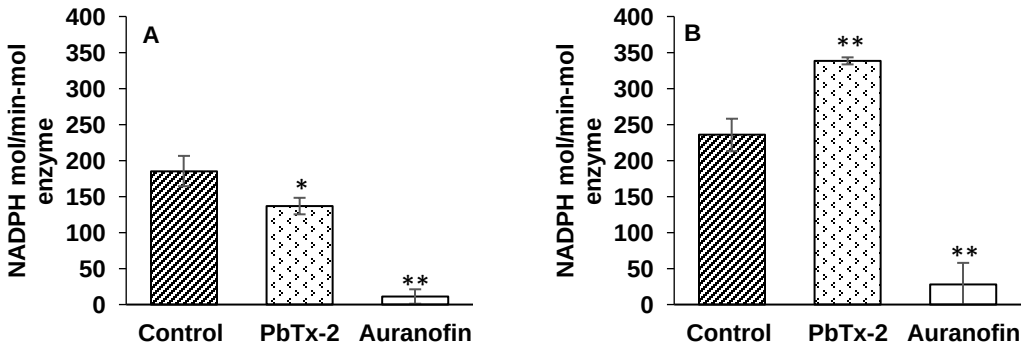

Figure 55. Hydrogen peroxide reduction by TrxR (50 nM) after 15 minutes incubation with PbTx-2 and auranofin (38.5 μM). **(A)** TrxR1; **(B)** mTrxR2 (CGUG). The data is expressed as NADPH consumption during reduction of H_2O_2. The number of asterisks indicate significant differences compared with control (* p <0.05, ** p <0.01)

Table 21. Rate of H_2O_2 reduction by TrxR after 15 minutes incubation with PbTx-2. NADPH consumption expressed as NADPH mol/min-mol enzyme

	TrxR1	**mTrxR2 (GCUG)**
Control	185 ± 21.1	235 ± 22.6
PbTx-2	137 ± 11.5*	338 ± 4.89**
Auranofin	11.1 ± 10.0**	27.9 ±29.9**

The number of asterisks indicate significant differences compared with control (* p <0.05, ** p <0.01)

4.3.9 NADPH oxidase activity of TrxR enzymes in the presence of PbTx-2 and PbTx-3

Adduction of the C-terminal Sec residue on TrxR induces NADPH oxidase activity of TrxR[49]. The consumption of NADPH in the absence of disulfide or diselenide substrate is monitored as a proxy for production of ROS. The consumption of NADPH was monitored for TrxR1, mTrxR2 (GCUG), mTrxR2 (GCCG), mTrxR2 (GSSG) and mTrxR2 (Δ8) in the presence of PbTx-2 and PbTx-3. The NADPH consumption by, mTrxR2 (GSSG) and mTrxR2 (Δ8) in the presence of PbTx-2 is increased by 25-fold, and 2.4-fold respectively when compared to their respective controls as listed in Table 22. On the other hand, PbTx-3 did not show an increase in NADPH consumption with any of the enzymes.

Table 22. NADPH consumption by TrxR in the presence of PbTx-2 and PbTx-3. NADPH consumption expressed as NADPH mol/min-mol enzyme

	TrxR1	**mTrxR2 (GCUG)**	**mTrxR2 (GCCG)**	**mTrxR2 (GSSG)**	**mTrxR2 (Δ8)**
Control	1.13 ± 0.09	0.93 ± 0.14	0.40 ± 0.15	0.11 ± 0.04	0.49 ± 0.43
PbTx-2	2.84 ± 1.63	1.17 ± 1.21	1.65 ± 1.24	2.80 ± 0.17**	1.18 ± 0.42*
PbTx-3	-	-0.88 ± 0.13	-	-	-1.29 ± 1.37

The number of asterisks indicate significant differences compared with control (* p <0.05, ** p <0.01)

4.3.10 Oxidative stress induced by PbTx-2 in GM02152 cells and use of antioxidants Trolox and ascorbic acid to mitigate the toxicity

The red tide exposed loggerhead sea turtles[61] and manatees[60] were reported to show increases in indicators of oxidative stress in peripheral blood leukocytes. Human lymphoblast cells (GM02152) cells were evaluated for signs of oxidative stress induced by PbTx-2.

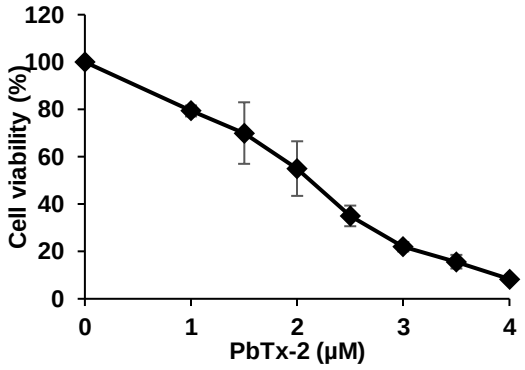

Figure 56. Dose response curve for PbTx-2 for GM02152 cells by MTT assay after 24 hours of treatment

The dose-response curve evaluated by MTT (3-(4, 5-dimethylthiazolyl-2)-2, 5-diphenyltetrazolium bromide) assay shows that PbTx-2 has an EC_{50} value of 2.3 µM as shown in Figure 56. The use of antioxidant Trolox (6-hydroxy-2,5,7,8-tetramethylchroman-2-carboxylic acid), water soluble version of vitamin E has been reported to mitigate the microcystin induced oxidative stress observed in tilapia[111]. The concentration of Trolox and Vitamin C (L-sodium ascorbate) used were 100 µM as no negative effect on the cells were observed at this concentration in MTT assay (Figure 57).

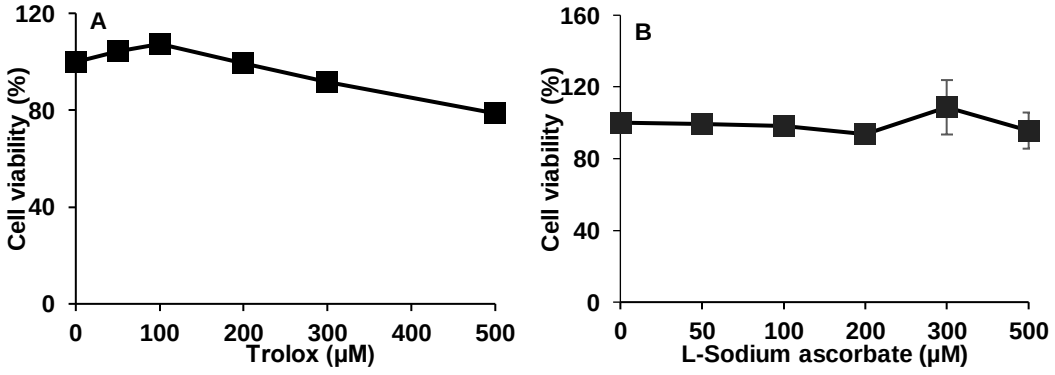

Figure 57. MTT assay after antioxidants treatment for 24 hours. **A.** Trolox; **B.** Vitamin C

Treatment of PbTx-2 (1 μM and 2 μM) in GM02125 cells for 24 hour reduced cell viability to 79 % and 55 % respectively of the untreated cells (Figure 58A). The simultaneous treatment of PbTx-2 (1 μM) and Trolox (100 μM) increased the cell viability to control levels. In comparison to Trolox treatment, vitamin C (100 μM) treatment was more effective at PbTx-2 concentration of 2 μM with cell viability of 98% (Figure 58B). The inhibition of TrxR will lead to an oxidized intracellular environment. Cellular glutathione level was reduced to 94% of the control for both PbTx-2 (1 μM) and PbTx-2/Trolox treatments. Free selenol content as determined from fluorescence probe Sel-green decreased to 89% and 87 % of control as shown in Figure 59A. The free radical can also degrade polyunsaturated fatty acid (PUFA) into lipid peroxide as reported in the larvae of coral *Porites astreoides* on exposure to *K. brevis*[106].The lipid peroxide is unstable and degraded into aldehyde compounds the most common of which is malondialdehyde (MDA). MDA can be monitored using a thiobarbaturic acid (TBA) to form MDA-TBA adduct. On the other hand, lipid peroxidation increased to 105 % in 1 μM PbTx-2 and 100 μM Trolox treated cell (Figure 59A) When the GM02152 cells were treated with higher dose of PbTx-2 (2.5 μM) the selenol content was decreased to 85% of untreated cells without any effect on lipid peroxidation (Figure 59B). The vitamin C (100 μM) treated sample has a free selenol content (87%) comparable to PbTx-2 (2 μM) treated samples (Figure 60).

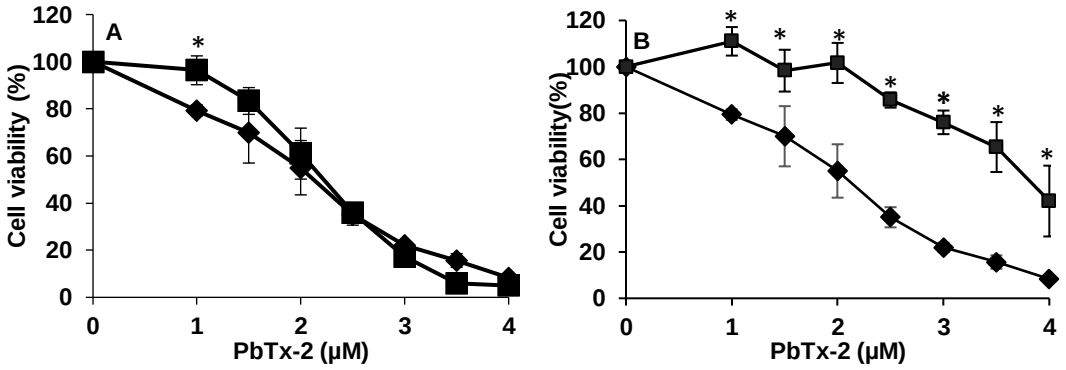

Figure 58. Dose-response curve for GM02152 cells (**A**) PbTx-2 ◆; PbTx-2 and Trolox (100 µM, ■) (**B**) PbTx-2 ◆; PbTx-2 and vitamin C (100 µM, ■). * indicates a statistically significant difference from the control ($p \leq 0.05$)

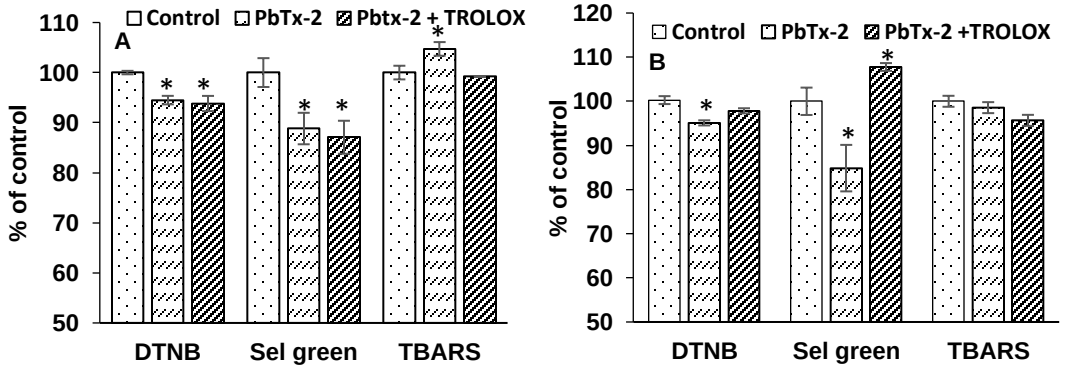

Figure 59. Measurement of oxidative stress indicators in GM02152 cells after 24 hours treatment of PbTx-2 and Trolox. (**A**) PbTx-2 (1 µM) and Trolox (100 µM); (**B**) PbTx-2 (2.5 µM) and Trolox (100 µM). * indicates a statistically significant difference from the control ($p \leq 0.05$)

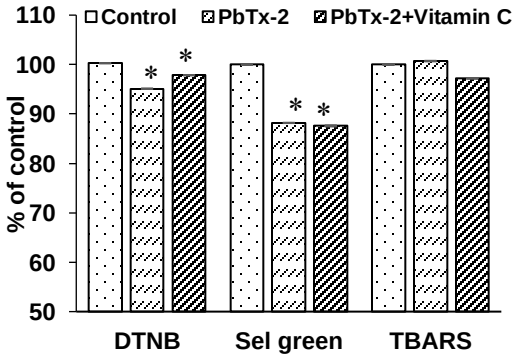

Figure 60. Measurement of oxidative stress indicators in GM02152 cells after 24 hours treatment of PbTx-2 (2 µM) and Vitamin C (100 µM). * indicates a statistically significant difference from the control ($p \leq 0.05$)

4.4 Conclusion

Compromising the C-terminal tail of TrxR can result in inactivation of the enzyme. Although both PbTx-2 and PbTx-3 can readily react with the amino acid selenocysteine as determined from the use of the Sel-green probe, only PbTx-2 inhibits Trx reduction by TrxR1. The inhibition of insulin reduction by TrxR1 in the presence of PbTx-2 suggests that the C-terminal redox center is compromised. The recovery of normal activity of TrxR1 after gel filtration suggests that the interaction between TrxR1 and PbTx-2 is either reversible or non-covalent. Binding of PbTx-3 may induce positive allosteric regulation of TrxR as is observed with many enzyme inhibitor complex[112] and thus the enzyme can still reduce substrates including insulin and selenocystine. The NADPH consumption by mTrxR2 (GSSG) in the presence of PbTx-2/PbTx-3 reveals that covalent modification of C-terminal redox center is not required for NADPH oxidase activity. Further, the activation of DTNB reduction with mTrxR variants as wells as DmTrxR variants occurs in a C-terminal Sec/Cys independent manner.

The reduction of selenocystine and H_2O_2 are more efficiently performed by Sec as compared to Cys[95]. In the presence of both the PbTx, the reduction of selenocystine is not compromised or partially compromised which reveals that these compounds may bind non-covalently or react reversibly with the C-terminal Cys which is available and is exposed to solvent rather than Sec[26] when the enzyme is in the reduced-waiting position. On the other hand, PbTx-2 inhibits reduction of H_2O_2 by 1.4-fold of TrxR1 control. This result signifies the formation of a reversible Michael adduct.

The free selenol and thiol content of PbTx-2 treated GM02152 cells were lower as compared to the control. The treatment of cells with the antioxidant, Trolox did not have

significant efficacy for restoring the thiol/selenol content. However, vitamin C significantly enhanced cell viability, the thiol/selenol content and lipid peroxidation was similar to Trolox treatment.

4.5 Materials and methods

2-Thiobarbituric acid (TBA) was purchased from MP biomedicals and 1,1,3,3-tetraethoxypropane (TEP) was purchased from Chem-Impex Int'l Inc.

DTNB reduction, reactivity with reduced selenocysteine, gel filtration, selenocystine, hydrogen peroxidase reduction and NADPH oxidase were performed according to procedure reported in section 3.5. All experiments are done in triplicate.

4.5.1 Preparation of cell lysates for biochemical assays

GM02152 cells (2.5×10^7) were seeded in 75 cm^2 flasks containing growth medium. After the cells reached log phase, growth medium was removed by centrifugation and replaced with fresh medium containing: 1 μM PbTx-2 or 1 μM PbTx-2 + 100 μM Trolox or DMSO alone. The cells were exposed for 24 hour after which they were resuspended in growth medium and centrifuged (720 ×g, 4 min). The supernatant was discarded, and the cells were lysed by the addition of 100 μL lysis buffer (10 mM Tris-HCl, 200 mM KCl, 2 mM EDTA, 40% glycerol, 0.2% TritonX-100, pH 7.5) by rotating at 4 °C for 2 hour as previously described. Cellular debris was removed by centrifugation at 17000 ×g at 4 °C for 30 min. Protein concentration of the lysate was determined by the Bradford method using the Coomassie protein assay reagent in duplicate. Typical concentrations of the lysate ranged from 10 to 15 mg/mL.

4.5.2 DTNB assay on cell lysates

DTNB (100 μL, 5 mM in 0.1 M sodium phosphate, 1 mM EDTA pH 8) solution was added to the cell lysate (90 μg of total protein/well) and absorbance was measured immediately at 410 nm. The assay was performed in triplicate.

4.5.3 Thiobarbituric acid-reactive substances (TBARS) assay on cell lysates

Lipid peroxidation was determined by measuring the level of thiobarbituric acid-reactive substances (TBARS) in cells. Proteins were precipitated from the cell lysate (160 μg of total protein) by the addition of trichloroacetic acid (500 μL, 20%) followed by centrifugation at 14,000 × g for 15 min. To the supernatant thiobarbituric acid solution (500 μL of 0.67% in 10% DMSO) was added. The mixture was then heated for 15 min at 90 °C. Absorbance was measured in triplicate at 532 nm.

4.5.4 Sel green assay on cell lysates

In a 96 well plate, Sel green probe (10 μL, 48 μM final concentration in 20% acetone in PBS) was added to cell lysate (75 μg of total protein/ well) to quantify the amount of selenocysteine. The mixture was incubated for 5 min and the fluorescence was measured at λ_{ex} = 502 and λ_{em} = 370 nm. Each treatment was analyzed in triplicate.

4.5.5 Statistical analysis of cytotoxicity and cell lysate assays

All data values are given as mean ± standard error. ANOVA was per- formed by a Tukey Honestly Significant Difference test using the JMP 13.0.0 Software

Chapter 5. Effect of MC-LR and reduced MC-LR on TrxR1, mTrxR and DmTrxR variants

5.1 Objective

Similar to PbTx-2, MCLR activates DTNB reduction by TrxR1. Most microcystin variants have a dehydroalanine residue within the peptide ring which could contribute to the formation of a Michael adduct with TrxR. The main objective of this chapter is to better understand the mechanism of activation of TrxR by microcystins which includes evaluation of the significance of the α, β-unsaturated carbonyl group in activation of DTNB reduction by TrxR. This goal will be accomplished by reducing the dehydroalanine of MC-LR with $NaBH_4$. Further the reactivity of MCLR with Sec of TrxR will be evaluated by using mutants of mTrxR and DmTrxR.

5.2 Introduction

Cyanobacteria are photosynthetic bacteria that are found in fresh, estuarine and marine waters. The cyanobacteria are prokaryotic and may produce cyanotoxins and some are also responsible for cyanobacterial harmful algal blooms (HABs). These algae are capable of forming blooms which can appear as a thick blue green mat like scum. The cause of the bloom is mainly a result of eutrophication. Phosphorus from agricultural land run-off to lakes and especially phosphorus promotes additional growth[113]. Cyanotoxins are broadly divided into neurotoxin like anatoxin-a(s) and saxitoxin, dermatoxin like lyngbyatoxin, and hepatoxin like nodularin, cylinderospermopsin, and microcystin. Toxins are released into the water when the algae die and cell wall break.

Microcystins (MC's) are cyclic heptapeptides as shown in Figure 61. About 80 congeners of microcystin have already been identified. Most of the microcystins have five constant amino acids and two variable amino acids (X and Y as shown in Table 23. One of the abundantly found microcystin is microcystin-LR (MC-LR). LR is named for two variable amino acids leucine (L) and arginine (R) at the X and Y positions respectively. They also possess the characteristic long-chain, β-amino acid, called Adda (all-*S*, all-*E*)-3-amino-9-methoxy-2, 6,8-trimethyl-10-phenyldeca-4, 6-dienoic acid.

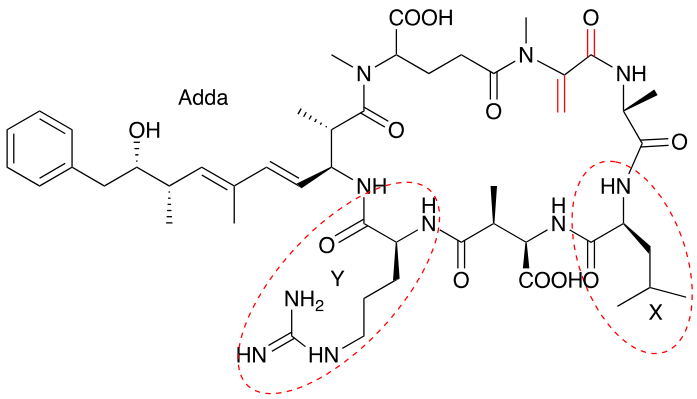

Figure 61. Microcystin LR

Table 23. Microcystin and some of the most common congeners

Name	X-position amino acid	Y-position amino acid	Molecular weight (Dalton)
Microcystin LA	Leucine (L)	Alanine (A)	910.06
Microcystin YR	Tyorosine (Y)	Arginine (R)	1045.19
Microcystin RR	Arginine (R)	Arginine (R)	1038.2
Microcystin LR	Leucine (L)	Arginine (R)	995.17

5.3 Effect of microcystin in human health

Drinking water is the major route for toxin of exposure in the human body. Microcystins have been reported to be present in treated water[114]. This poses a major challenge for municipalities that use surface water as their drinking water source. Other routes can be food chain, ingestion or inhalation of contaminated water during recreational use. Once in the body, microcystin are carried to the liver cells by Organic Anion Transporting Polypeptides (OATP) where they covalently link to active cysteine residue of protein phosphatase 2A and protein phosphatase 1 in the cytosol[115] and inhibit these enzymes. This enzyme cleaves phosphate groups from the proteins. As a result, phosphorylated proteins accumulate in the liver cell. Numerous physiological processes are regulated by phosphorylation and dephosphorylation of enzymes thus the inhibition of dephosphorylation disrupts cellular homeostasis. This is the primary mechanism of toxicity. However, like many inhibitors of TrxR, MC-LR also has the presence of α, β- unsaturated carbonyl in the dehydroalanine amino acid, which can serve as a Michael acceptor and inhibit the enzyme. The requirement of this functional group has been evaluated by reducing dehydroalanine of MC-LR. Further to understand if MC-LR interacts with Sec of TrxR site-specific mTrxR and DmTrxR variants are used.

5.4 Results and Discussion

5.4.1 Reduction of MC-LR

The dehydroalanine in MC-LR, the site thought to be responsible for forming Michael adduct is reduced as previously described[116] using $NaBH_4$ for 96 hours as shown

in reaction in Figure 62. The completion of reduction was confirmed with MALDI-MS (Matrix Assisted Laser Desorption/Ionization-Mass spectrometry) as shown in Figure 63.

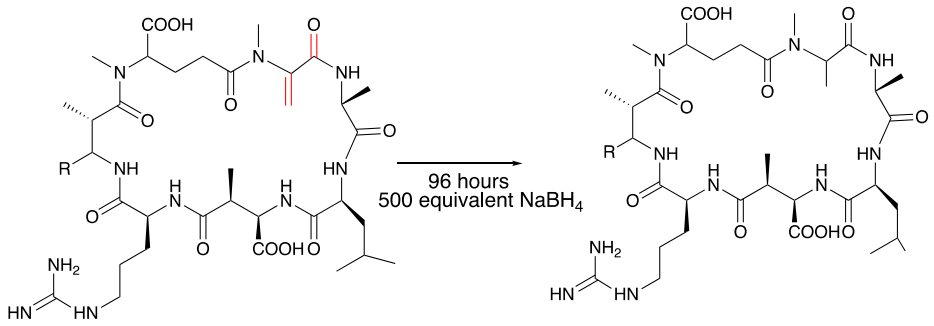

Figure 62. Reduction of MC-LR. MC-LR (0.5 mg) reduced with freshly prepared $NaBH_4$ in H_2O (9ml, 1mg/ml) for 96 hours. The reduced MC-LR was cleaned with C-18 column and inspected with MALDI-MS. Adda moiety is represented as R

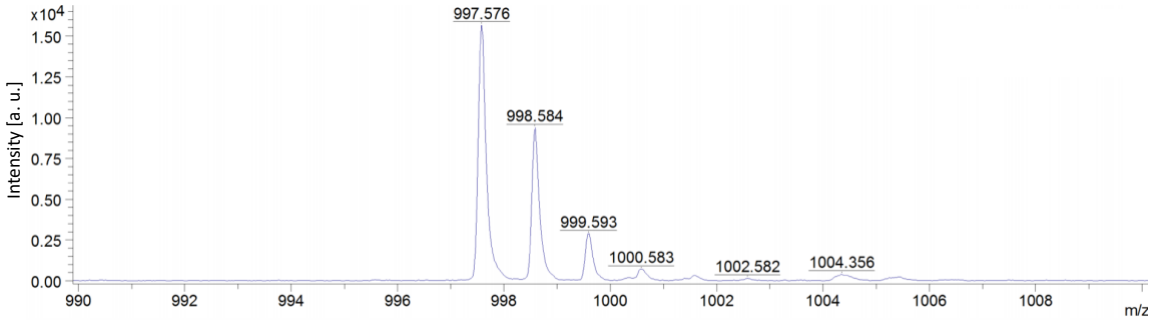

Figure 63. MALDI-MS result for reduced MC-LR. The absence of *m/z* 995.55 peak which corresponds to M+1 of MC-LR and appearance of *m/z* at 997.576 (corresponding to M+1 of reduced MC-LR) represents the complete reduction of MC-LR

5.4.2 Reactivity of MC-LR and reduced MC-LR with seleno-*L*-cysteine

The reactivity of MC-LR with reduced selenocysteine suggests that dehydroalanine of MC-LR could be the possible site for reactivity with Sec of TrxR. Reduced MC-LR fails to react with selenocystine. If the dehydroalanine is required for the activation of TrxR then we would predict that dihydro MC-LR would not avtivate TrxR (Figure 64).

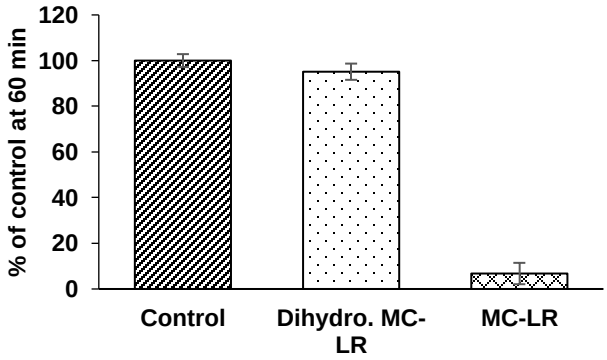

Figure 64. Reaction of reduced seleno-*L*-cysteine (20 μM) with Sel-green probe (20 μM) after incubation with the MC-LR and dihydro MC-LR (20 μM for 60 min)

5.4.3 DTNB as a substrate for TrxR1 and mTrxR variants

MC-LR activates DTNB reduction of TrxR1, mTrxR2 (GCUG), mTrxR2 (GCCG) and mTrxR2 (Δ8) by 3.3-fold, 2.9-fold, 2.3-fold and 4.2-fold respectively as shown in Figure 65 and Table 24. The DTNB reduction in the presence of dihydro MC-LR (Figure 66) also exhibits the activation comparable to unreduced MC-LR. This fact emphasizes that MC-LR does not require a dehydroalanine for activation of DTNB reduction by TrxR. This fact is further supported by activation of DTNB reduction in the presence of MCLR by the dead tail and truncated mutants of mTrxR, neither of which has a C-terminal active site Cys or Sec.

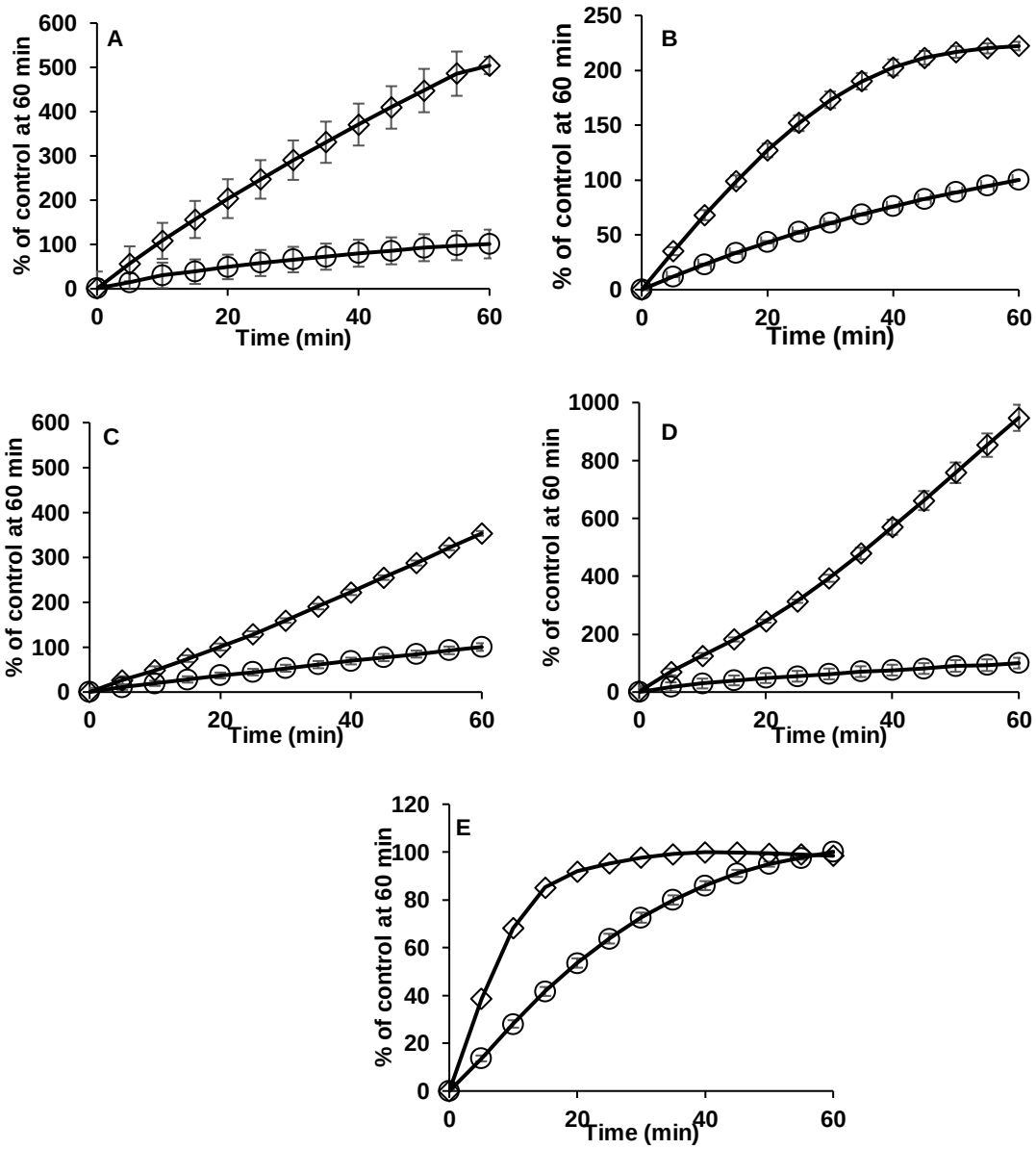

Figure 65. Reduction of DTNB (2 mM) by TrxR in the presence of MC-LR (20 μM). (**A**) TrxR1 (5.12 nM); (**B**) mTrxR2 (GCUG) (5.12 nM); (**C**) mTrxR2 (GCCG) (5.12 nM); (**D**) mTrxR2 (GSSG) (5.12 nM); (**E**) mTrxR2 (Δ8) (10 nM). MC-LR (◇). Control (DMSO only, ○).

Table 24. Enzyme activity expressed as TNB^{2-} mol/min-mol enzyme for TrxR control and activation of DTNB reduction reported as relative rate for MC-LR and dihydro MC-LR with respect to control. The consumption of DTNB was calculated from standard curve of TNB^{2-}

	TrxR1	**mTrxR2 (GCUG)**	**mTrxR2 (GCCG)**	**mTrxR2 (GSSG)**	**mTrxR2 (Δ8)**
Control	634 ± 47.3	785 ± 11.0	249 ± 23.2	226 ± 17.0	995 ± 65.5
MC-LR	3.32**	2.90**	2.25**	4.21**	2.42**
Dihydro MC-LR	3.55**	0.89**	0.99	1.27	1.14

The number of asterisks indicate significant differences compared with control (** p <0.01)

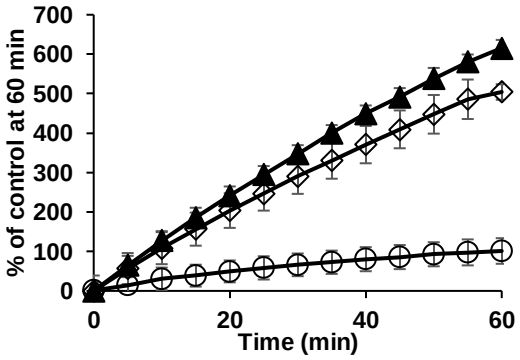

Figure 66. Reduction of DTNB (2 mM) by TrxR1 (5.12 nM) in the presence of dihydro MC-LR (20 μM, ▲) and MC-LR. (20 μM, ◇); Control (DMSO only, ○)

5.4.4 DTNB as a substrate for DmTrxR variants

MC-LR activates DTNB reduction of DmTrxR (SCUG) and DmTrxR (Δ8) by 1.7-fold and 2.5-fold respectively as shown in Figure 67 and Table 25.

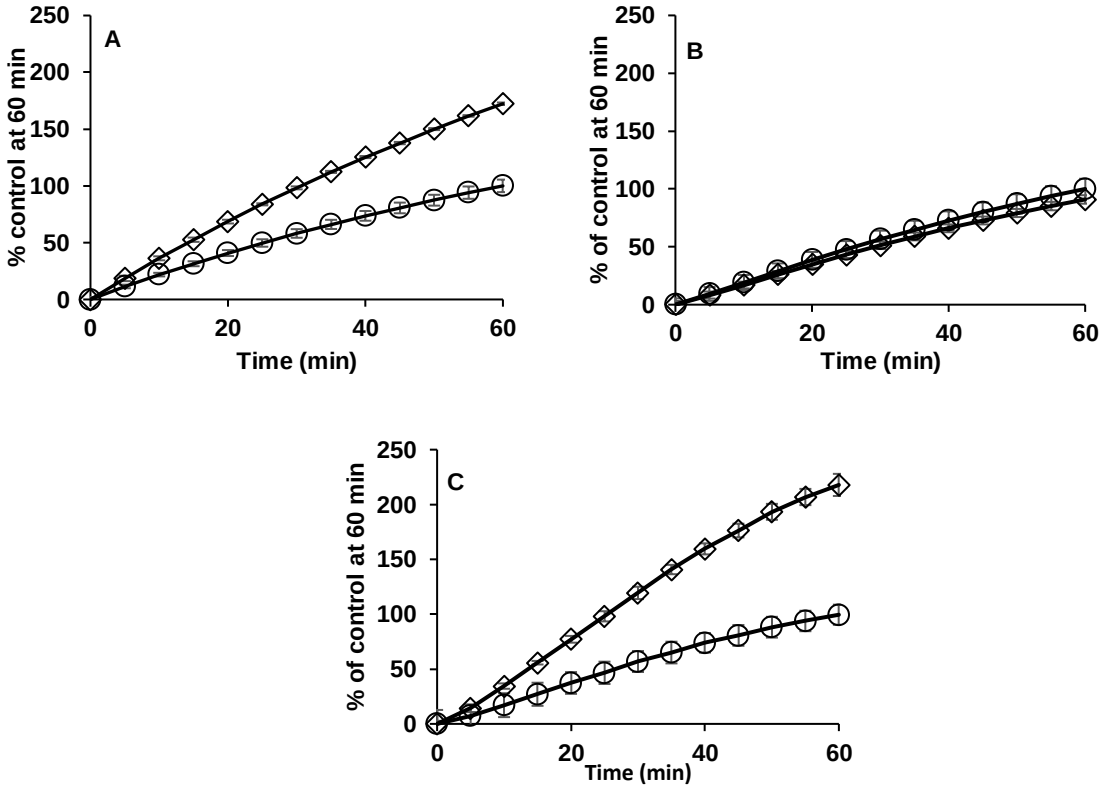

Figure 67. Reduction of DTNB (2 mM) by DmTrxR in the presence of MCLR (20 μM). (**A**) DmTrxRSCUG (10 nM); (**B**) DmTrxRSCCS (50 nM); (**C**) DmTrxR (Δ8) (10 nM). MCLR (◇); Control (DMSO only, ○)

Table 25. Enzyme activity expressed as TNB^{2-} mol/min-mol enzyme for DmTrxR control and activation of DTNB reduction reported as relative rate for MC-LR with respect to control. The consumption of DTNB was calculated from standard curve of TNB^{2-}

	DmTrxR (SCUG)	**DmTrxR (SCCS)**	**DmTrxR (Δ8)**
Control	70.4 ± 2.25	34.5 ± 10.3	24.6 ± 5.03
MC-LR	1.68**	1.15	2.49**

The number of asterisks indicate significant differences compared with control (** p <0.01)

5.4.5 Irreversible inhibition TrxR by MC-LR

In order to determine if the MC-LR covalently formed an adduct with the C-terminal redox center of TrxR, DTNB reduction was performed as usual with TrxR1, mTrxR2 (GCUG) and mTrxR2 (GCCG) incubated with MCLR (4.2 μM) after size

exclusion chromatography to remove unbound MCLR. After incubation, the mixture was passed through a gel filtration column (MW cutoff of 6000 amu) followed by a 30 min incubation with additional NADPH to reduce TrxR (Figure 68). The reduction of DTNB by TrxR enzymes incubated with MC-LR as well as TrxR reduced only after passing through size exclusion column was not activated in any of the enzymes, revealing either non-covalent or reversible covalent interaction between the enzymes (TrxR1, mTrxR2 (GCUG) and mTrxR2 (GCCG)) and MC-LR. Such interaction is not possible with dead tail and truncated enzyme due to lack of C-terminal active site.

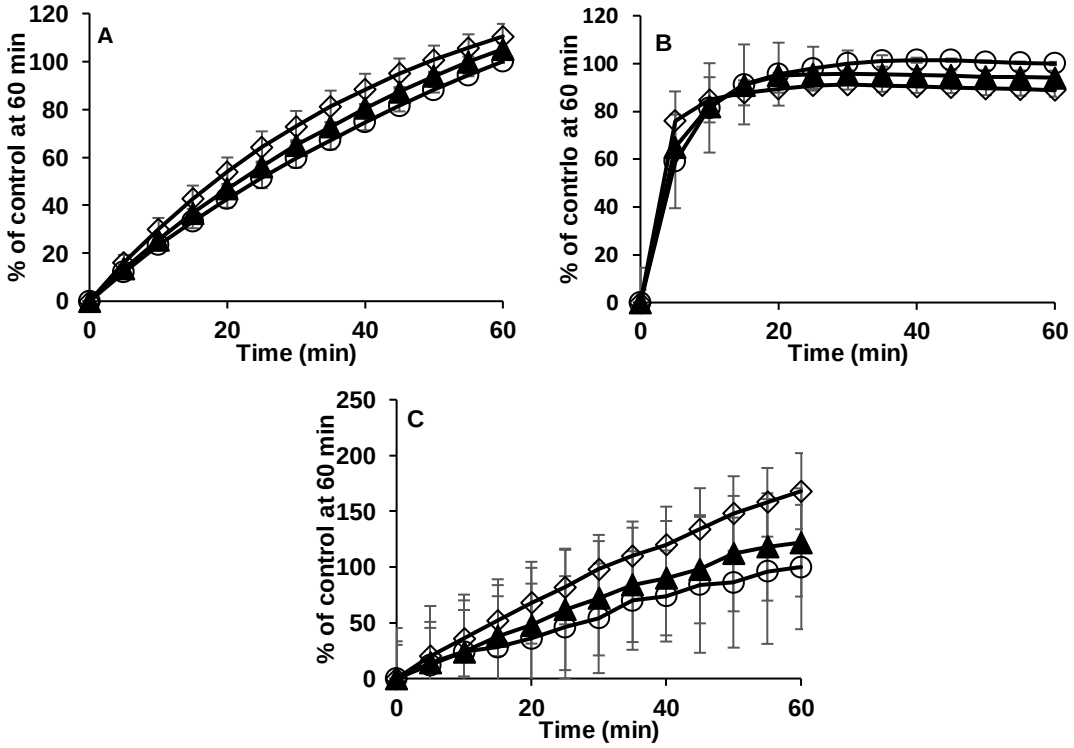

Figure 68. Test of irreversibility of inhibition of DTNB reduction by TrxR in the presence of MC-LR (4.2 μM). (**A**) TrxR1 (5.2 nM); (**B**) mTrxR2 (GCUG) (5.2 nM); (**C**) mTrxR2 (GCCG) (5.2 nM). TrxR reduced only after removal of activator/test compounds by gel filtration (◇); Control (no MC-LR, ○); MC-LR removed by gel filtration after incubation with reduced TrxR (▲)

5.4.6 TrxR/Trx insulin reduction in the presence of MC-LR

Neither MC-LR nor reduced MC-LR inhibit insulin reduction by TrxR, which support the hypothesis that these compounds either non-covalently or irreversibly interact with TrxR (Figure 69).

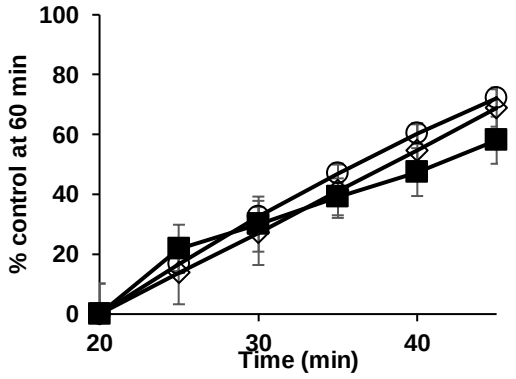

Figure 69. TrxR1/Trx reduction in the presence of MC-LR (◇, 20 μM) and dihydro MC-LR (■, 20 μM).

5.4.7 Reactivity of TrxR1 and mTrxR variants with substrate selenocystine in the presence of MC-LR

Unlike auranofin, the reduction of selenocystine is not compromised in the presence of MC-LR. The reduction of selenocystine requires a C-terminal redox site. Mutation of the C-terminal Sec to Cys reduces the rate of selenocystine reduction by 5-fold [25]. As shown in Figure 70 and Table 26, a comparison of the selenocystine reduction in the presence of MC-LR by all enzymes reveals that Sec remains free to reduce selenocystine when not pre-incubated with reduced TrxR.

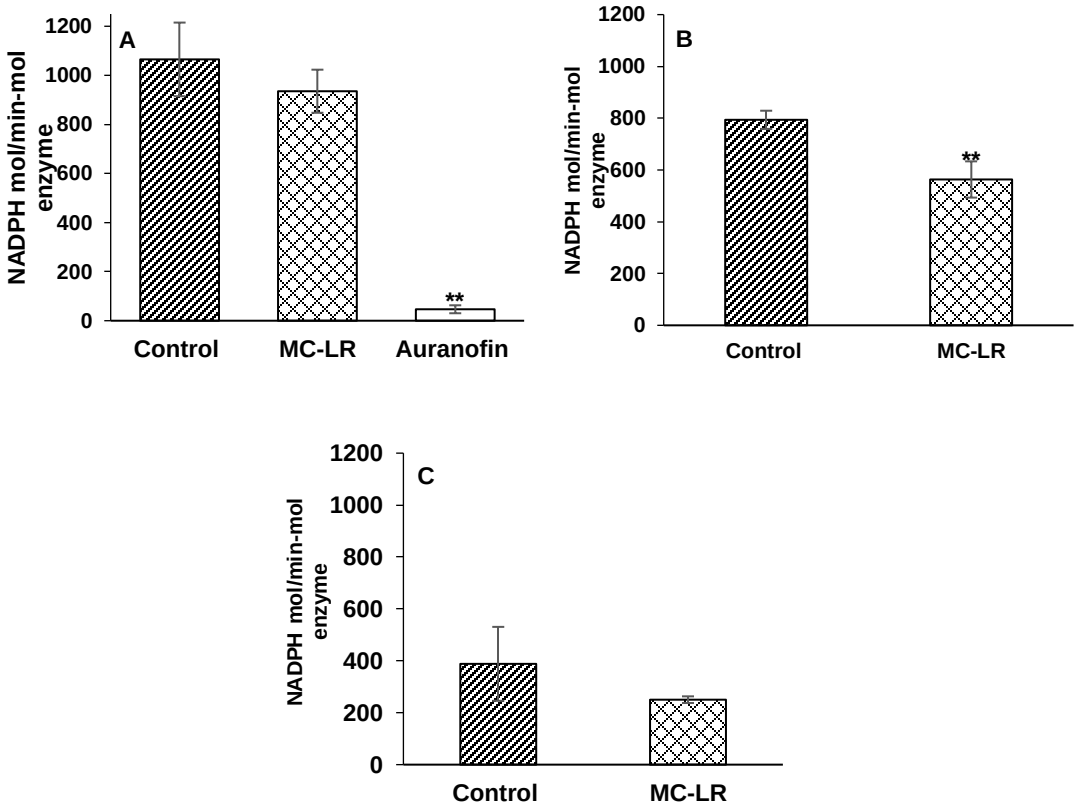

Figure 70. Reduction of selenocystine (120 μM) by TrxR (20 nM) in the presence of MC-LR and auranofin (38.5 μM); (**A**) TrxR1; (**B**) mTrxR2 (GCUG); (**C**) mTrxR2 (GCCG)**.** The number of asterisks indicate significant differences compared with control (* p <0.05, ** p <0.01)

Table 26. Rates of selenocystine reduction by TrxR enzymes in the presence of MC-LR. NADPH consumption expressed as NADPH mol/min-mol enzyme

	TrxR1	**mTrxR2 (GCUG)**	**mTrxR2 (GCCG)**
Control	1065 ± 150	794 ± 35.1	388 ± 142
MC-LR	935 ± 87.8	563 ± 69.9**	250 ± 12.8

The number of asterisks indicate significant differences compared with control (* p <0.05, ** p <0.01)

As shown in Figure 71 and Table 27, the selenocystine reduction after incubation (15 minutes) of MC-LR with reduced TrxR resulted in decrease of 1.3-fold in the presence of MC-LR as compared to mTrxR2 (GCUG) control. On the other hand, auranofin completely inhibited the reduction of selenocystine either incubated with MC-LR or not with all the enzymes.

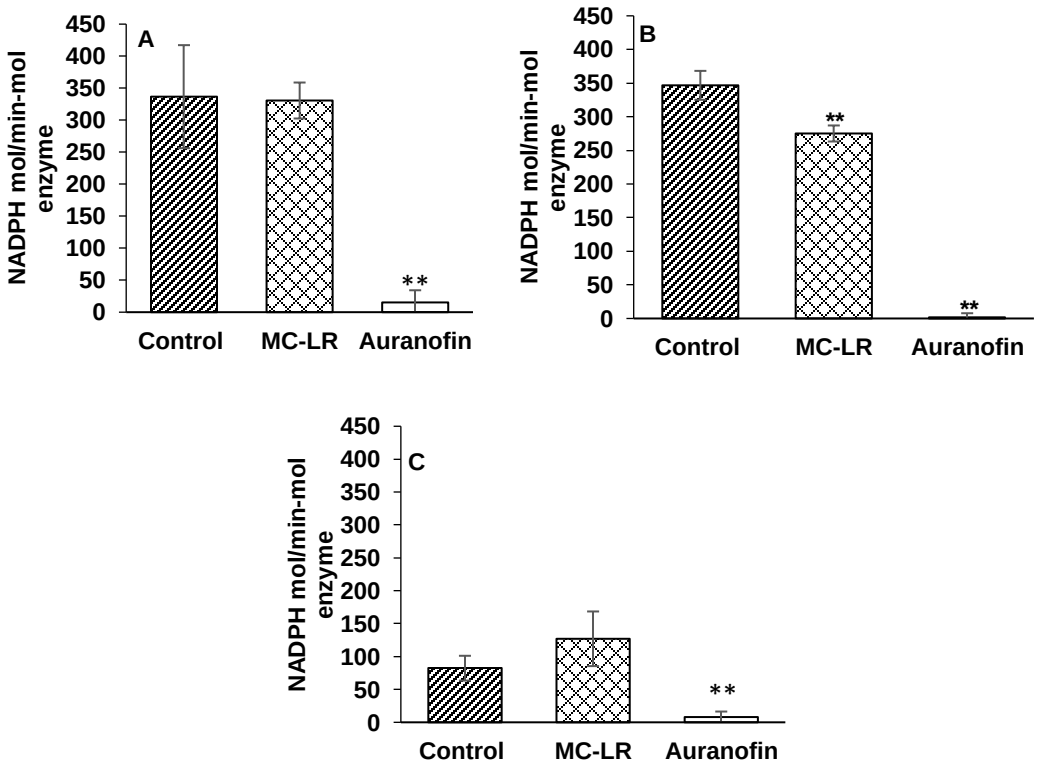

Figure 71. Reduction of selenocystine (120 μM) by TrxR (20 nM) after 15 minutes incubation with MC-LR and auranofin (38.5 μM); **(A)** TrxR1; **(B)** mTrxR2 (GCUG); **(C)** mTrxR2 (GCCG). The number of asterisks indicate significant differences compared with control (* p <0.05, ** p <0.01)

Table 27. Rates of selenocystine reduction by TrxR enzymes after 15 minutes incubation with MC-LR. NADPH consumption expressed as NADPH mol/min-mol enzyme

	TrxR1	**mTrxR2 (GCUG)**	**mTrxR2 (GCCG)**
Control	337 ± 80.5	347 ± 21.5	82.2 ± 18.8
MC-LR	331 ± 28.1	275 ± 11.9**	127 ± 41.5
Auranofin	15.2 ± 19.0**	1.67 ± 6.14**	8.00 ±8.35**

The number of asterisks indicate significant differences compared with control (* p <0.05, ** p <0.01)

5.4.8 Reactivity of TrxR1 and mTrxR2 (GCUG) with substrate hydrogen peroxide in the presence of MC-LR

In the presence of MC-LR, hydrogen peroxidase activity was not compromised as shown in Figure 72 and Table 28. Reduction of H_2O_2 requires C-terminal Sec^{97-98}. The

result presented below shows that MC-LR does not interact with Sec in absence of pre-incubation.

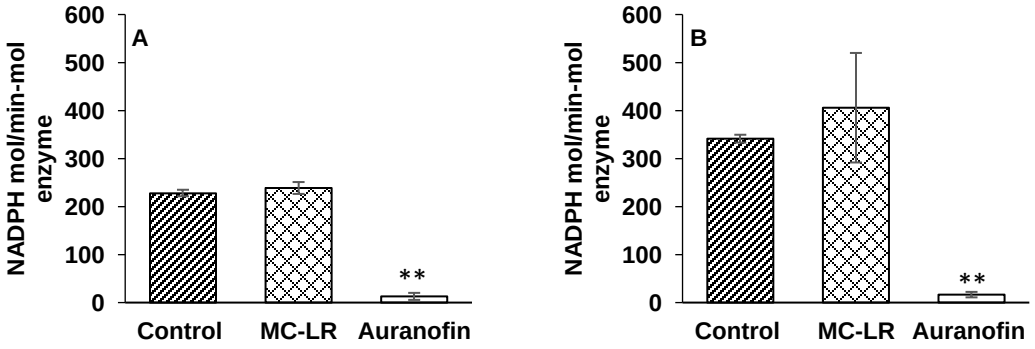

Figure 72. Hydrogen peroxide reduction by TrxR (50 nM) in the presence of MC-LR and auranofin (38.5 μM). (**A**) TrxR1; (**B**) mTrxR2 (CGUG). The data is expressed as NADPH consumption during reduction of H_2O_2. The number of asterisks indicate significant differences compared with control (* p <0.05, ** p <0.01)

Table 28. Rate of H_2O_2 reduction by TrxR in the presence of MC-LR and auranofin. NADPH consumption expressed as NADPH mol/min-mol enzyme

	TrxR1	**mTrxR2 (GCUG)**
Control	228± 6.84	341± 8.20
MC-LR	239 ± 12.36	406±114
Auranofin	12.89 ±7.29**	16.6 ±5.71**

The number of asterisks indicate significant differences compared with control (* p <0.05, ** p <0.01)

MC-LR induced 1.4-fold increase in H_2O_2 reduction as compared to mTrxR2 (GCUG) control when incubated for 15 minutes, as shown Figure 73 and Table 29 while no significant change is observed with TrxR1.

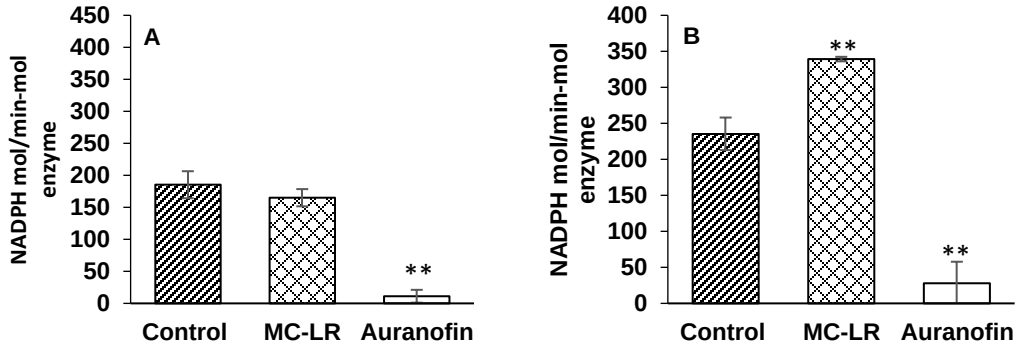

Figure 73. Hydrogen peroxide reduction by TrxR (50 nM) after 15 minutes incubation with MC-LR and auranofin (38.5 μM). (**A**) TrxR1; (**B**) mTrxR2 (CGUG). The data is expressed as NADPH consumption during reduction of H_2O_2. The number of asterisks indicate significant differences compared with control (* p <0.05, ** p <0.01)

Table 29. Rate of H_2O_2 reduction by TrxR after 15 minutes incubation with MC-LR and auranofin. NADPH consumption expressed as NADPH mol/min-mol enzyme

	TrxR1	**mTrxR2 (GCUG)**
Control	185 ± 21.0	235 ± 22.6
MC-LR	165 ± 13.4	339± 3.12**
Auranofin	11.1 ± 10.0**	27.9 ±29.9**

The number of asterisks indicate significant differences compared with control (* p <0.05, ** p <0.01)

5.4.9 NADPH oxidase activity of TrxR enzymes in the presence of MC-LR

Modification of the C-terminal Sec of TrxR by alkylation or coordination with a noble metal induces the NADPH oxidase activity of TrxR [49]. This can be measured by monitoring NADPH consumption in the absence of a disulfide or diselenide substrate. In the presence of MC-LR, NADPH consumption by TrxR1 increased by 1.3-fold as compared to controls as listed in in Table 30.

Table 30. NADPH consumption by TrxR in the presence of MC-LR (38.5 μM). NADPH consumption expressed as NADPH mol/min-mol enzyme

	TrxR1	**mTrxR2 (GCUG)**	**mTrxR2 (GCCG)**	**mTrxR2 (GSSG)**	**mTrxR2 (Δ8)**
Control	3.63 ± 3.37	0.93 ± 0.14	0.40 ± 0.15	0.55 ± 0.40	0.49 ± 0.43
MCLR	4.82 ± 5.49	1.27 ± 0.24	0.72 ± 0.66	0.39 ± 0.09	0.85 ± 1.07

The number of asterisks indicate significant differences compared with control (* p <0.05, ** p <0.01)

5.5 Conclusion

The summary of all the enzymatic assays in the presence of MC-LR is given in Table 31.

Table 31. Summary of TrxR activity in the presence of MC-LR

	TrxR1	**mTrxR2 (GCUG)**	**mTrxR2 (GCCG)**	**mTrxR2 (GSSG)**	**mTrxR2 (Δ8)**
DTNB reduction	Activate	Activate	Activate	Activate	Activate
Insulin reduction	No inhibition	-	-	-	-
DTNB reduction after size exclusion	No activation	No activation	No activation	-	-
NADPH oxidase	No activation	No activation	No activation	No activation	No activation
Selenocystine reduction	No activation	Inhibit	No activation	No activation	No activation
Selenocystine reduction (15 minutes incubation)	No activation	Inhibit	No activation	-	-
H_2O_2 reduction	No activation	No activation	-	-	-
H_2O_2 reduction (15 minutes incubation)	No activation	Activate	-	-	-

MC-LR activates DTNB reduction with all the enzymes tested. On the other hand, reduced MC-LR that does not have α, β-unsaturated carbonyl group activates DTNB reduction by TrxR1 while it has little effect on the other enzymes. Failure to inhibit selenocystine reduction and failure to activate DTNB reduction after removal of MC-LR by size exclusion also indicates that the interaction between TrxR and MC-LR is either non-covalent or reversible. Further this hypothesis is supported by the failure of both MC-LR and reduced MC-LR to inhibit insulin reduction in a Trx dependent reaction.

5.6 General experiment

Microcystin-LR was purified from biomass collected during an algae bloom[117] according to published protocols[116]. Dihdro MC-LR was prepared according to published methods[118] and analyzed by MALDI-MS. The Sel-green probe was synthesized according to published methods[93] . All assays were performed in triplicate. Results are presented as an average of three trials ±standard deviation. Error limits on graphs represent the standard deviation of three trials.

DTNB reduction, reactivity with reduced selenocysteine, gel filtration, selenocystine, hydrogen peroxidase reduction and NADPH oxidase were performed according to procedure reported in section 3.5

5.6.1 Preparation, purification and analysis of dihydro MCLR

The dehydroalanine of MC-LR (0.5 mg, 0.5 μmol) was reduced with 0.23 mmol of freshly prepared $NaBH_4$ in H_2O for 96 hours. Fresh batch of $NaBH_4$ (500 μL) was added every 6 hours.

The reduced MC-LR was separated from inorganic by-products using a C-18 SPE column (10 gm). The SPE column was conditioned ith 100 ml of MeOH (followed by 100 ml distilled H_2O. The reduced sample was loaded in the column and washed with 100 ml of H_2O to remove the impurities. Finally, the reduced MC-LR was eluted with 50 ml of 100% MeOH and reconstituted in 1 mg/ml final concentration.

MALDI-TOF-MS analysis was conducted on a Bruker AutoFlex III instrument, utilizing the dried droplet technique. The instrument was operated in the reflectron mode and positive (+) ion polarity. The sample was diluted in a 1:10 ratio with 50/50 H_2O:MeCN, before being mixed in a 1:1 ratio with a matrix solution composed of α-cyanno-4-hydroxycinnamic acid (α-CHCA) in a solvent system consisting of 50/50 H_2O:MeCN with 0.5% TFA. For Reduced MCLR, mass spectrometry analysis detected a peak at m/z =997.576 with a mass error of + 4.32 ppm corresponding to the theoretical m/z = 997.572 for the $[M+H]^+$ ion of formula $C_{49}H_{76}N_{10}O_{12}$. In addition, a peak was observed at *m/z* = 1019. 596 with a mass error of + 9.8 ppm with respect to the theoretical *m/z* = 1019.554 for the $[M+Na]^+$ for formula $C_{49}H_{76}N_{10}O_{12}$. Other ions were also detected at *m/z* = 1015.596, 1031.583, 1037.536, 1041.541, and 1063.540.

5.6.2 DTNB reduction with reduced MC-LR

The DTNB reduction with reduced MC-LR is performed in the similar way as regular DTNB assay, refer to Section 3.5.1. The concentration of reduced MC-LR was estimated form absorption of the Adda group at 238 nm by comparing with standard unreduced MC-LR. The control sample has an equal amount of DMSO.

Chapter 6. Effect of antibiotics on TrxR1, mTrxR and DmTrxR

6.1 Objective

Manumycin, an antitumor compound with several α, β-unsaturated carbonyl moieties is a potent inhibitor of TrxR1 and induce apoptosis by generating ROS. The effect of antibiotics (Ga, Rf and Th) with similar electrophilic functional groups on TrxR will be studied in this chapter using WT and mutants of mTrxR and DmTrxR.

6.2 Introduction

Geldanamycin (Ga) and rifamycins are bacterial ansamycin antibiotics that have aromatic group linked by an aliphatic chain. Ga binds to highly conserved pocket of heat shock protein 90 (Hsp90) and inhibit the enzyme[119]. Hsp are a family of chaperone proteins that regulates many critical functions in cells including refolding, protein stabilization[120-121]and indirectly controling apoptosis by inhibiting caspsase[122]. HSP is upregulated in numerous cancer and tumor cells[123-124] because of which it has been a primary target for cancer treatment[125-131].

The rifamycin class includes derivatives of rifamycin including rifamycin SV (Rf). The family of rifamycin drug has been effective in treatment of disease involving bacteria mycobacterium and act by inhibiting bacterial RNA polymerase[132] . Rifamycins have multiple targets including transcriptional repression protein BCL6 (B cell lymphoma 6 protein)[133] and organic anion transporting polypeptide[134].

Th, a naturally occurring antibacterial oligopeptide that inhibits bacterial protein synthesis by binding to ribosomal RNA but does not affect eukaryotic protein synthesis[135]. It is also an inhibitor of peroxiredoxin (Prx 3) an important scavenger of

H_2O_2 and lipid peroxide, and is upregulated in cancerous cell[136]. As the result of inhibition of peroxiredoxin, FOXM1 (Forkhead box M1) an important oncogenic transcription factor[137] is downregulated.

Cancer cells treated with these antibiotics have been known to produce ROS. The napthohydroquinone of Rf and quinione of Ga can accept one or two electrons from NADPH and undergo oxidation or reduction in the presence of appropriate reductase and dehyrogenases. Rf can undergo redox recycling in the presence of NADPH/NADH, rat liver microsomes and Fe catalyst[138] to produce $^{\cdot}OH$, H_2O_2 and $O_2^{-\cdot}$ radical. Similarly, one electron reduction of Ga by cytochrome P450 reductase in the presence of NADPH produces $O_2^{-\cdot}$ radical [139-140]. The $O_2^{-\cdot}$ radical has been reported to be produced in malignant mesothelioma cells as a result of Prx3 inhibition by Th[137].

6.3 Results and Discussion

6.3.1 Reactivity of antibiotics with seleno-*L*-cysteine

The reactivity with reduced selenocysteine in the reaction monitored by release of fluorophore from Sel-green probe[93] indicates all the antibiotics may react with TrxR, as shown from Figure 74.

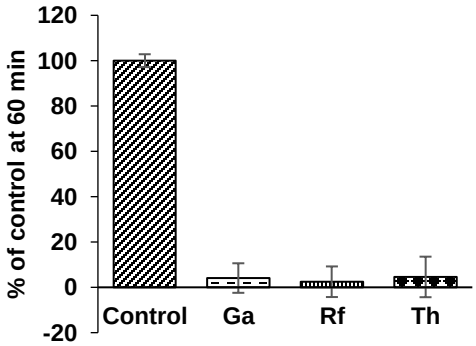

Figure 74. Reaction of reduced seleno-*L*-cysteine (20 μM) with Sel-green probe (20 μM) after incubation with the Ga, Rf and Th (20 μM for 60 min)

6.3.2 DTNB as a substrate for TrxR1 and mTrxR variants

Ga, Rf and Th activates the reduction of DTNB by TrxR1, mTrxR2 (GCUG), mTrxR2 (GCCG) and mTrxR2 (Δ8) as shown in Figure 75 and Table 32.

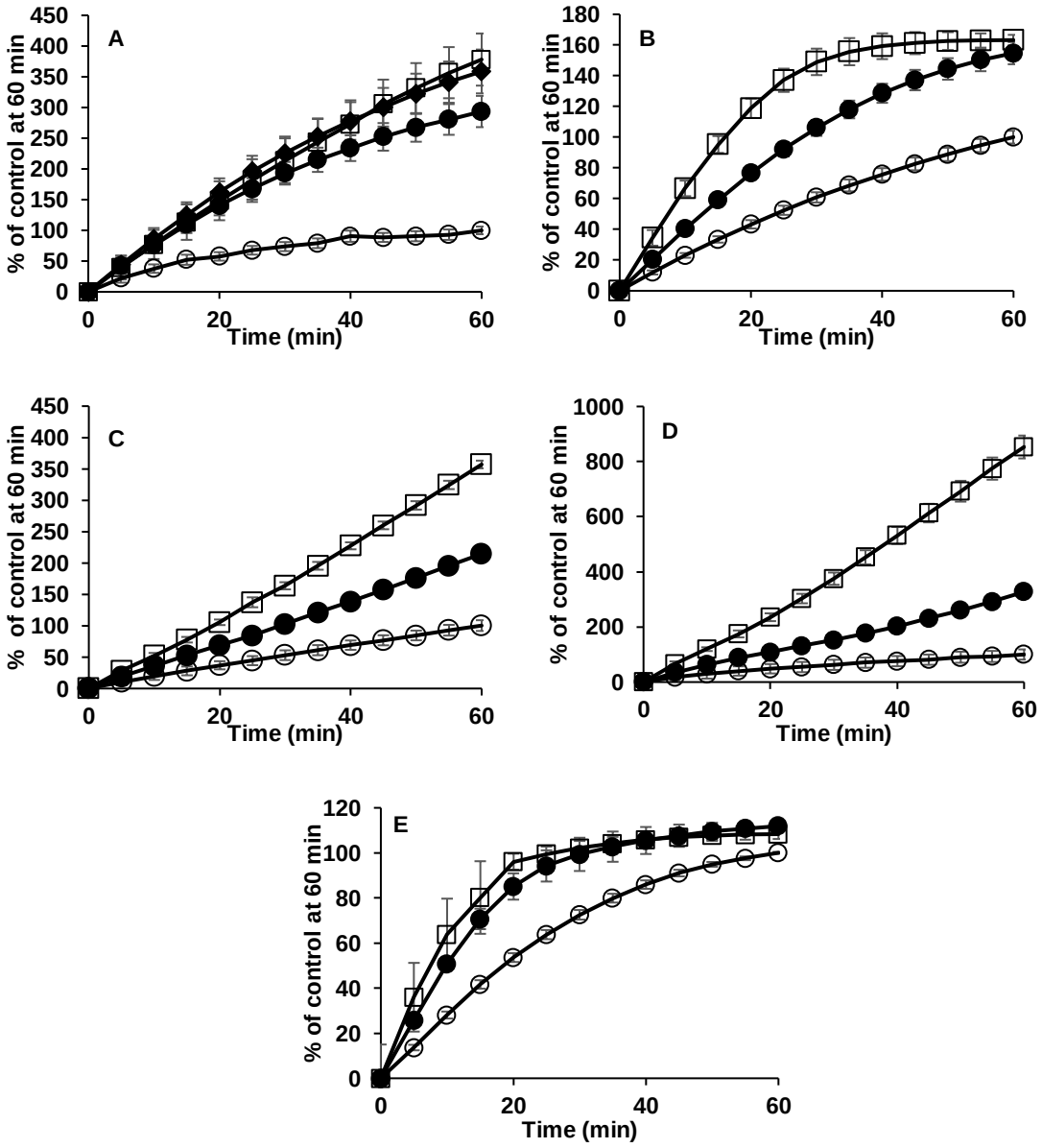

Figure 75. Reduction of DTNB (2 mM) by TrxR (5.12 nM) in the presence of Ga; Rf and Th (20 μM). (**A**) TrxR1; (**B**) mTrxR2 (GCUG); (**C**) mTrxR2 (GCCG); (**D**) mTrxR2 (GSSG); (**E**) mTrxR2 (Δ8). Ga (◆); Rf (●); Th (□) and Control (DMSO only, ○)

Table 32. Enzyme activity expressed as TNB^{2-} mol/min-mol enzyme for TrxR control and activation of DTNB reduction reported as relative rate for Ga, Rf and Th with respect to control.

	TrxR1	**mTrxR2 (GCUG)**	**mTrxR2 (GCCG)**	**mTrxR2 (GSSG)**	**mTrxR2 (Δ8)**
Control	634 ± 47.3	785 ± 11.0	249 ± 23.2	226 ± 17.0	995 ± 65.5
Ga	2.67**	-	-	-	-
Rf	2.33**	1.96**	1.53**	1.82**	2.01**
Th	2.35**	3.04**	2.40**	4.42**	2.37**

The number of asterisks indicate significant differences compared with control (** p <0.01)

6.3.3 DTNB as a substrate for DmTrxR variants

Ga, Rf and Th activate the DTNB reduction of DmTrxR (SCUG), DmTrxR (SCCS) and DmTrxR (Δ8) as shown in Figure 76 and Table 33.

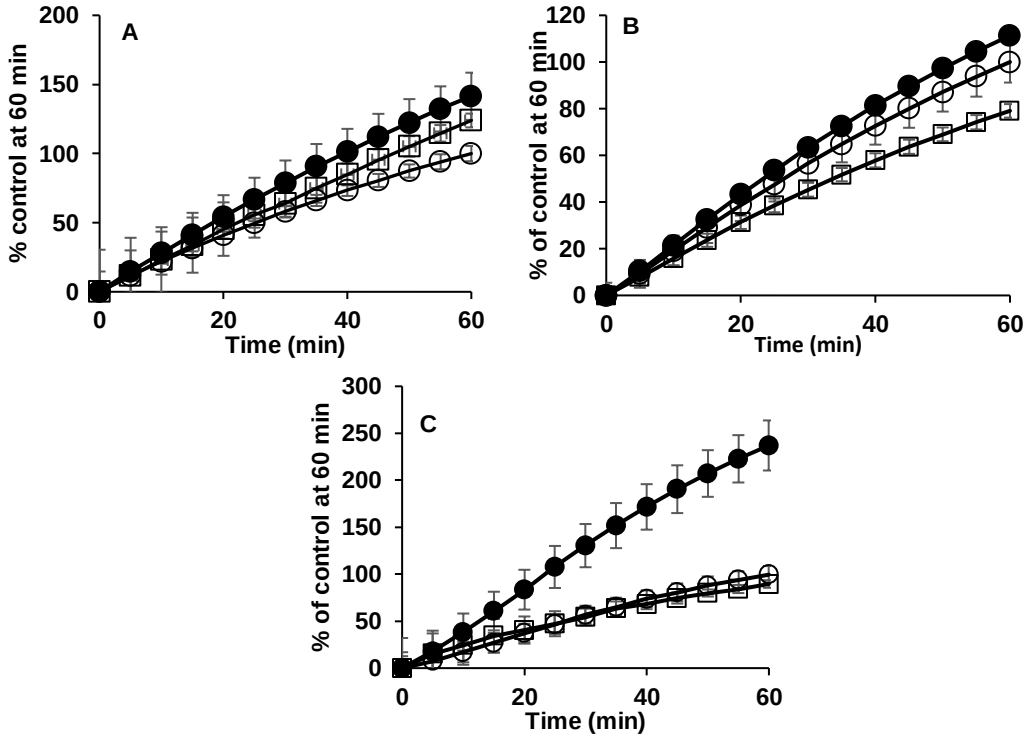

Figure 76. Reduction of DTNB (2 mM) by DmTrxR in the presence of Rf and Th (20 µM). (**A**) DmTrxRSCUG (10 nM); (**B**) DmTrxRSCCS (50 nM); (**C**) DmTrxRΔ8 (10 nM). The control sample was prepared by adding an equal volume of DMSO. Rf (20 µM, ●); Th (20 µM, □) and Control (DMSO only, ○)

Table 33. Enzyme activity expressed as TNB^{2-} mol/min-mol enzyme for DmTrxR control and activation of DTNB reduction reported as relative rate for Ga, Rf and Th with respect to control.

	DmTrxR (SCUG)	**DmTrxR (SCCS)**	**DmTrxR (Δ8)**
Control	70.4 ± 2.25	34.5 ± 10.3	24.6 ± 5.03
Rf	1.32**	1.44*	2.64**
Th	1.03	1.02	1.13**

The number of asterisks indicate significant differences compared with control (* p <0.05, ** p <0.01)

6.3.4 Reduction of DTNB by TrxR1 in the simultaneous the presence of curcumin and antioxidants

The TrxR is known to react with the residue of TrxR1. Competition assays with C-terminal Sec two inhibitor inhibitor curcumin and the test compounds for TrxR1 could

help to isolate the site of interaction. When TrxR1 was incubated first with curcumin (20 μM, 30 minutes) followed by either Ga, Rf or Th (20 μM, 30 minutes), DTNB reduction was comparable to the curcumin only, as shown in Table 34 (not significantly different). When TrxR1 was incubated with the test compounds first followed by curcumin, the Ga, Rf and Th treated enzyme remains active (336, 289 and 154% of the curcumin control respectively). The thiostrepton treated samples retain about 50% of the original enzyme activity. The pre-treatment of TrxR1 with three of the test compounds, Ga, Rf and Th prevented the curcumin induced inhibition of DTNB reduction by TrxR1 suggesting competition for the same site.

Table 34. Initial rates (V_0) of DTNB reduction in the presence of the test compounds (20 μM) vs curcumin (20 μM) relative to the control. Control rate; 634 ± 47.2 mole TNB^{2-}/min-mol TrxR

	Curcumin first	**Curcumin second**
Curcumin only	0.01	0.01
Ga	1.22	3.36
Rf	0.22	2.89
Th	0.2	1.54

6.3.5 TrxR1/Trx insulin reduction in the presence of antioxidants

None of the antibiotics inhibit insulin reduction by TrxR1(Figure 77) which is contradicting as in the competition with curcumin added second, these compounds still showed activation (Section 6.3.4). The possibility of reversible or non-covalent interaction with C-terminal redox site of TrxR1 could explain the observed reduction of insulin.

The other possibility of such result would be if the interaction of antibiotics with TrxR1 would expose N-terminal thiols. The reduced thiol could then reduce the insulin (6

kDa) directly without reduction of large Trx (11.7 kDa) In order to evaluate this hypothesis, insulin reduction assay was performed in absence of hTrx-1. As shown in Figure 78, in the absence of hTrx-1 and the presence of Ga (20 μM) the reduction of insulin is prevented which suggest that insulin reduction only occurs via reduced hTrx-1.

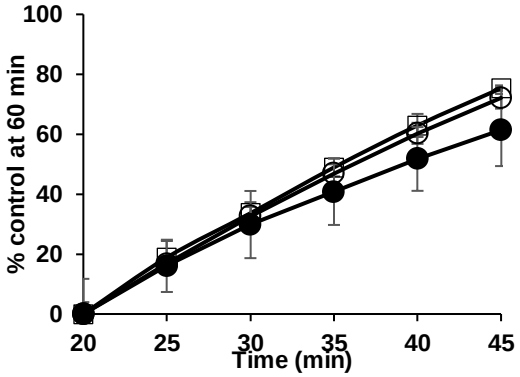

Figure 77. TrxR1/Trx reduction in the presence of Rf and Th (20 μM). Rf (●); Th (□) and control (DMSO only, ○)

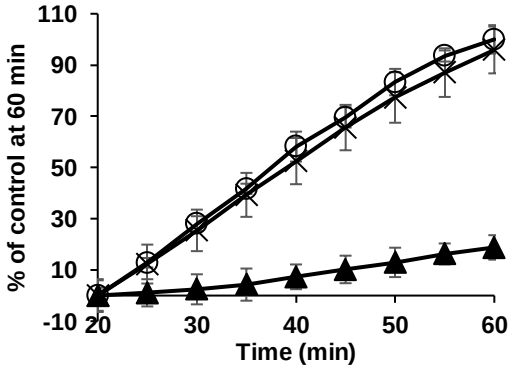

Figure 78. TrxR1/Trx inhibition in the absence of hTrx-1and in the presence of Ga (20 μM). Ga (×); Control (○); Ga without hTrx-1 (▲). Data expressed as % of control at 60 min.

6.3.6 Native PAGE gel for determination of disruption of TrxR1 by Ga

Ladder shaped polyether compounds like desulfated yessotoxin and brevetoxin-2 are known to interact with the α-helix and disrupt the oligomeric glycophorin A, a transmembrane protein in erythrocytes[141]. If disruption of TrxR1 is induced by these compounds each monomer could reduce DTNB via the N-terminal redox center, by-passing the C-terminal redox center, and might explain the result observed with DTNB reduction. Similar result of enhanced activity has been reported as the result of acetylation of TrxR1 at Lys^{141}, Lys^{200} and Lys^{307} which increases the population of active dimeric TrxR1[142]. A native PAGE gel (as SDS is known to disrupt TrxR dimers)[143] was run to test this hypothesis. The disruption of the TrxR dimer should result in monomeric band at 55 kDa. The comparison of control and Ga treated TrxR in a native gel is shown in Figure 79. This result demonstrates that Ga does not disrupt TrxR1 dimers which contradict the original hypothesis.

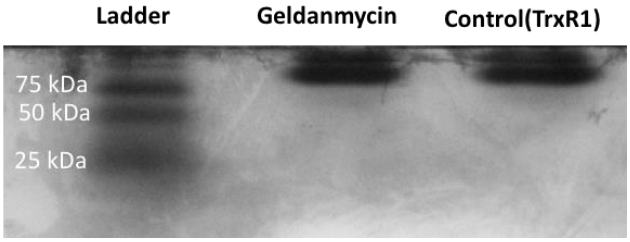

Figure 79. Native PAGE for determination of disruption of TrxR1 by Ga. Rat recombinant TrxR1 (4.7 μg) was incubated with (2.5 mM) Ga for an hour. The control sample have equivalent amount of DMSO.

6.3.7 Reactivity of TrxR1 and mTrxR variants with substrate selenocystine in the presence of antibiotics

As shown in Figure 80 and Table 35, TrxR enzymes are not inhibited in the presence of these antibiotics and the rates are either comparable to or higher than the respective controls. In the presence of Ga and Rf, the selenocystine reduction increased

by 1.6-fold and 1.4-fold as compared to mTrxR2 (GCUG) control while Rf and Th induced 1.7-fold and 1.7-fold of activation of selenocystine reduction when compared to mTrxR2 (GCCG) control. Because this reaction is faster when there is a free selenol in the C-terminal redox center, this resut suggests involvement of Sec in reduction of selenocystine which could only be possible when these antibiotics react non-covalently or reversible with enzymes.

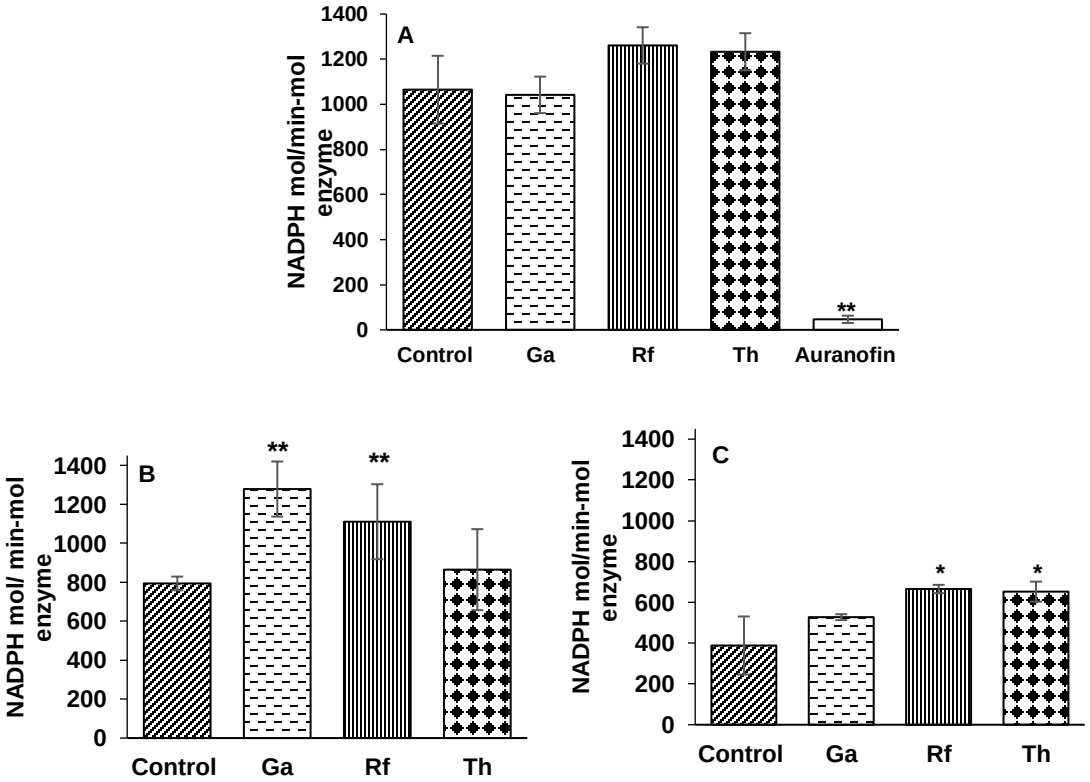

Figure 80. Reduction of selenocystine by TrxR (20 nM) in the presence of Ga; Th; Rf (38.5 μM) and auranofin (62.5 μM). (**A**) TrxR1; (**B**) mTrxR2 (GCUG); (**C**) mTrxR2 (GCCG). The number of asterisks indicate significant differences compared with control (* p <0.05, ** p <0.01)

Table 35. Rates of of selenocystine reduction by TrxR enzymes in the presence of Ga, Rf, auranofin and Th with respect to control. NADPH consumption expressed as NADPH mol/min-mol enzyme

	TrxR1	**mTrxR2 (GCUG)**	**mTrxR2 (GCCG)**
Control	1065 ± 150	794 ± 35.1	388 ± 142
Ga	1042 ± 80.8	1278 ± 141**	527 ± 14.4
Rf	1261 ± 80.6	1110 ± 193**	665 ± 20.4*
Th	1233 ± 82.3	865 ± 208	652 ± 49.0*

The number of asterisks indicate significant differences compared with control (* p <0.05, ** p <0.01)

As shown in Figure 81 and Table 36, the selenocystine reduction after incubation (15 minutes) of Ga, Rf and Th with reduced TrxR resulted in increase of 1.5-fold in the presence of Th as compared to TrxR1 control. Similarly, Ga, Rf and Th induced 1.2-fold, 1.2-fold and 1.6-fold as compared to mTrxR2 (GCUG) control respectively while only Th induced 2.5-fold increase in selenocystine reduction as compared to mTrxR2 (GCCG) control. On the other hand, auranofin completely inhibited the reduction of selenocystine either incubated with antioxidants or not with all the enzymes.

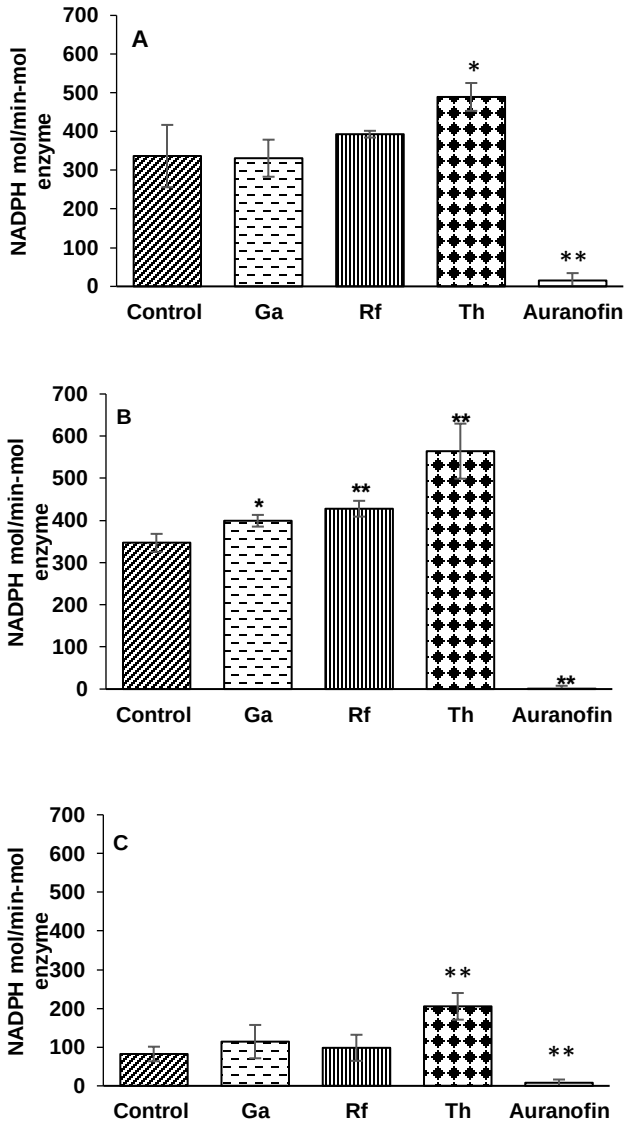

Figure 81. Reduction of selenocystine by TrxR (20 nM) after 15 minutes incubation with Ga; Th and Rf (38.5 μM) and auranofin (62.5 μM); (**A**) TrxR1; (**B**) mTrxR2 (GCUG); (**C**) mTrxR2 (GCCG). The number of asterisks indicate significant differences compared with control (* p <0.05, ** p <0.01)

Table 36. Rates of of selenocystine reduction by TrxR enzymes after 15 minutes incubation with Ga, Rf, auranofin and Th with respect to control. NADPH consumption expressed as NADPH mol/min-mol enzyme

	TrxR1	**mTrxR2 (GCUG)**	**mTrxR2 (GCCG)**
Control	337 ± 80.5	347 ± 21.5	82.2 ± 18.8
Ga	331 ± 47.9	399 ± 13.9*	114 ± 43.1
Rf	393 ± 8.70	428 ± 18.8**	98.2 ± 33.6
Th	489 ± 36.0*	564 ± 65.3**	205 ± 34.5**
Auranofin	15.23 ± 19.0**	1.67 ± 6.14**	8.00 ± 8.35**

The number of asterisks indicate significant differences compared with control (* p <0.05, ** p <0.01)

6.3.8 Reactivity of TrxR1 and mTrxR2 (GCUG) with substrate hydrogen peroxide in the presence of antibiotics

In the presence of antioxidants, hydrogen peroxidase activity was not compromised as shown in Figure 82 and Table 37. Reduction of H_2O_2 requires C-terminal Sec[97-98]**.**The result presented below shows that these antioxidants do not interact with Sec.

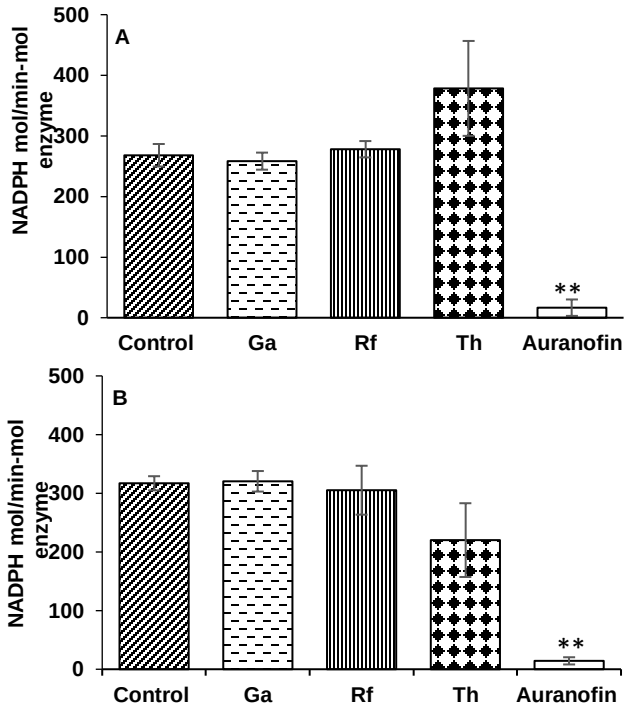

Figure 82. Hydrogen peroxide reduction by TrxR (50 nM) in the presence of Ga; Rf, Th and auranofin (38.5 μM). (**A**) TrxR1; (**B**) mTrxR2 (CGUG). The data is expressed as NADPH consumption during reduction of H_2O_2. The number of asterisks indicate significant differences compared with control (* p <0.05, ** p <0.01)

Table 37. Rate of H_2O_2 reduction by TrxR1 and mTrxR2 (GCUG) in the presence of Ga, Rf, auranofin and Th with respect to control. NADPH consumption expressed as NADPH mol/min-mol enzyme

	TrxR1	**mTrxR2 (GCUG)**
Control	268± 18.6	317±12.0
Ga	258 ± 14.0	320±17.5
Rf	278± 13.5	305±41.6
Th	378± 78.3	220±62.8
Auranofin	16.6±13.6**	14.3 ±6.15**

The number of asterisks indicate significant differences compared with control (* p <0.05, ** p <0.01)

However, only Th induced 1.7-fold increase in H_2O_2 reduction as compared to mTrxR2 (GCUG) control when incubated for 15 minutes. Other antibiotics did not vary

significantly with their control except for auranofin which completely inhibit reduction of H_2O_2 with or without 15 minutes incubation, as shown in Figure 83 and Table 38. This increased activity of selenocystine reduction by TrxR in the presence of Th could be the possible result of increase in number of TrxR dimer.

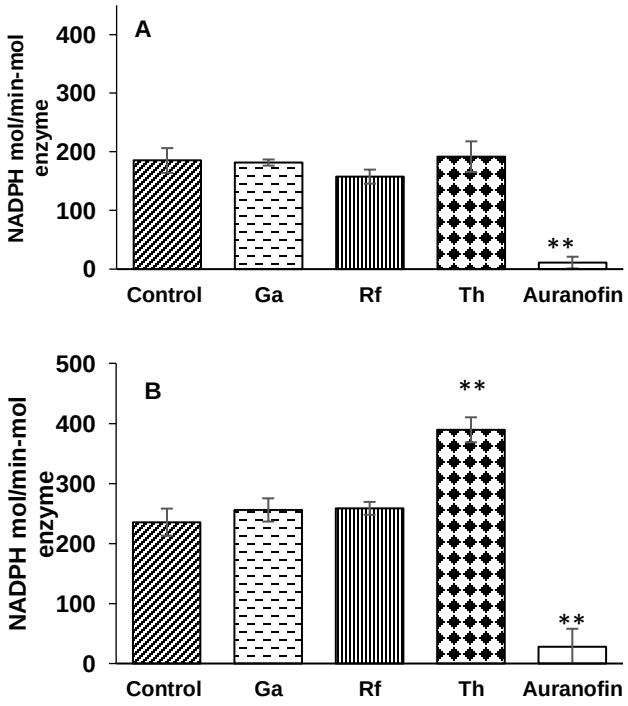

Figure 83. Hydrogen peroxide reduction by TrxR (50 nM) after 15 minutes incubation with Ga; Rf; Th and auranofin (38.5 μM). (**A**) TrxR1; (**B**) mTrxR2 (CGUG). The data is expressed as NADPH consumption during reduction of H_2O_2 at 10 minutes. The number of asterisks indicate significant differences compared with control (* p <0.05, ** p <0.01)

Table 38. Rate of H_2O_2 reduction by TrxR1 and mTrxR2 (GCUG) after 15 minutes incubation with Ga, Rf, auranofin and Th with respect to control. NADPH consumption expressed as NADPH mol/min-mol enzyme

	TrxR1	**mTrxR2 (GCUG)**
Control	185± 21.0	235±22.6
Ga	182 ± 5.26	256±19.3
Rf	158 ± 11.9	258±10.7
Th	192± 26.2	389±20.8**
Auranofin	11.1 ±10.0**	27.9 ±29.9**

The number of asterisks indicate significant differences compared with control (* p <0.05, ** p <0.01)

6.3.9 NADPH oxidase activity of TrxR enzymes in the presence of antibiotics

Inhibition of TrxR at the C-terminal redox center induces NADPH oxidase activity. Rf enhanced NADPH oxidase activity by 7.8-fold with TrxR1, 5.2-fold with mTrxR2 (GCUG) and 3.9-fold with mTrxR2 (Δ8), as shown in Table 39. Th enhanced NADPH oxidase activity by 3.4-fold with mTrxR2 (GCUG) and 7.2-fold with mTrxR2 (Δ8).

Table 39. NADPH consumption by TrxR in the presence of Ga, Rf and Th. NADPH consumption expressed as NADPH mol/min-mol enzyme

	TrxR1	**mTrxR2 (GCUG)**	**mTrxR2 (GCCG)**	**mTrxR2 (GSSG)**	**mTrxR2 (Δ8)**
Control	1.13 ± 0.09	0.93 ± 0.14	2.04 ± 1.39	0.11 ± 0.04	0.49 ± 0.43
Ga	1.88 ± 0.90	0.55 ± 0.28	0.68 ± 0.25	0.07 ± 0.01	0.10 ± 0.07
Rf	8.76 ± 0.33**	4.81 ± 0.52**	-1.29 ± 2.42	0.10 ± 0.07	1.94 ± 0.94**
Th	2.88 ± 2.49	3.13 ± 0.27**	3.92 ± 2.03	2.09 ± 1.13*	3.52 ± 2.34**

The number of asterisks indicate significant differences compared with control (* p <0.05, ** p <0.01)

6.4 Conclusion

Although all antibiotics tested activate DTNB reduction by TrxR1 and mTrxR2 enzymes, DmTrxR enzymes are not affected by Th and Rf. Failure to inhibit insulin reduction by TrxR1 indicates a non-covalent or reversible interaction with C-terminal redox center also supported by selenocystine reduction. Rf and Th induced NADPH oxidase activity in TrxR1, mTrxR2 (GCUG) and mTrxR2 (Δ8). Rf having a napthoquinone that can undergo autoxidation in the presence of metal ion[135] have known to produce ROS such as $^{\cdot}OH$, $O_2^{-\cdot}$ and H_2O_2. Based on this fact, the NADPH oxidase induced by Rf on TrxR1 can be explained.

6.5 Materials and methods

Ga was purchased from TSZ Chem, Rf from MP Biomedicals and Th from Cayman Chemical. All assays were performed in triplicate. Results are presented as an average of three trials ±standard deviation. Error limits on graphs represent the standard deviation of three trials.

DTNB reduction, reactivity with reduced selenocysteine, gel filtration, selenocystine, hydrogen peroxidase reduction and NADPH oxidase were performed according to procedure reported in section 3.5.

6.5.1 Native page gel for disruption of TrxR1 dimer by Ga

TrxR1 (3.5 μL,12 μM) was reduced with NADPH (4.5 μL,1.34 mM) and incubated for 1 hour in the presence of Ga (2 μL,2.5 mM) in 0.5 M Tris-HCl pH 6.8 for. The control sample has equivalent volume of DMSO. The samples were analyzed by

native PAGE gel (10% acrylamide) in 1X Tris glycine buffer (25 mM Tris-base, 192 mM glycine) for 15 hours at 0^0C. The gel was stained with coomassie brilliant blue.

6.5.2 TrxR1/Trx inhibition assay without hTrx-1 in presence of Ga

The assay was performed in 384 well black flat bottom plate in a final volume of 100 µL. Rat TrxR1 (10 µL, 1 µM, 0.2 mg/mL BSA, 50 mM Tris-Cl, 1 mM EDTA pH 7.5) was pre-reduced with NADPH (5 µL, 5.37 mM) in the presence of Ga (10 µL, 200 µM in 25% DMSO) final concentrations of 20 µM. After 30 minutes, human Trx-1 (10 µL, 1 µM) was added to Ga control sample only but not for Ga without hTrx-1 sample and incubated for an additional 30 minutes. Fluorescent substrate (20 µL, 0.4 mg/ml, eosin labeled bovine insulin) was added to the enzyme/Ga mixture (80 µL) to initiate the reaction. The fluorescence was monitored at λex/λem= 520nm/545 nm every 5 minutes for 1 hour.

6.5.3 Reduction of DTNB by TrxR1 in the simultaneous the presence of curcumin and antioxidants

The assay was performed by addition of curcumin (20 µM) added first and incubated for 30 minutes followed by addition of testcompounds or vice versa. DTNB (20 µL, 10 mM) in 0.1 M sodium phosphate and 1 mM EDTA, pH 7.5 was added to initiate the reaction. The reduction of DTNB was monitored at 412 nm every 5 minutes for 1 hour.

Chapter 7. Summary and future direction of research work

7.1 Summary of DTNB reduction

Except Man-A and deoxyman-A all other test compounds resulted in activation as shown in Table 40. The activation induced by test compounds on dead tail and truncated enzymes reveals the fact that covalent adducts at Sec or Cys is not required.

Table 40. Summary for DTNB reduction assay with all the enzymes and test compounds

	TrxR1	**mTrxR2 (GCUG)**	**mTrxR2 (GCCG)**	**mTrxR2 (GSSG)**	**mTrxR2 (Δ8)**
PbTx-3	Activate	Activate	Activate	Activate	Activate
PbTx-2	Activate	Activate	Activate	Activate	Activate
MC-LR	Activate	Activate	Activate	Activate	Activate
Dihydro MC-LR	Activate	*	*	*	*
Nodularin	Activate	#	#	#	#
Ga	Activate	#	#	#	#
Rf	Activate	Activate	Activate	Activate	Activate
Th	Activate	Activate	Activate	Activate	Activate
Man-A	Inhibit	Activate	Activate	Activate	Activate
Dihydroman-A	Activate	#	#	#	#
Deoxyman-A	Inhibit	#	#	#	#

Indicate test compound have not been tested

*Indicate no difference between control and sample

7.2 Summary for TrxR/Trx reduction

The reduction of insulin occurs via reduced Trx which in turn is reduced by reduced TrxR. When the C-terminal redox center is alkylated, this would interrupt the flow of electron and hence prevent the reduction of insulin, as shown by PbTx-2 and Man-A (Table 41). In the presence of rest of the test compounds the insulin reduction is not interrupted which would imply that these compounds are interacting non-covalently or reversibly with C-terminal redox center.

Table 41. Summary for TrxR/Trx reduction with all the enzymes and test compounds

	TrxR1	**mTrxR2 (GCUG)**
PbTx-3	*	#
PbTx-2	Inhibit	#
MC-LR	*	#
Dihydro MC-LR	*	#
Nodularin	#	#
Ga	*	#
Rf	*	#
Th	*	#
Man-A	Inhibit	Inhibit

Indicate test compound have not been tested

*Indicate no difference between control and sample

7.3 Summary of selenocystine reduction

The reduction of selenocystine requires the C-terminal Sec/Cys, Sec being more efficient than Cys. The pre-incubation of Man-A with reduced TrxR1 and mTrxR2 (GCCG) resulted in inhibition of selenocystine reduction (Table 42). Reaction of Man-A with TrxR1 is time dependent and the results indicate the initial alkylation at Cys followed by covalent adduct at Sec (also proved by gel filtration chromatography). On the other hand, Man-A activates slenocystine reduction of mTrxR2 (GCUG). Such activation can also be observed with other test compounds revealing the non-covalent interaction at Cys.

When the test compounds were not pre-incubated, most of the test compounds activate the selenocystine reduction (Table 42) which could be possible when the Cys of TrxR is adducted leaving the Sec to reduce selenocystine. The activation observed in the presence of test compounds also directs the possibility of selenocystine to be reduced by N-terminal. MC-LR is the only one compounds that inhibit the reduction of selenocystine indicating the interaction at C-terminal Sec.

Table 42. Summary of selenocystine reduction with and without pre-incubation

	Pre-incubation			No pre-incubation		
	TrxR1	**mTrxR2 (GCUG)**	**mTrxR2 (GCCG)**	**TrxR1**	**mTrxR2 (GCUG)**	**mTrxR2 (GCCG)**
PbTx-2	*	Activate	Activate	*	*	*
MC-LR	*	Inhibit	*	*	Inhibit	*
Ga	*	Activate	*	*	Activate	*
Rf	*	Activate	*	*	Activate	Activate
Th	Activate	Activate	Activate	*	*	Activate
Man-A	Inhibit	Activate	Inhibit	Activate	Activate	*

*Indicate no difference between control and sample

7.4 Summary of H_2O_2 reduction

The reduction of H_2O_2 absolutely requires the presence of C-terminal Sec. In the presence of Man-A, the reduction of H_2O_2 by TrxR1 and mTrxR2 (GCUG) is prevented when not pre-incubated (Table 43). Interaction of Man-A with Cys of TrxR could prevent the reduction of oxidized Sec (SeOH) and result in inhibition. The pre-incubation of Man-A with reduced TrxR alkylates the Sec (also proved by prevention of selenocystine reduction in the presence of Man-A).

Table 43. Summary of H_2O_2 reduction with and without pre-incubation

	Pre-incubation		No pre-incubation	
	TrxR1	**mTrxR2 (GCUG)**	**TrxR1**	**mTrxR2 (GCUG)**
PbTx-2	Inhibit	Activate	*	Inhibit
MC-LR	*	Activate	*	*
Ga	*	*	*	*
Rf	*	*	*	*
Th	*	Activate	*	*
Man-A	Inhibit	Inhibit	Inhibit	Inhibit

*Indicate no difference between control and sample

7.5 Summary of NADPH oxidase activity

Man-A induced NADPH oxidase activity with all the enzymes (Table 44). It is known that Man-A inhibit Sec of TrxR which induce production of $O_2^{-\cdot}$ by forming SecTRAP. The dead tail and truncated enzyme also consumed more NADPH in the presence of Man-A as well as Rf, Th and PbTx-2. This fact suggests that alkylation at Sec is not required for activation of NADPH consumption.

Table 44. Summary of NADPH oxidase activity

	TrxR1	**mTrxR2 (GCUG)**	**mTrxR2 (GCCG)**	**mTrxR2 (GSSG)**	**mTrxR2 (Δ8)**
PbTx-3	#	*	#	#	*
PbTx-2	*	*	*	Activate	Activate
MC-LR	*	*	*	*	*
Ga	*	*	*	#	*
Rf	Activate	Activate	*	*	Activate
Th	*	Activate	*	*	Activate
Man-A	Activate	Activate	Activate	Activate	Activate

Indicate test compound have not been tested

*Indicate no difference between control and sample

The test compounds were selected because of their similar size and molecular weight and electrophilic functional groups. All of the test compounds activate DTNB reduction by TrxR1 and mTrxR2 to different degrees except Man-A which inhibits TrxR1. Man-A acts by activating DTNB reduction by mTrxR2. TrxR1 and mTrxR2 enzymes are isoforms and have similar mechanism of reducing substrates. All the above results, it can be concluded that Man-A reacts with both C-terminal Cys/Sec. The reaction of Man-A with Sec is time dependent and covalent, possibly forms Michael adduct, as represented by path A in Figure 84. On the other hand, the reaction with Cys is reversible and takes place instantaneously as represented by path B in Figure 84. Most of the other

test compounds also react in similar way. Additional experiments are required to understand the underlying mechanism to prove the above stated hypothesis.

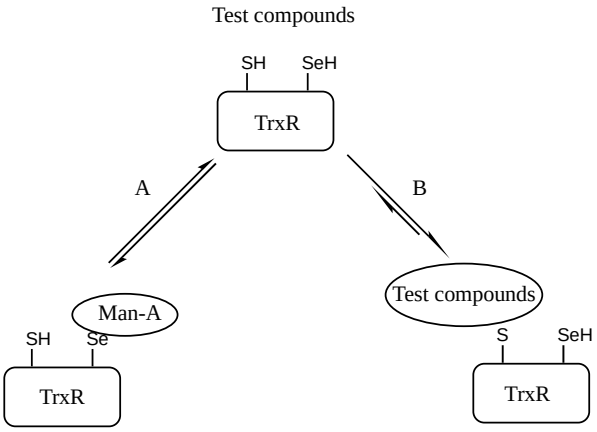

Figure 84. Hypothesized mechanism of interaction of test compounds with TrxR

7.6 Future direction

7.6.1 Evaluation of disruption of TrxR multimers

It still remains unclear the reason behind activation of DTNB reduction by TrxR in the presence of test compounds. We tried to reason if the increase in TrxR1 activity is due to disruption of TrxR1 dimer in the presence of Ga (presented in section 6.3.6) but did not observe as expected. Acetylation of Lys residue of TrxR1 increased the enzyme activity by destabilizing low activity multimers[140]. It could be possible that these test compounds may act in a similar manner by disrupting the TrxR multimers. This can be achieved by separating low activity tetramers of TrxR by passing through size exclusion chromatography. The quantification of active dimers can be then achieved by western blot technique.

7.6.2 Irreversible inhibition of TrxR by test compounds

The gel filtration chromatography experiment is inconclusive as these experiments are performed at very low concentration of 4.2 μM compared to 20 μM for DTNB reduction assay. Hence gel filtration experiment should be performed at 20 μM concentration. If the interaction of test compounds with TrxR is covalent then similar fold of activation should be observed in the sample incubated with test compounds after passing through size exclusion column in DTNB reduction.

7.6.3 Mass spectroscopy approach to identify the adduct

Our approach to identify the PbTx-2 + TrxR1 adduct was inconclusive as PbTx-2 being a large polyether compound forbid to ionize and hence was not observed in mass spectrometry. Alternatively, MC-LR being a peptide TrxR + MC-LR adduct could be observed in mass spectroscopy. Another alternative is to study X-ray crystal the test compound and TrxR.

References

1. Cremers, C. M.; Jakob, U. Oxidant sensing by reversible disulfide bond formation. *J. Biol. Chem.* **2013***, 288*, 26489-26496.

2. Miranda-Vizuete, A.; Damdimopoulos, A. E.; Spyrou, G. cDNA cloning, expression and chromosomal localization of the mouse mitochondrial thioredoxin reductase gene1. *Biochim Biophys. Acta, Gene Struct. Expression.* **1999***, 1447*, 113-118.

3. Conrad, M.; Jakupoglu, C.; Moreno, S. G.; Lippl, S.; Banjac, A.; Schneider, M.; Beck, H.; Hatzopoulos, A. K.; Just, U.; Sinowatz, F.; Schmahl, W.; Chien, K. R.; Wurst, W.; Bornkamm, G. W.; Brielmeier, M. Essential role for mitochondrial thioredoxin reductase in hematopoiesis, heart development, and heart function. *Mol. Cell. Biol.* **2004***, 24*, 9414-9423.

4. Jakupoglu, C.; Przemeck, G. K.; Schneider, M.; Moreno, S. G.; Mayr, N.; Hatzopoulos, A. K.; de Angelis, M. H.; Wurst, W.; Bornkamm, G. W.; Brielmeier, M.; Conrad, M. Cytoplasmic thioredoxin reductase is essential for embryogenesis but dispensable for cardiac development. *Mol. Cell. Biol.* **2005***, 25*, 1980-1988.

5. Park, U.; Han, H.; Um, E.; An, X.; Kim, E.; Um, S. Redox regulation of transcriptional activity of retinoic acid receptor by thioredoxin glutathione reductase (TGR). *Biochem. Biophys. Res. Commun.* **2009***, 390*, 241-246.

6. Tinkov, A. A.; Bjørklund, G.; Skalny, A. V.; Holmgren, A.; Skalnaya, M. G.; Chirumbolo, S.; Aaseth, J. The role of the thioredoxin/thioredoxin reductase system in the metabolic syndrome: towards a possible prognostic marker? *Cell. Mol. Life Sci.* **2018,** *75*, 1567-1586.

7. Lu, J.; Holmgren, A. The thioredoxin antioxidant system. *Free Radical Biol. Med.* **2014***, 66*, 75-87.

8. Waksman, G.; Krishna, T. S.; Williams, C. H.; Kuriyan, J. Crystal structure of *E. coli* thioredoxin reductase refined at 2 Å resolution: Implication for a large conformational change during catalysis. *J. Mol. Biol.* **1994***, 236*, 800-816.

9. McWilliam, H.; Li, W.; Uludag, M.; Squizzato, S.; Park, Y. M.; Buso, N.; Cowley, A. P.; Lopez, R., Analysis tool web services from the EMBL-EBI. *Nucleic acids research* **2013**, *41* (W1), W597-W600.

10. Osborne, S. A.; Tonissen, K. F. Genomic organization and alternative splicing of mouse and human thioredoxin reductase 1 genes. *BMC Genomics.* **2001***, 2*, 10.

11. Miranda-Vizuete, A.; Damdimopoulos, A. E.; Pedrajas, J. R.; Gustafsson, J.; Spyrou, G. Human mitochondrial thioredoxin reductase. *The FEBS J.* **1999***, 261*, 405-412.

12. Sun, Q. A.; Wu, Y.; Zappacosta, F.; Jeang, K. T.; Lee, B. J.; Hatfield, D. L.; Gladyshev, V. N. Redox regulation of cell signaling by selenocysteine in mammalian thioredoxin reductases. *J. Biol. Chem.* **1999***, 274*, 24522-24530.

13. Schmidt, R. L.; Simonović, M. Synthesis and decoding of selenocysteine and human health. *Croat. Med. J.* **2012,** *53*, 535-550.

14. Forchhammer, K.; Leinfelder, W.; Böck, A. Identification of a novel translation factor necessary for the incorporation of selenocysteine into protein. *Nature.* **1989***, 342*, 453-456.

15. Forchhammer, K.; Bock, A. Selenocysteine synthase from *Escherichia coli*. Analysis of the reaction sequence. *J. Biol. Chem.* **1991***, 266*, 6324-6328.

16. Leinfelder, W.; Forchhammer, K.; Veprek, B.; Zehelein, E.; Bock, A. In vitro synthesis of selenocysteinyl-tRNA (UCA) from seryl-tRNA (UCA): involvement and characterization of the selD gene product. *Proc. Natl. Acad. Sci. U. S. A.* **1990***, 87*, 543-547.

17. Brandt, W.; Wessjohann, L. A. The Functional Role of Selenocysteine (Sec) in the Catalysis Mechanism of Large Thioredoxin Reductases: Proposition of a Swapping Catalytic Triad Including a Sec-His-Glu State. *ChemBioChem.* **2005,** *6*, 386-394.

18. Gromer, S.; Wessjohann, L. A.; Eubel, J.; Brandt, W. Mutational studies confirm the catalytic triad in the human selenoenzyme thioredoxin reductase predicted by molecular modeling. *Chembiochem.* **2006,** *7*, 1649-1652.

19. Cheng, Q.; Sandalova, T.; Lindqvist, Y.; Arner, E. S. Crystal structure and catalysis of the selenoprotein thioredoxin reductase 1. *J. Biol. Chem.* **2009***, 284*, 3998-4008.

20. Bauer, H.; Massey, V.; Arscott, L. D.; Schirmer, R. H.; Ballou, D. P.; Williams, C. H. The mechanism of high Mr thioredoxin reductase from *Drosophila melanogaster*. *J. Biol. Chem.* **2003***, 278*, 33020-33028.

21. Council, N. R.; Council, N. R. Dietary reference intakes for vitamin C, vitamin E, selenium, and carotenoids. Washington, DC: National Academy Press: 2000.

22. Risher, J. Toxicological profile for selenium; Agency for Toxic Substances and Disease Registry: 2003.

23. Kryukov, G. V.; Castellano, S.; Novoselov, S. V.; Lobanov, A. V.; Zehtab, O.; Guigó, R.; Gladyshev, V. N. Characterization of mammalian selenoproteomes. *Science.* **2003***, 300*, 1439-1443.

24. Reich, H. J.; Hondal, R. J. Why nature chose selenium? *ACS Chem. Biol.* **2016***, 11*, 821-841.

25. Lothrop, A. P.; Snider, G. W.; Ruggles, E. L.; Hondal, R. J. Why is mammalian thioredoxin reductase 1 so dependent upon the use of selenium? *Biochemistry.* **2014***, 53*, 554-565.

26. Fritz-Wolf, K.; Urig, S.; Becker, K. The structure of human thioredoxin reductase 1 provides insights into C-terminal rearrangements during catalysis. *J. Mol. Biol.* **2007***, 370*, 116-127.

27. Su, D.; Novoselov, S. V.; Sun, Q. A.; Moustafa, M. E.; Zhou, Y.; Oko, R.; Hatfield, D. L.; Gladyshev, V. N. Mammalian selenoprotein thioredoxin-glutathione reductase. Roles in disulfide bond formation and sperm maturation. *J. Biol. Chem.* **2005***, 280*, 26491-26498.

28. Williams, D. L.; Bonilla, M.; Gladyshev, V. N.; Salinas, G. Thioredoxin glutathione reductase-dependent redox networks in platyhelminth parasites. *Antioxid. Redox Signaling.* **2013***, 19*, 735-745.

29. Rhee, S. G.; Woo, H. A.; Kil, I. S.; Bae, S. H. Peroxiredoxin functions as a peroxidase and a regulator and sensor of local peroxides. *J. Biol. Chem.* **2012***, 287*, 4403-4410.

30. Wang, Z.; Feng, B.; Xiao, G.; Zhou, Z. Roles of methionine oxidation in E200K prion protein misfolding: Implications for the mechanism of pathogenesis in E200K linked familial Creutzfeldt–Jakob disease. *Biochim. Biophys Acta, Proteins Proteomics*. **2016***, 1864*, 346-358.

31. Shao, L.; Diccianni, M. B.; Tanaka, T.; Gribi, R.; Yu, A. L.; Pullen, J. D.; Camitta, B. M.; Yu, J. Thioredoxin expression in primary T-cell acute lymphoblastic leukemia and its therapeutic implication. *Cancer Res.* **2001***, 61*, 7333-7338.

32. Kakolyris, S.; Giatromanolaki, A.; Koukourakis, M.; Powis, G.; Souglakos, J.; Sivridis, E.; Georgoulias, V.; Gatter, K. C.; Harris, A. L. Thioredoxin expression is associated with lymph node status and prognosis in early operable non-small cell lung cancer. *Clin. Cancer Res.* **2001***, 7*, 3087-3091.

33. Fujii, S.; Nanbu, Y.; Nonogaki, H.; Konishi, I.; Mori, T.; Masutani, H.; Yodoi, J. Coexpression of adult T-cell leukemia-derived factor, a human thioredoxin homologue,

and human papillomavirus DNA in neoplastic cervical squamous epithelium. *Cancer.* **1991**, *68*, 1583-1591.

34. Nakamura, H.; Masutani, H.; Tagaya, Y.; Yamauchi, A.; Inamoto, T.; Nanbu, Y.; Fujii, S.; Ozawa, K.; Yodoi, J. Expression and growth-promoting effect of adult t-cell leukemia-derived factor a human thioredoxin homologue in hepatocellular carcinoma. *Cancer.* **1992**, *69*, 2091-2097.

35. Yoshioka, J.; Schreiter, E. R.; Lee, R. T. Role of thioredoxin in cell growth through interactions with signaling molecules. *Antioxid. Redox Signaling.* **2006**, *8*, 2143-2151.

36. Saitoh, M.; Nishitoh, H.; Fujii, M.; Takeda, K.; Tobiume, K.; Sawada, Y.; Kawabata, M.; Miyazono, K.; Ichijo, H. Mammalian thioredoxin is a direct inhibitor of apoptosis signal-regulating kinase (ASK) 1. *EMBO J.* **1998**, *17*, 2596-2606.

37. Gotoh, Y.; Cooper, J. A. Reactive oxygen species-and dimerization-induced activation of apoptosis signal-regulating kinase 1 in tumor necrosis factor-α signal transduction. *J. Biol. Chem.* **1998**, *273*, 17477-17482.

38. Schulze, P. C.; De Keulenaer, G. W.; Yoshioka, J.; Kassik, K. A.; Lee, R. T. Vitamin D3-upregulated protein-1 (VDUP-1) regulates redox-dependent vascular smooth muscle cell proliferation through interaction with thioredoxin. *Circ. Res.* **2002**, *91*, 689-695.

39. Wang, Y.; De Keulenaer, G. W.; Lee, R. T. Vitamin D (3)-up-regulated protein-1 is a stress-responsive gene that regulates cardiomyocyte viability through interaction with thioredoxin. *J. Biol. Chem.* **2002**, *277*, 26496-26500.

40. Karin, M. How NF-κB is activated: the role of the IκB kinase (IKK) complex. *Oncogene.* **1999**, *18*, 6867-6874.

41. Hirota, K.; Matsui, M.; Iwata, S.; Nishiyama, A.; Mori, K.; Yodoi, J. AP-1 transcriptional activity is regulated by a direct association between thioredoxin and Ref-1. *Proc. Natl. Acad. Sci. U. S. A.* **1997**, *94*, 3633-3638.

42. Soini, Y.; Kahlos, K.; Näpänkangas, U.; Kaarteenaho-Wiik, R.; Säily, M.; Koistinen, P.; Pääakkö, P.; Holmgren, A.; Kinnula, V. L. Widespread expression of thioredoxin and thioredoxin reductase in non-small cell lung carcinoma. *Clin. Cancer Res.* **2001**, *7*, 1750-1757.

43. Kawahara, N.; Tanaka, T.; Yokomizo, A.; Nanri, H.; Ono, M.; Wada, M.; Kohno, K.; Takenaka, K.; Sugimachi, K.; Kuwano, M. Enhanced coexpression of thioredoxin and high mobility group protein 1 genes in human hepatocellular carcinoma and the possible association with decreased sensitivity to cisplatin. *Cancer Res.* **1996**, *56*, 5330-5333.

44. Wakita, H.; Yodoi, J.; Masutani, H.; Toda, K.; Takigawa, M. Immunohistochemical distribution of adult T-cell leukemia-derived factor/thioredoxin in epithelial components of normal and pathologic human skin conditions. *J. Invest. Dermatol.* **1992***, 99*, 101-107.

45. Nakamura, H.; Bai, J.; Nishinaka, Y.; Ueda, S.; Sasada, T.; Ohshio, G.; Imamura, M.; Takabayashi, A.; Yamaoka, Y.; Yodoi, J. Expression of thioredoxin and glutaredoxin, redox-regulating proteins, in pancreatic cancer. *Cancer Detect. Prev.* **2000***, 24*, 53-60.

46. Guaiquil, V. H.; Vera, J. C.; Golde, D. W. Mechanism of vitamin C inhibition of cell death induced by oxidative stress in glutathione-depleted HL-60 cells. *J. Biol. Chem.* 2001*, 276*, 40955-40961.

47. Ruebhart, D. R.; Wickramasinghe, W.; Cock, I. E. Protective efficacy of the antioxidants vitamin E and Trolox against *Microcystis aeruginosa* and microcystin-LR in *Artemia franciscana* nauplii. *J. Toxicol. Environ. Health, Part A.* **2009***, 72*, 1567-1575.

48. Forrest, V. J.; Kang, Y.; McClain, D. E.; Robinson, D. H.; Ramakrishnan, N. Oxidative stress-induced apoptosis prevented by Trolox. *Free Radical Biol. Med.* **1994***, 16*, 675-684.

49. Angelucci, F.; Sayed, A. A.; Williams, D. L.; Boumis, G.; Brunori, M.; Dimastrogiovanni, D.; Miele, A. E.; Pauly, F.; Bellelli, A. Inhibition of *Schistosoma mansoni* thioredoxin-glutathione reductase by auranofin: structural and kinetic aspects. *J. Biol. Chem.* **2009***, 284*, 28977-28985.

50. Noll, D. M.; Mason, T. M.; Miller, P. S. Formation and repair of interstrand cross-links in DNA. *Chem. Rev.* **2006***, 106*, 277-301.

51. Millet, R.; Urig, S.; Jacob, J.; Amtmann, E.; Moulinoux, J.; Gromer, S.; Becker, K.; Davioud-Charvet, E. Synthesis of 5-nitro-2-furancarbohydrazides and their cis-diamminedichloroplatinum complexes as bitopic and irreversible human thioredoxin reductase inhibitors. *J. Med. Chem.* **2005***, 48*, 7024-7039.

52. Anestål, K.; Prast-Nielsen, S.; Cenas, N.; Arnér, E. S. Cell death by SecTRAPs: thioredoxin reductase as a prooxidant killer of cells. *PloS One.* **2008***, 3*, e1846.

53. Urig, S.; Becker, K. On the potential of thioredoxin reductase inhibitors for cancer therapy. *Semin. Cancer Biol*. **2006**, *16*, 452-465.

54. Arnér, E. S.; Nakamura, H.; Sasada, T.; Yodoi, J.; Holmgren, A.; Spyrou, G. Analysis of the inhibition of mammalian thioredoxin, thioredoxin reductase, and glutaredoxin by cis-diamminedichloroplatinum (II) and its major metabolite, the glutathione-platinum complex. *Free Radical Biol. Med.* **2001***, 31*, 1170-1178.

55. Lu, J.; Chew, E. H.; Holmgren, A. Targeting thioredoxin reductase is a basis for cancer therapy by arsenic trioxide. *Proc. Natl. Acad. Sci. U. S. A.* **2007**, *104*, 12288-12293.

56. Fang, J.; Lu, J.; Holmgren, A. Thioredoxin reductase is irreversibly modified by curcumin: a novel molecular mechanism for its anticancer activity. *J. Biol. Chem.* **2005**, *280*, 25284-25290.

57. Liu, Z.; Huang, S.; Li, M.; Huang, Z.; Lee, K. S.; Gu, L. Inhibition of thioredoxin reductase by mansonone F analogues: Implications for anticancer activity. *Chem. Biol. Interact.* **2009**, *177*, 48-57.

58. Carvalho, C. M.; Chew, E. H.; Hashemy, S. I.; Lu, J.; Holmgren, A. Inhibition of the human thioredoxin system. A molecular mechanism of mercury toxicity. *J. Biol. Chem.* **2008**, *283*, 11913-11923.

59. Palomero, J.; Pye, D.; Kabayo, T.; Spiller, D. G.; Jackson, M. J. In situ detection and measurement of intracellular reactive oxygen species in single isolated mature skeletal muscle fibers by real time fluorescence microscopy. *Antioxid. Redox Signaling.* **2008**, *10*, 1463-1474.

60. Walsh, C. J.; Butawan, M.; Yordy, J.; Ball, R.; Flewelling, L.; de Wit, M.; Bonde, R. K. Sublethal red tide toxin exposure in free-ranging manatees (*Trichechus manatus*) affects the immune system through reduced lymphocyte proliferation responses, inflammation, and oxidative stress. *Aquat. Toxicol.* **2015**, *161*, 73-84.

61. Walsh, C. J.; Leggett, S. R.; Carter, B. J.; Colle, C. Effects of brevetoxin exposure on the immune system of loggerhead sea turtles. *Aquat. Toxicol.* **2010**, *97*, 293-303.

62. Cassell, R. T.; Chen, W.; Thomas, S.; Liu, L.; Rein, K. S. Brevetoxin, the dinoflagellate neurotoxin, localizes to thylakoid membranes and interacts with the light-harvesting complex II (LHCII) of photosystem II. *Chembiochem.* **2015**, *16*, 1060-1067.

63. Chen, W.; Tuladhar, A.; Rolle, S.; Lai, Y.; del Rey, F. R.; Zavala, C. E.; Liu, Y.; Rein, K. S. Brevetoxin-2, is a unique inhibitor of the C-terminal redox center of mammalian thioredoxin reductase-1. *Toxicol. Appl. Pharmacol.* **2017**, *329*, 58-66.

64. Paz, M. M.; Zhang, X.; Lu, J.; Holmgren, A. A new mechanism of action for the anticancer drug mitomycin C: mechanism-based inhibition of thioredoxin reductase. *Chem. Res. Toxicol.* **2012**, *25*, 1502-1511.

65. Riener, C. K.; Kada, G.; Gruber, H. J. Quick measurement of protein sulfhydryls with Ellman's reagent and with 4, 4′-dithiodipyridine. *Anal. Bioanal. Chem.* **2002**, *373*, 266-276.

66. Ellman, G. L. Tissue sulfhydryl groups. *Arch. Biochem. Biophys.* **1959***, 82*, 70-77.

67. Cenas, N.; Nivinskas, H.; Anusevicius, Z.; Sarlauskas, J.; Lederer, F.; Arner, E. S. Interactions of quinones with thioredoxin reductase: a challenge to the antioxidant role of the mammalian selenoprotein. *J. Biol. Chem.* **2004***, 279*, 2583-2592.

68. Hara, M.; Akasaka, K.; Akinaga, S.; Okabe, M.; Nakano, H.; Gomez, R.; Wood, D.; Uh, M.; Tamanoi, F. Identification of Ras farnesyltransferase inhibitors by microbial screening. *Proc. Natl. Acad. Sci. U.S.A.* **1993**, *90*, 2281-2285.

69. Downward, J. Targeting RAS signalling pathways in cancer therapy. *Nat. Rev. Cancer.* **2003**, *3*, 11-22.

70. Papke, B.; Der, C. J. Drugging RAS: Know the enemy. *Science.* **2017**, *355*, 1158-1163.

71. Fletcher, S.; Keaney, E. P.; Cummings, C. G.; Blaskovich, M. A.; Hast, M. A.; Glenn, M. P.; Chang, S.-Y.; Bucher, C. J.; Floyd, R. J.; Katt, W. P. Structure-based design and synthesis of potent, ethylenediamine-based, mammalian farnesyltransferase inhibitors as anticancer agents. *J. Med. Chem.***2010**, *53*, 6867-6888.

72. Sousa, S. F.; Fernandes, P. A.; Ramos, M. J. Farnesyltransferase inhibitors: a detailed chemical view on an elusive biological problem. *Curr. Med. Chem.* **2008**, *15*, 1478-1492.

73. Capell, B. C.; Erdos, M. R.; Madigan, J. P.; Fiordalisi, J. J.; Varga, R.; Conneely, K. N.; Gordon, L. B.; Der, C. J.; Cox, A. D.; Collins, F. S. Inhibiting farnesylation of progerin prevents the characteristic nuclear blebbing of Hutchinson-Gilford progeria syndrome. *Proc. Natl. Acad. Sci. U.S.A.* **2005**, *102*, 12879-12884.

74. Buckner, F. S.; Eastman, R. T.; Nepomuceno-Silva, J. L.; Speelmon, E. C.; Myler, P. J.; Van Voorhis, W. C.; Yokoyama, K. Cloning, heterologous expression, and substrate specificities of protein farnesyltransferases from *Trypanosoma cruzi* and *Leishmania major*. *Mol. Biochem. Parasitol.* **2002**, *122*, 181-188.

75. Esteva, M. I.; Kettler, K.; Maidana, C.; Fichera, L.; Ruiz, A. M.; Bontempi, E. J.; Andersson, B.; Dahse, H.-M.; Haebel, P.; Ortmann, R. Benzophenone-based farnesyltransferase inhibitors with high activity against *Trypanosoma cruzi*. *J. Med. Chem.* **2005**, *48*, 7186-7191.

76. Glenn, M. P.; Chang, S. Y.; Hucke, O.; Verlinde, C. L.; Rivas, K.; Hornéy, C.; Yokoyama, K.; Buckner, F. S.; Pendyala, P. R.; Chakrabarti, D. Structurally simple farnesyltransferase inhibitors arrest the growth of malaria parasites. *Angew. Chem. Int. Ed.* **2005**, *44*, 4903-4906.

77. Ibrahim, M.; Azzouz, N.; Gerold, P.; Schwarz, R. T. Identification and characterisation of *Toxoplasma gondii* protein farnesyltransferase. *Int. J. Parasitol.* **2001**, *31*, 1489-1497.

78. Kainuma, O.; Asano, T.; Hasegawa, M.; Kenmochi, T.; Nakagohri, T.; Tokoro, Y.; Isono, K. Inhibition of growth and invasive activity of human pancreatic cancer cells by a farnesyltransferase inhibitor, manumycin. *Pancreas.* **1997**, *15*, 379-383.

79. Nagase, T.; Kawata, S.; Tamura, S.; Matsuda, Y.; Inui, Y.; Yamasaki, E.; Ishiguro, H.; Ito, T.; Miyagawa, J.; Mitsui, H. Manumycin and gliotoxin derivative KT7595 block Ras farnesylation and cell growth but do not disturb lamin farnesylation and localization in human tumour cells. *Br. J. Cancer.* **1997**, *76*, 1001-1010.

80. Bernier, M.; Kwon, Y.-K.; Pandey, S. K.; Zhu, T.-N.; Zhao, R.-J.; Maciuk, A.; He, H.-J.; DeCabo, R.; Kole, S. Binding of manumycin A inhibits IκB kinase β activity. *J. Biol. Chem.* **2006**, *281*, 2551-2561.

81. Ito, T.; Kawata, S.; Tamura, S.; Igura, T.; Nagase, T.; Miyagawa, J. i.; Yamazaki, E.; Ishiguro, H.; Matsuzawa, Y. Suppression of human pancreatic cancer growth in BALB/c nude mice by manumycin, a farnesyl: protein transferase inhibitor. *Jpn. J. Cancer Res.* **1996**, *87*, 113-116.

82. Sears, K. T.; Daino, H.; Carey, G. B. Reactive oxygen species-dependent destruction of MEK and Akt in Manumycin stimulated death of lymphoid tumor and myeloma cell lines. *Int. J. Cancer.* **2008**, *122*, 1496-1505.

83. Ahmad, R.; Sylvester, J.; Ahmad, M.; Zafarullah, M. Involvement of H-Ras and reactive oxygen species in proinflammatory cytokine-induced matrix metalloproteinase-13 expression in human articular chondrocytes. *Arch. Biochem. Biophys.* **2011**, *507*, 350-355.

84. Ahmad, F.; Ghosh, S.; Sinha, S.; Joshi, S. D.; Mehta, V. S.; Sen, E. TGF-β-induced hCG-β regulates redox homeostasis in glioma cells. *Mol. Cell. Biochem.* **2015**, *399*, 105-112.

85. Carey, G. B.; Roy, S. K.; Daino, H. The natural tumorcide Manumycin-A targets protein phosphatase 1α and reduces hydrogen peroxide to induce lymphoma apoptosis. *Exp. Cell Res.* **2015**, *332*, 136-145.

86. Chang, M.-C.; Chen, Y.-J.; Chang, H.-H.; Chan, C.-P.; Yeh, C.-Y.; Wang, Y.-L.; Cheng, R.-H.; Hahn, L.-J.; Jeng, J.-H. Areca nut components affect COX-2, cyclin B1/cdc25C and keratin expression, PGE2 production in keratinocyte is related to reactive oxygen species, CYP1A1, Src, EGFR and Ras signaling. *PloS One.* **2014**, *9*, e101959.

87. Dixit, D.; Sharma, V.; Ghosh, S.; Koul, N.; Mishra, P. K.; Sen, E. Manumycin inhibits STAT3, telomerase activity, and growth of glioma cells by elevating intracellular reactive oxygen species generation. *Free Radical Biol.Med.* **2009**, *47*, 364-374.

88. Pan, J.; She, M.; Xu, Z.-X.; Sun, L.; Yeung, S.-C. J. Farnesyltransferase inhibitors induce DNA damage via reactive oxygen species in human cancer cells. *Cancer Res.* **2005**, *65*, 3671-3681.

89. She, M.-R.; Yang, H.; Sun, L.; Yeung, S.-C. J. Redox control of manumycin A-induced apoptosis in anaplastic thyroid cancer cells: involvement of the xenobiotic apoptotic pathway. *Cancer Biol. Ther.* **2006**, *5*, 275-280.

90. Zhang, J.; Jiang, H.; Xie, L.; Hu, J.; Li, L.; Yang, M.; Cheng, L.; Liu, B.; Qian, X. Antitumor effect of manumycin on colorectal cancer cells by increasing the reactive oxygen species production and blocking PI3K-AKT pathway. *OncoTargets Ther.* **2016**, *9*, 2885-2895.

91. Yu, Y.; Fan, S.-M.; Ye, Y.-C.; Tashiro, S.-i.; Onodera, S.; Ikejima, T. The tyrphostin AG1478 augments oridonin-induced A431 cell apoptosis by blockage of JNK MAPK and enhancement of oxidative stress. *Free Radical Res.* **2012**, *46*, 1393-1405.

92. Montano, S. J.; Lu, J.; Gustafsson, T. N.; Holmgren, A. Activity assays of mammalian thioredoxin and thioredoxin reductase: fluorescent disulfide substrates, mechanisms, and use with tissue samples. *Anal.l Biochem.* **2014**, *449*, 139-146.

93. Zhang, B.; Ge, C.; Yao, J.; Liu, Y.; Xie, H.; Fang, J. Selective selenol fluorescent probes: design, synthesis, structural determinants, and biological applications. *J. Am. Chem. Soc.* **2015**, *137*, 757-769.

94. Fang, J.; Holmgren, A. Inhibition of thioredoxin and thioredoxin reductase by 4-hydroxy-2-nonenal in vitro and in vivo. *J. Am. Chem. Soc.* **2006**, *128*, 1879-1885.

95. Powis, G.; Wipf, P.; Lynch, S. M.; Birmingham, A.; Kirkpatrick, D. L. Molecular pharmacology and antitumor activity of palmarumycin-based inhibitors of thioredoxin reductase. *Mol.r Cancer Ther.* **2006**, *5*, 630-636.

96. Zhang, Q.; Tsukahara, F.; Maru, Y. N-acetyl-cysteine enhances growth in BCR-ABL-transformed cells. *Cancer Sci.* **2005**, *96*, 240-244.

97. Zhong, L.; Holmgren, A. Essential role of selenium in the catalytic activities of mammalian thioredoxin reductase revealed by characterization of recombinant enzymes with selenocysteine mutations. *J. Biol. Chem.* **2000,** *275* , 18121-18128.

98. Zhong, L.; Arnér, E. S.; Holmgren, A. Structure and mechanism of mammalian thioredoxin reductase: the active site is a redox-active selenolthiol/selenenylsulfide

formed from the conserved cysteine-selenocysteine sequence. *Proc. Natl. Acad. Sci. U.S.A.* **2000,** *97*, 5854-5859.

99. Reuter, C. W.; Morgan, M. A.; Bergmann, L. Targeting the Ras signaling pathway: a rational, mechanism-based treatment for hematologic malignancies? *Blood.* **2000**, *96*, 1655-1669.

100. Pierce, R.; Henry, M. Harmful algal toxins of the Florida red tide (*Karenia brevis*): natural chemical stressors in South Florida coastal ecosystems. *Ecotoxicology.* **2008**, *17*, 623-631.

101. Shimizu, Y.; Bando, H.; Chou, H.-N.; Van Duyne, G.; Clardy, J. C. Absolute configuration of brevetoxins. *J. Chem. Soc., Chem. Commun.* **1986**, *22*, 1656-1658.

102. Baden, D. G.; Bourdelais, A. J.; Jacocks, H.; Michelliza, S.; Naar, J. Natural and derivative brevetoxins: historical bakground, multiplicity, and effects. *Environ. Health Perspect.* **2005**, *113*, 621-625.

103. Landsberg, J. H. The effects of harmful algal blooms on aquatic organisms. *Rev. Fish. Sci.* **2002**, *10*, 113-390.

104. Tian, L.; Wang, M.; Li, X.; Lam, P. K. S.; Wang, M.; Wang, D.; Chou, H. N.; Li, Y.; Chan, L. L. Proteomic modification in gills and brains of medaka fish (*Oryzias melastigma*) after exposure to a sodium channel activator neurotoxin, brevetoxin-1. *Aquat. Toxicol.* **2011**, *104*, 211-217.

105. Radwan, F. F.; Ramsdell, J. S. Characterization of in vitro oxidative and conjugative metabolic pathways for brevetoxin (PbTx-2). *Toxicol. Sci.*. **2005**, *89*, 57-65.

106. Ross, C.; Ritson-Williams, R.; Pierce, R.; Bullington, J. B.; Henry, M.; Paul, V. J. Effects of the Florida red tide dinoflagellate, *Karenia brevis*, on oxidative stress and metamorphosis of larvae of the coral *Porites astreoides*. *Harmful Algae.* **2010**, *9*, 173-179.

107. Washburn, B. S.; Baden, D. G.; Gassman, N. J.; Walsh, P. J. Brevetoxin: tissue distribution and effect on cytochrome P450 enzymes in fish. *Toxicon.* **1994**, *32*, 799-805.

108. Walsh, C. J.; Leggett, S. R.; Henry, M. S.; Blum, P. C.; Osborn, S.; Pierce, R. H. Cellular metabolism of brevetoxin (PbTx-2) by a monocyte cell line (U-937). *Toxicon.* **2009**, *53*, 135-145.

109. Sayer, A.; Hu, Q.; Bourdelais, A. J.; Baden, D. G.; Gibson, J. E. The effect of brevenal on brevetoxin-induced DNA damage in human lymphocytes. *Arch. Toxicol.* **2005**, *79*, 683-688.

110. Murrell, R. N.; Gibson, J. E. Brevetoxins 2, 3, 6, and 9 show variability in potency and cause significant induction of DNA damage and apoptosis in Jurkat E6-1 cells. *Arch.Ttoxicol.* **2009**, *83*, 1009-1019.

111. Prieto, A. I.; Jos, A.; Pichardo, S.; Moreno, I.; de Sotomayor, M. Á.; Moyano, R.; Blanco, A.; Cameán, A. M. Time-dependent protective efficacy of Trolox (vitamin E analog) against microcystin-induced toxicity in tilapia (*Oreochromis niloticus*). *Environ. Toxicol.* **2009**, *24*, 563-579.

112. Savvides, S. N.; Karplus, P. A. Kinetics and crystallographic analysis of human glutathione reductase in complex with a xanthene inhibitor. *J. Biol. Chem.* **1996,** *271*, 8101-8107.

113. Xu, H.; Paerl, H. W.; Qin, B.; Zhu, G.; Gaoa, G. Nitrogen and phosphorus inputs control phytoplankton growth in eutrophic Lake Taihu, China. *Limnol. Oceanogr.* **2010**, *55*, 420-432.

114. Paerl, H. W.; Otten, T. G. Harmful cyanobacterial blooms: causes, consequences, and controls. *Microb. Ecol.* **2013**, *65*, 995-1010.

115. Robinson, N. A.; Matson, C. F.; Pace, J. G. Association of microcystin-LR and its biotransformation product with a hepatic-cytosolic protein. *J. Biochem. Mol. Toxicol.* **1991**, *6*, 171-180.

116. Namikoshi, M.; Rinehart, K. L.; Sakai, R.; Stotts, R. R.; Dahlem, A. M.; Beasley, V. R.; Carmichael, W. W.; Evans, W. R. Identification of 12 hepatotoxins from a Homer Lake bloom of the cyanobacteria *Microcystis aeruginosa*, *Microcystis viridis*, and *Microcystis wesenbergii*: nine new microcystins. *J. Org. Chem.***1992**, *57*, 866-872.

117. Oehrle, S.; Rodriguez-Matos, M.; Cartamil, M.; Zavala, C.; Rein, K. S. Toxin composition of the 2016 *Microcystis aeruginosa* bloom in the St. Lucie Estuary, Florida. *Toxicon.* **2017**, *138*, 169-172.

118. Williams, D. E.; Kent, M. L.; Andersen, R. J.; Klix, H.; Holmes, C. F. Tissue distribution and clearance of tritium-labeled dihydromicrocystin-LR epimers administered to Atlantic salmon via intraperitoneal injection. *Toxicon.* **1995**, *33*, 125-131.

119. Stebbins, C. E.; Russo, A. A.; Schneider, C.; Rosen, N.; Hartl, F. U.; Pavletich, N. P. Crystal structure of an Hsp90–Ga complex: targeting of a protein chaperone by an antitumor agent. *Cell*. **1997**, *89*, 239-250.

120. Sullivan, W.; Toft, D. Mutational analysis of hsp90 binding to the progesterone receptor. *J. Biol. Chem.* **1993**, *268*, 20373-20379.

121. Whitesell, L.; Cook, P. Stable and specific binding of heat shock protein 90 by Ga disrupts glucocorticoid receptor function in intact cells. *Mol. Endocrinol.* **1996**, *10*, 705-712.

122. Lianos, G. D.; Alexiou, G. A.; Mangano, A.; Mangano, A.; Rausei, S.; Boni, L.; Dionigi, G.; Roukos, D. H. The role of heat shock proteins in cancer. *Cancer let.* **2015**, *360*, 114-118.

123. Zhao, M.; Shen, F.; Yin, Y.; Yang, Y.; Xiang, D.; Chen, Q. Increased expression of heat shock protein 27 correlates with peritoneal metastasis in epithelial ovarian cancer. *Reprod. Sci.* **2012**, *19*, 748-753.

124. Kubota, H.; Yamamoto, S.; Itoh, E.; Abe, Y.; Nakamura, A.; Izumi, Y.; Okada, H.; Iida, M.; Nanjo, H.; Itoh, H. Increased expression of co-chaperone HOP with HSP90 and HSC70 and complex formation in human colonic carcinoma. *Cell Stress Chaperones.* **2010**, *15*, 1003-1011.

125. Wachsberger, P. R.; Lawrence, Y. R.; Liu, Y.; Rice, B.; Feo, N.; Leiby, B.; Dicker, A. P. Hsp90 inhibition enhances PI-3 kinase inhibition and radiosensitivity in glioblastoma. *J. Cancer Res. Clin. Oncol.* **2014**, *140*, 573-582.

126. Floris, G.; Sciot, R.; Wozniak, A.; Van Looy, T.; Wellens, J.; Faa, G.; Normant, E.; Debiec-Rychter, M.; Schöffski, P. The Novel HSP90 inhibitor, IPI-493, is highly effective in human gastrostrointestinal stromal tumor xenografts carrying heterogeneous KIT mutations. *Clin. Cancer Res.* **2011**, *17*, 5604-5614.

127. Lin, P.; Yi, Y.; Lu, M.; Wang, M.; Yang, Y.; Lu, Y.; Song, S.; Zheng, Z.; Deng, X.; Zhang, L. Heat shock protein 90 inhibitor mycoepoxydiene modulates kinase signaling in cervical cancer cells and inhibits in-vivo tumor growth. *Anticancer Drugs.* **2015**, *26*, 25-34.

128. Ferraldeschi, R.; Welti, J.; Powers, M. V.; Yuan, W.; Smyth, T.; Seed, G.; Riisnaes, R.; Hedayat, S.; Wang, H.; Crespo, M. Second-generation HSP90 inhibitor onalespib blocks mRNA splicing of androgen receptor variant 7 in prostate cancer cells. *Cancer Res.* **2016**, *76*, 2731-2742.

129. Che, Y.; Best, O. G.; Zhong, L.; Kaufman, K. L.; Mactier, S.; Raftery, M.; Graves, L. M.; Mulligan, S. P. Christopherson, R. I. Hsp90 inhibitor SNX-7081 dysregulates proteins involved with DNA repair and replication and the cell cycle in human chronic lymphocytic leukemia (CLL) cells. *J. Proteome. Res.* **2013**, *12*, 1710-1722.

130. Jang, W. J.; Jung, S. K.; Kang, J. S.; Jeong, J. W.; Bae, M. K.; Joo, S. H.; Park, G. H.; Kundu, J. K.; Hong, Y. S.; Jeong, C. H. Anti-tumor activity of WK88-1, a novel geldanamycin derivative, in gefitinib-resistant non-small cell lung cancers with Met amplification. *Cancer Sci.* **2014**, *105*, 1245-1253.

131. Wang, J.; Li, Z.; Lin, Z.; Zhao, B.; Wang, Y.; Peng, R.; Wang, M.; Lu, C.; Shi, G.; Shen, Y. 17-DMCHAG, a new geldanamycin derivative, inhibits prostate cancer cells through Hsp90 inhibition and survivin downregulation. *Cancer lett.* **2015**, *362*, 83-96.

132. Campbell, E. A.; Korzheva, N.; Mustaev, A.; Murakami, K.; Nair, S.; Goldfarb, A.; Darst, S. A. Structural mechanism for rifampicin inhibition of bacterial RNA polymerase. *Cell*. **2001**, *104*, 901-912.

133. Evans, S. E.; Goult, B. T.; Fairall, L.; Jamieson, A. G.; Ferrigno, P. K.; Ford, R.; Schwabe, J. W.; Wagner, S. D. The ansamycin antibiotic, rifamycin SV, inhibits BCL6 transcriptional repression and forms a complex with the BCL6-BTB/POZ domain. *PloS One.* **2014**, *9*, e90889.

134. Vavricka, S. R.; Van Montfoort, J.; Ha, H. R.; Meier, P. J.; Fattinger, K. Interactions of rifamycin SV and rifampicin with organic anion uptake systems of human liver. *Hepatology.* **2002**, *36*, 164-172.

135. Bausch, S. L.; Poliakova, E.; Draper, D. E. Interactions of the N-terminal domain of ribosomal protein L11 with Th and rRNA. *J. Biol. Chem.* **2005**, *280*, 29956-29963.

136. Li, L.; Yu, A.-Q. The functional role of peroxiredoxin 3 in reactive oxygen species, apoptosis, and chemoresistance of cancer cells. *J. Cancer Res. Clin. Oncol.* **2015**, *141*, 2071-2077.

137. Newick, K.; Cunniff, B.; Preston, K.; Held, P.; Arbiser, J.; Pass, H.; Mossman, B.; Shukla, A.; Heintz, N. Peroxiredoxin 3 is a redox-dependent target of thiostrepton in malignant mesothelioma cells. *PloS One.* **2012**, *7*, e39404.

138. Kukiełka, E.; Cederbaum, A. Stimulation of NADH-dependent microsomal DNA strand cleavage by rifamycin SV. *Biochem. J.* **1995**, *307*, 361-367.

139. Guo, W.; Reigan, P.; Siegel, D.; Ross, D. Enzymatic reduction and glutathione conjugation of benzoquinone ansamycin heat shock protein 90 inhibitors: relevance for toxicity and mechanism of action. *Drug Metab. Dispos.* **2008**, *36*, 2050-2057.

140. Piper, P. W.; Millson, S. H. Mechanisms of resistance to Hsp90 inhibitor drugs: a complex mosaic emerges. *Pharmaceuticals*. **2011,** *4*, 1400-1422.

141. Mori, M.; Oishi, T.; Matsuoka, S.; Ujihara, S.; Matsumori, N.; Murata, M.; Satake, M.; Oshima, Y.; Matsushita, N.; Aimoto, S. Ladder-shaped polyether compound, desulfated yessotoxin, interacts with membrane-integral α-helix peptides. *Bioorganic Med. Chem.* **2005**, *13*, 5099-5103.

142. Wright, D. E.; Altaany, Z.; Bi, Y.; Alperstein, Z.; O'Donoghue, P. Acetylation regulates thioredoxin reductase oligomerization and activity. *Antioxid.. Redox Signaling.* **2017**. DOI: 10.1089/ars.2017.7082.

143. Rackham, O.; Shearwood, A.-M. J.; Thyer, R.; McNamara, E.; Davies, S. M.; Callus, B. A.; Miranda-Vizuete, A.; Berners-Price, S. J.; Cheng, Q.; Arnér, E. S. Substrate and inhibitor specificities differ between human cytosolic and mitochondrial thioredoxin reductases: Implications for development of specific inhibitors. *Free Radical Biol. Med.* **2011**, *50*, 689-699.

VITA

ANUPAMA TULADHAR
Kathmandu, Nepal

2008-2010 M.S., Chemistry
Tribhuvan University
Kathmandu, Nepal

2013-2018 Doctoral Candidate
Florida International University
Miami, Fl

PRESENTATIONS AND PUBLICATION

- Anupama Tuladhar, Wei Chen, Shantell Rolle, Yuan Liu and Kathleen S. Rein (09/18/2016-09/23/2016), Poster presentation on title "The effect of Trolox on brevetoxicosis in human lymphoblast cells." at International Society on Toxinology, Miami Beach.

- Anupama Tuladhar, Kathleen S. Rein (07/21/2018-07/25/2018), Poster presentation on title "Manumycin-A: Inhibitor of cytoplasmic TrxR and activator of mitochondrial TrxR." at The American Society of Pharmacognosy (ASP).

- Anupama Tuladhar, Wei Chen, Shantell Rolle, Yuan Liu and Kathleen S. Rein. (05/04/2017-05/06/2017), Oral presentation on title "The mechanism of brevotoxin induced oxidative stress and effect of antioxidant." at 92nd Florida Annual Meeting and Exposition (FAME).

- Anupama Tuladhar, Kathleen S. Rein. (03/19/2018-03/20/2018), Oral presentation on title "Manumycin-A is a potent inhibitor of mammalian cytoplasmic TrxR." GPSC, FIU.

- Anupama Tuladhar, Kathleen S. Rein. (05/04/2018-04/06/2018), Oral presentation on title "Manumycin-A is a potent inhibitor of mammalian cytoplasmic TrxR and activator of mitochondrial TrxR." at 93rd Florida Annual Meeting and Exposition (FAME).

- Chen, W.; Tuladhar, A.; Rolle, S.; Lai, Y.; del Rey, F. R.; Zavala, C. E.; Liu, Y.; Rein, K.S. Brevetoxin-2, is a unique inhibitor of the C-terminal redox center of mammalian thioredoxin reductase-1. *Toxicol. Appl. Pharmacol.* 2017, *329*, 58-66.

- ❖ Tuladhar, A.; Rein, K. S. Manumycin A is a potent inhibitor of mammalian thioredoxin reductase-1 (TrxR-1). *ACS Med. Chem. Lett.* 2018, *9*, 318-322.

- ❖ Tuladhar, A.; Rein, K. S. Effectors of thioredoxin reductase. Brevetoxins and manumycin A. *Comparative Biochemistry and Physiology Part C: Toxicology and Pharmacology.* 2018. https://doi.org/10.1016/j.cbpc.2018.11.015.

- ❖ Tuladhar, A.; Rein, K. S. Effectors of thioredoxin reductase. Microcystin-LR and dihydro-microcystin-LR. In preparation.